DISS. ETH No. 22056

Gait Control and Locomotor Recovery after Spinal Cord Injury

A thesis submitted to attain the degree of

DOCTOR OF SCIENCES of ETH ZURICH
(Dr. sc. ETH Zürich)

presented by

Lea Awai
MSc ETH HMS

born on 2nd July 1984
Citizen of Untervaz (GR) and Japan

accepted on the recommendations of

Prof. Dr. Martin E. Schwab
Prof. Dr. Armin Curt
Prof. Dr. Grégoire Courtine

~ 2014 ~

Contents

Summary

The gait of patients with an incomplete spinal cord injury (iSCI) has been studied previously. The most widely examined parameters to characterize iSCI gait are walking speed and time-distance measures (e.g., step length, step frequency, gait-cycle phases). In a clinical setting, the functional recovery of iSCI patients is routinely captured by specific outcome measures such as the 10-meter walk test (10mWT), the 6-minute walk test (6minWT) or the walking index for spinal cord injury (WISCI), which has been specifically established for this particular group of patients to score their walking ability. These measures are useful to monitor gross motor function and recovery during rehabilitation, but lack the ability to elucidate underlying mechanisms of gait alterations and recovery or subtle changes in locomotor pattern. In order to be able to appreciate the injury-induced deficits in locomotor control and to capture changes in motor function that may not be visible to the naked eye a sensitive and comprehensive tool is of need.

The easiest way of assessing walking capacity is to collect data of walking speed and distance. Yet, one of the most obvious gait alterations in subjects with iSCI is an impaired gait quality. In the past, gait quality has been scored by trained investigators that rate defined features of walking. However, more complex movements that require precise spatial and temporal coordination of several joints and body segments are not easy to detect by mere observation. In the first study of this thesis, we evaluated the lower-limb coordination by means of combined hip-knee angular profiles (cyclograms). Patients showed distinct types and extents of cyclogram alterations and were thereupon categorized into four groups of impairment. The cyclogram seemed to reflect the underlying deficits as it correlated well with walking performance (speed) but could not be modulated with increasing speeds in contrast to a converging normalization in all control subjects. The intralimb coordination apparently is a sensitive indicator of motor-control impairment after spinal cord injury.

We next evaluated a variety of gait-related parameters in order to find alterations of locomotor control after iSCI. With the aim of establishing a comprehensive framework to examine the organization of walking behavior in humans and how this organization gets distorted by insults to the spinal cord we

chose a data-driven holistic approach for analyzing a multivariate set of data. This approach prevents a certain investigator-induced bias that arises when more or less arbitrarily pre-selecting a specific outcome measure. Multivariate in this case means variables of different modalities, i.e., objective electrophysiological measures that represent the integrity and electrical conductivity of specific spinal fiber tracts, kinematic measures that describe the extent of movements and body-segment coordination (i.e., gait quality) as well as measures that quantify locomotor performance such as walking speed and distance. Hence, clusters of parameters were identified that were or were not altered in iSCI patients and that were distinctly modulated with respect to speed. These findings suggest that there are distinguishable domains of neural control of walking that may be differently affected in specific neurological disorders.

Consequently, the question arises as to which of these parameters change over time and what this might reveal about the mechanisms of recovery. These questions were addressed in the third study where the gait of iSCI patients was analyzed at several time points during rehabilitation in order to reveal those parameters that most strongly contribute to recovery, and also to reveal the responsiveness of the multimodal factors to an improvement in walking speed. Interestingly, the responsiveness of a single measure did not necessarily contribute to recovery, which is rather affected by the contribution of mutually interacting parameters.

It remains to be elucidated where exactly the plastic changes leading to functional recovery take place and by what mechanisms they are mediated. The great challenge of spinal cord research is the cure for paralysis, or, in other words, a way to induce functional neural repair in the growth-inhibiting environment of the central nervous system (CNS). Even though it is known that spontaneous regeneration of severed neural tissue does virtually not occur in the CNS, recovery on a functional basis does happen. In the fourth study we demonstrated that the spinal cord is capable of extensive plastic changes induced by pathological processes in the absence of motor deficits and only minor sensory impairments.

To accelerate the success of future clinical trials, the bridging from bench to bedside needs to be encouraged. Outcome measures should be standardized across species in order to appreciate differences and similarities. It could be shown that after a cervical hemisection of the spinal cord, equivalent to a the Brown-Séquard Syndrome in patients, humans and primates show superior recovery of function mediated by the corticospinal tract compared to rats. These findings support the importance of studies performed in primates to minimize the gap between preclinical and clinical outcome.

Zusammenfassung

Der Gang von inkomplett querschnittgelähmten Patienten (iSCI, *engl.* incomplete spinal cord injury) wird bereits seit längerem untersucht. Die am häufigsten verwendeten Grössen um das iSCI Gangbild zu charakterisieren sind Gehgeschwindigkeit und Gangzyklus Parameter (z.B. Schrittlänge, Schrittfrequenz, Phasen des Ganzyklus). Im klinischen Alltag wird die funktionelle Erholung von iSCI Patienten mittels spezifischer Messgrössen bestimmt, wie z.B. der 10-Meter Gehtest (10mWT), der 6-Minuten Gehtest (6minWT) oder der *walking index for spinal cord injury* (WISCI), der eigens für diese spezifische Patientengruppe etabliert wurde um ihre Gehfähigkeit bewerten zu können. Diese Messgrössen eignen sich gut um die allgemeine motorische Funktion und deren Erholung während der Rehabilitation zu verfolgen, sind jedoch nicht in der Lage die zugrundeliegenden Mechanismen, die zu Gangstörungen führen sowie deren Erholung oder subtile Unterschiede des Gangmusters zu erkennen. Um die verletzungsbedingten Defizite der Lokomotionskontrolle und Veränderungen der motorischen Funktion, die sich dem blossen Auge entziehen, erfassen zu können, braucht es sensitive und umfassende Tools.

Die einfachste Methode um Gehfähigkeit erfassen zu können ist das Messen von Gehgeschwindigkeit und –distanz. Die offensichtlichste Veränderung des Ganges von iSCI Patienten ist jedoch die beeinträchgte Gangqualität. Bislang wurde die Gangqualität durch geschulte Untersucher anhand von definierten Merkmalen bewertet. Die komplexe Abfolge von zeitlich und räumlich präzise ablaufenden Bewegungen von mehreren Gelenken und Körpersegmenten ist jedoch nicht einfach mittels Beobachtung zu beurteilen. In der ersten Studie dieser Dissertation wurde die Koordination der unteren Extremitäten mittels kombinierten Hüft-Knie Winkelverläufen (Zyklogramm) evaluiert. Patienten zeigten unterscheidbare Typen und Ausprägungen von Zyklogrammveränderungen aufgrund derer sie in vier Gruppen von Schweregraden eingeteilt wurden. Das Zyklogramm schien die zugrundeliegenden Defizite zu widerspiegeln, da es gut mit der Gehgeschwindigkeit korrelierte, jedoch nicht entsprechend einer höheren Geschwindigkeit moduliert werden konnte, ganz im Gegensatz zu einer einheitlichen Normalisierung in allen Kontrollpersonen. Die Koordination innerhalb eines Beins ist offensichtlich ein

sensitiver Indikator für eine Beeinträchtigung der motorischen Kontrolle nach einer Rückenmarksverletzung.

Daraufhin untersuchten wir eine Vielzahl von Gang-assoziierten Parametern um Veränderungen der Lokomotionskontrolle nach inkompletter Querschnittlähmung zu finden. Mit dem Ziel ein umfassendes Konzept zur Untersuchung der Organisation des Gehverhaltens beim Menschen und deren Veränderung nach einer Verletzung zu entwickeln, haben wir den datengetriebenen holistischen Ansatz einer multivariaten Datenanalyse gewählt. Dadurch wird eine Verzerrung durch den Untersucher verhindert, die durch eine willkürliche Wahl einer Zielgrösse entstehen würde. In diesem Fall bezieht sich ‚multivariat' auf die unterschiedlichen Modalitäten der Variablen, wie z.B. objektive elektrophysiologische Messgrössen, die die Integrität und elektrische Leitfähigkeit von spezifischen spinalen Bahnen messen, kinematische Grössen, die das Bewegungsausmass und die Koordination von Körpersegmenten (d.h. Gangqualität) umschreiben sowie Messgrössen, die die Gehleistung in Form von Geschwindigkeit und zurückgelegter Distanz quantifizieren. Als Folge konnten Ansammlungen von Parametern identifiziert werden, die beim iSCI Patienten verändert oder eben unverändert waren und unterschiedlich moduliert waren in Bezug auf die Gehgeschwindigkeit. Diese Erkenntnisse lassen vermuten, dass es unterschiedliche Domänen von neuronaler Kontrolle des Gehens gibt, die nach spezifischen neurologischen Erkrankungen unterschiedlich betroffen sind.

Folglich stellt sich die Frage, welche dieser Parameter sich im Verlauf ändern und was dies bezüglich der zugrundeliegenden Mechanismen von Erholung bedeutet. Diese Fragen wurden in der dritten Studie angegangen, wo das Gangmuster von iSCI Patienten zu unterschiedlichen Zeitpunkten während ihrer Rehabilitation analysiert wurde um diejenigen Parameter zu finden, die am stärksten zur Erholung beitragen und die am ehesten mit einer verbesserten Geschwindigkeit einhergehen. Interessanterweise waren nicht zwingend jene Parameter, die sich am meisten veränderten auch jene, die zur Erholung beitrugen. Diese ist vielmehr von der Wechselwirkung unterschiedlicher Parameter abhängig.

Wo genau die plastischen Veränderungen stattfinden, die zu einer funktionellen Verbesserung führen und durch welche Mechanismen diese vermittelt werden bleibt Gegenstand von Untersuchungen. Die grosse Herausforderung der Rückenmarksforschung ist die Heilung von Querschnittlähmung, oder, mit anderen Worten, einen Weg zu finden um funktionelle neurale Wiederherstellung im wachstumsinhibierenden Zentralnervensystem herbeizuführen. Obwohl bekannt ist, dass eine spontane Regeneration von verletzten Nervenzellen im Zentralnervensystem kaum stattfindet, geschieht eine Verbesserung auf funktioneller Ebene. In der vierten Studie zeigten wir, dass das Rückenmark zu weitreichenden plastischen Veränderungen in der Lage ist, die durch pathologische Prozesse hervorgerufen wurden ohne die Manifestation von motorischen Defiziten und nur geringen sensorischen Beeinträchtigungen.

Um den Erfolg von klinischen Studien in Zukunft zu beschleunigen muss ein Brückenschlag *from bench to bedside* gefördert werden. Messparameter sollten zwischen den unterschiedlichen Spezies standardisiert werden um Unterschiede und Gemeinsamkeiten feststellen zu können. Es konnte gezeigt werden, dass nach einer Hemisektion des zervikalen Rückenmarks, vergleichbar mit dem Brown-Séquard Syndrom bei Patienten, der Mensch und der Primate eine bessere Erholung der Funktionen zeigen, die durch die Kortikospinalbahn gesteuert werden, im Vergleich zu Ratten. Diese Erkenntnisse unterstützen die Wichtigkeit von Studien in Primaten, damit der Abstand zwischen präklinischem und klinischem Erfolg verringert werden kann.

General Introduction

Spinal cord injury (SCI) is a debilitating condition where the most obvious deficit is an impaired motor function ranging from minor deficits to complete paralysis of those parts of the body innervated by spinal segments below the level of lesion. However, an insult to the spinal cord most often additionally involves sensory deficits and autonomic dysfunctions. An incomplete spinal cord injury (iSCI) refers to a partial disruption of spinal neural pathways sparing various amounts of intact neural tissue. In more than 50% of SCIs the injury is said to be incomplete and thus motor and sensory functions are impaired but not completely abolished (National SCI Statistical Center). The most widely used classification for the degree of impairment in SCI patients was established by the American Spinal Injury Association (ASIA) where complete SCI is divided into motor and sensory complete impairments (ASIA A) and motor complete and sensory incomplete deficits (ASIA B) while incomplete SCI is subdivided into a group with low residual voluntary motor function (ASIA C) mostly not able to move against gravity while at least half of the assessed key muscles can produce movements against gravity in ASIA D patients. The ASIA impairment scale might be useful for a crude distinction of SCI patients but is not sensitive enough to reveal more precise information on the functional state of patients.

The aims of rehabilitation interventions are a maximal recovery of function and the relearning of activities of daily living with the ultimate goal of greater independence of patients and improved quality of life. Despite longstanding efforts to find a cure for paralysis (i.e., regeneration of severed axons across the lesion site) SCI remains an irremediable neurological disorder. To date, promising treatment approaches in preclinical studies performed in animals could not be successfully translated to human subjects (Hug and Weidner 2012). Current endeavors to improve recovery of function aim at promoting compensatory mechanisms. However, the exact mechanisms of recovery remain largely unidentified not least because of sparsely available sensitive parameters. In humans, recovery is routinely monitored by different means. Magnetic resonance images (MRI) provide insights into morphological changes within the central nervous system (CNS), but whether these changes result in functional improvements cannot be revealed

using imaging techniques. Neurophysiological assessments reveal the integrity of central and peripheral neural pathways where the derived evoked potentials (EPs) contain information on conduction velocity (EP latency) and amount of conducting fibers (EP amplitude). Alterations of the EPs may therefore unveil changes in myelination of axons or the number of neurons and synapses involved in conducting the stimulus. Interestingly, the latency of motor evoked potentials (MEPs) in SCI patients does neither correlate with functional improvements nor with increases in motor strength (Curt et al. 2008). Similarly, MEP amplitudes only change in a small subset of SCI patients with relatively mild impairments despite significant recovery of muscle force and functional ability. These previous results suggest that recovery is likely to occur via compensatory mechanisms and plastic changes of undamaged tissue rather than repair of injured fibers. By what means functional recovery is possible in the absence of repair processes remains to be elucidated. Thus, finding sensitive parameters that might reveal information on underlying mechanisms of plasticity leading to functional changes are of need.

Early studies in vertebrates showed that neurons within the spinal cord are capable of producing rhythmic motor output in the absence of supraspinal and even sensory input (Grillner 1985, Kiehn 2006). The neuronal network producing the rhythmic motor output was termed central pattern generator (CPG). Later on it was shown that these locomotion-generating neuronal networks also exist in mammals such as the cat that can walk on a treadmill in the absence of supraspinal input (Barbeau and Rossignol 1987, Lovely et al. 1986). The rat spinal cord seems to be less autonomous with respect to the generation of patterned motor output. When the spinal cord is completely transected in rats they are unable to produce walking movements. Only after the administration of pharmacological agents and/or electrical stimulation of the dorsal aspect of the spinal cord are they able to produce a physiological stepping pattern (Courtine et al. 2009). To date, no one has reported ambulatory function in human subjects with a complete SCI. However, muscle activity may be elicited during passive ambulation in patients with a clinically complete injury (Dietz et al. 1994, Dietz et al. 1995). Fictive walking could be induced in human subjects via electrical or magnetic stimulation of the spinal cord (Dimitrijevic et al. 1998, Gurfinkel et al. 1998). Therefore, similar to the rat, the human spinal cord seems to be capable of

producing rhythmic, reciprocal motor output without any input from brain centers. The isolated human spinal cord is obviously less sovereign in orchestrating locomotion but has a preserved ability to integrate sensory information in order to produce subsequent motor activity, therefore suggesting the presence of a spinal pattern generator in humans.

Aims

One major aim of the present thesis was to elucidate specific gait parameters that are sensitive enough to measure impairment and recovery in iSCI. Ideally, distinct parameters may reveal complementary information and thus unmask distinguishable mechanisms of gait control and locomotor recovery. In the light of translational research, it is crucial to find similarities and differences of recovery mechanisms across species that enable a prediction and appropriate planning of clinical trials outcome in order to ameliorate the transfer from bench to bedside.

Despite the relative rigidity of the CNS it has been shown that it may allow for certain plasticity. This ability for adaptive changes has mainly been shown for the brain while the plastic potential of the spinal cord was less investigated. We therefore aimed at filling this gap.

Study 1

Intralimb coordination as a sensitive indicator of motor-control impairment after spinal cord injury

Lea Awai, Armin Curt

Frontiers in Human Neuroscience (2014)

»» I would like to thank Barbara Huber, who assisted me during the conduct of this study. ««

1.1 Abstract

Recovery of walking function after neurotrauma, e.g. after spinal cord injury, is routinely captured using standardized walking outcome measures of time and distance. However, these measures do not provide information on possible underlying mechanisms of recovery, nor do they tell anything about the quality of gait. Subjects with an incomplete spinal cord injury are a very heterogeneous group of people with a wide range of functional impairments. A stratification of these subjects would allow increasing sensitivity for hypothesis testing and a more targeted treatment strategy.

The gait of incomplete spinal cord injured subjects was compared to healthy control subjects by analyzing kinematic data obtained by a 3-D motion capture system. Hip-knee angle-angle plots (cyclograms) informed on the qualitative aspect of gait and the intralimb coordination. Features of the cyclogram, e.g. shape of the cyclogram, cycle-to-cycle consistency and its modulation due to changes in walking speed were discerned and used to stratify spinal cord injured subjects.

Spinal cord injured subjects were unable to modulate their cyclogram configuration when increasing speed from slow to preferred. Their gait quality remained clearly aberrant and showed even higher deviations from normal when walking at preferred speed. Qualitative categorization of spinal cord injured subjects based on their intralimb coordination was complemented by quantitative measures of cyclogram shape comparison.

Spinal cord injured subjects showed distinct distortions of intralimb coordination as well as limited modulation to changes in walking speed. The specific changes of the cyclograms revealed complementary insight in the disturbance of lower-limb control in addition to measures of time and distance and may be a useful tool for patient categorization and stratification prior to clinical trial inclusion.

1.2 Introduction

The most obvious impairment after spinal cord injury (SCI) is the complete or partial loss of lower-limb motor function, clinically assessed as decreased walking speed and alterations in time-distance measures (e.g. step length, step frequency, double- and single limb support phase) (Krawetz and Nance 1996, Pepin et al. 2003). These parameters are often used to monitor recovery and to capture locomotor capacity, but they lack the ability to unveil underlying neurological mechanisms (Dobkin et al. 2006, Tamburella et al. 2013). However, the quality of walking, especially the ability to coordinate lower-limb segments and joints, represents aspects of gait that complement the information about walking capacity and additionally provides insights into underlying mechanisms. A clinical inventory for gait quality assessment, relying on a subjective evaluation of SCI walking by a trained therapist has been developed (Field-Fote et al. 2001). Yet, it is not easy to quantify and scale gait quality and even compare it across different neuromotor disorders (Robinson and Smidt 1981). The latter may be one of the reasons for the limited amount of published studies performing quantitative kinematic analysis of gait quality. Previous studies in healthy people have shown that, irrespective of walking speed, lower-limb segments are controlled interdependently as quantified by the co-variation of the elevation angles (Borghese et al. 1996, Grasso et al. 1998, Lacquaniti et al., 1999). This constraint in multi-segmental coordination suggests an underlying rule of motor control ensuring secure upright locomotion. The controlled behavior of multiple segments subserves the ultimate goal of controlling limb endpoints, which is believed to be controlled on different levels within very restricted boundaries. At the cost of aberrant muscle-activity pattern, the endpoint is controlled in a way that its trajectory shows very little variability in healthy individuals and gets closer to normal during training in iSCI subjects (Ivanenko et al. 2003, Winter 1992). Compared to elevation angles, joint angles seem to be more variable and less reproducible (Borghese et al. 1996, Grasso et al., 1998). Lower-limb kinematics (i.e. hip-, knee- and ankle-angle profiles) have been assessed in SCI (Abel et al. 2002, Gil-Agudo et al. 2011) and reveal aberrant and heterogeneous behaviors. But the simple description of joint angles during a gait cycle does not inform on intersegmental coordination. The intralimb coordination, measured as the simultaneous coordination of hip- and knee angles, was found to

be distorted in incomplete spinal cord injury (iSCI) and to be less amendable after locomotor training (Field-Fote and Tepavac 2002, Nooijen et al. 2009). However, the degree of distortion has not been quantified and the measure of intralimb coordination has not been further analyzed. Also, the speed modulation of the intralimb coordination has not been considered, which might reveal information on underlying deficits. The aim of the present study was to characterize intralimb coordination of iSCI subjects qualitatively as well as quantitatively by means of hip-knee cyclograms. These measures may reveal different patterns and categories of walking impairment in iSCI subjects and may uncover mechanisms of lower-limb motor control. The latter findings may be applied to improve the stratification of patients for tailored (i.e. specific to the impairment) interventions to improve walking outcomes in acute as well as chronic iSCI.

1.3 Materials and methods

Subjects

iSCI inclusion criteria: a diagnosed incomplete spinal cord injury; age: 18 years or older; iSCI subjects need to be able to at least stand and walk without the assistance of another person (no manual leg movement by therapist). *Exclusion criteria*: Subjects suffering from neurological disorders other than SCI; gait impairments not caused by SCI. Healthy subjects with no neurological disorders or gait impairments served as the control group. The study was approved by the ethics committee of the Canton of Zurich, Switzerland. Participants gave their written informed consent. 19 iSCI subjects (4f, 15m; age: 50.0 ± 15.9 years; height: 172.6 ± 7.7 cm; weight: 75.8 ± 13.2 kg; Table 1.1) and 19 healthy control subjects (10f, 9m; age: 40.7 ± 13.7 years; height: 173.2 ± 9.3 cm; 68.9 ± 13.0 kg) were included in this study.

Materials

Kinematic data was recorded using 8 infrared cameras (T10, Vicon motion systems Ltd., Oxford, UK) at 200 Hz and two synchronized digital high-speed video cameras (pilot series, Basler AG, Ahrensburg, D) at 100 Hz. 16 reflective markers (16 mm diameter) were placed on bony landmarks according to the Vicon Plug-in Gait lower-body model. During treadmill (TM) walking pressure sensors underneath the TM belt recorded the force distribution of the footsoles at 120 Hz (Zebris FDM-T, zebris Medical GmbH, Isny im Allgäu, D). Kinematic data was recorded and post-processed using the Vicon Nexus Software (1.7.1). Trajectories were smoothed and gaps interpolated using Woltring's cross-validatory quintic-spline routine with a mean squared error (MSE) of 10 mm^2. Continuous data from ~20 consecutive gait cycles was cut into individual gait cycles and time-normalized using linear interpolation. Data from the pressure sensors underneath the TM belt was recorded by the same PC using the Zebris WinFDM-T software (02.01.01). Recordings were synchronized via a ±5V trigger signal.

Protocol

Subjects walked barefooted both overground (OG) and on a TM, where walking speed could be controlled and varied. iSCI subjects were allowed to use assistive devices for OG walking or to hold handrails when walking on the TM. Subjects were first asked to walk OG to assess their preferred walking speed. On the TM, iSCI subjects were then asked to walk at a slow speed (0.5 km/h ≈ 0.14 m/s) and at preferred OG walking speed.

Outcome variables

~20 gait cycles were analyzed per walking speed. The hip and knee angles were time-normalized to one gait cycle (500 samples) using linear interpolation. The intralimb coordination was illustrated by hip-knee cyclograms whose vertical and horizontal expansion corresponded to the maximal hip- and knee range of motion (ROM [°]) during walking, respectively. The within-subject cycle-to-cycle consistency of these cyclograms was quantified using the angular component of coefficient of correspondence (ACC) (Field-Fote and Tepavac 2002). Inter-subject (within-group) variability of the cyclogram was assessed after translation of the centroids of cyclograms to the origin. The inter-subject variability was calculated as the cumulative ellipse area with half axes (a and b, see equation (1)) corresponding to the between-subject standard deviation of hip- and knee angles, respectively, for 20 equal bins of time-normalized cyclograms:

$$\mathrm{Var}_n = \sum_{i=1}^{20} \Pi * a_{n,i} b_{n,i} \qquad (1)$$

Index n refers to subject number, i describes the bin number. The shape difference between two cyclograms was quantified as the square root of the sum of squared distances (SSD) after uniform scaling and translation of the cyclogram centroids to the origin:

$$SSD_{j,k} = \sqrt{\sum_i \left(\alpha_{j,i} - \alpha_{k,i}\right)^2 + \left(\beta_{j,i} - \beta_{k,i}\right)^2} \quad (2)$$

Equation (2) compares cyclogram j to cyclogram k where α and β correspond to the scaled and transformed hip- and knee angles, respectively, at sample point i. Within-group SSD was calculated as the average SSD of every pairing of subjects within a group (mean of n*(n-1)/2 SSDs). The between group SSD was calculated by comparing the mean cyclograms of two groups. Data analysis was performed using custom-written Matlab scripts (Matlab R2013a; The MathWorks Inc., Natick, MA, USA). A categorization based on the presence or absence of specific characteristics of the cyclogram shape was performed with the goal of stratifying patients into different groups of impairment. Within each group, iSCI subjects were additionally ranked according to the severity of alterations, resulting in a continuous ranking of iSCI subjects based on their cyclogram (lower ranking meaning worse cyclogram).

Statistical analysis

Normality of data distribution was tested using histograms and QQ plots. Non-normally distributed ACC values were compared using the non-parametric Kruskal-Wallis test and, if revealing significance, the following post-hoc tests were applied: independent data was tested using a Mann-Whitney U test and a Wilcoxon signed rank test was employed for paired data samples. The significance level was corrected for using Bonferroni correction resulting in an α-value of 0.05/4 = 0.0125. In order to assess the relation between the qualitative cyclogram ranking and objective measures (i.e. walking speed, hip- and knee ROM) non-parametric Spearman correlation coefficient ρ (rho) was calculated. Matlab R2013a was used for all statistical analyses.

1.4 Results

iSCI subjects exhibited a mean preferred walking speed of 0.57 ± 0.32 m/s while control subjects preferably walked at 1.16 ± 0.15 m/s.

Table 1.1 - Descriptive data of patients

ID	Age [years]	Sex	Cause of SCI	Level of SCI	Disease progress	LEMS	Assistive device
01	73	m	Traumatic	C5	chronic	24.5	wheeler
02	24	m	Traumatic	C3	chronic	24.5	-
08	60	f	Spinal ischemia	T5	122 d	23.0	wheeler
09	48	f	Traumatic	T7	chronic	15.0	one stick
10	39	f	Spinal myelitis	C, T	46 d	19.0	wheeler
12	65	m	Hematoma	C6	chronic	24.0	-
13	23	m	Traumatic	C7	1 year	9.5	wheeler
15	78	m	Diverse	C3/4	50 d	22.5	wheeler
16	60	m	Spinal canal stenosis	T9/10	76 d	25.0	-
17	55	m	Cervical myelopathy	C5	chronic	19.5	-
18	63	f	Epidural abscess	T4	chronic	23.0	crutches
19	43	m	Traumatic	C2	chronic	24.0	two sticks
20	61	m	Disc prolapse	C2	chronic	25.0	-
21	40	m	Traumatic	C5	chronic	22.5	-
22	64	m	Spondylitis, abscess	T4	chronic	23.5	-
23	32	m	Traumatic	T11	75 d	8.0	crutches
24	36	m	Traumatic	L4/5	78 d	23.5	-
25	41	m	Traumatic	C7	1 year	24.0	-
26	48	f	Disc prolapse	T10	15 d	24.0	two sticks

LEMS = mean value of left and right lower extremity motor score (max = 25).

Patient categorization

The cyclograms of healthy control subjects at preferred speed exhibited typical characteristics that could be found in all subjects. These features are listed in the box on the left of **Figure 1.1A**.

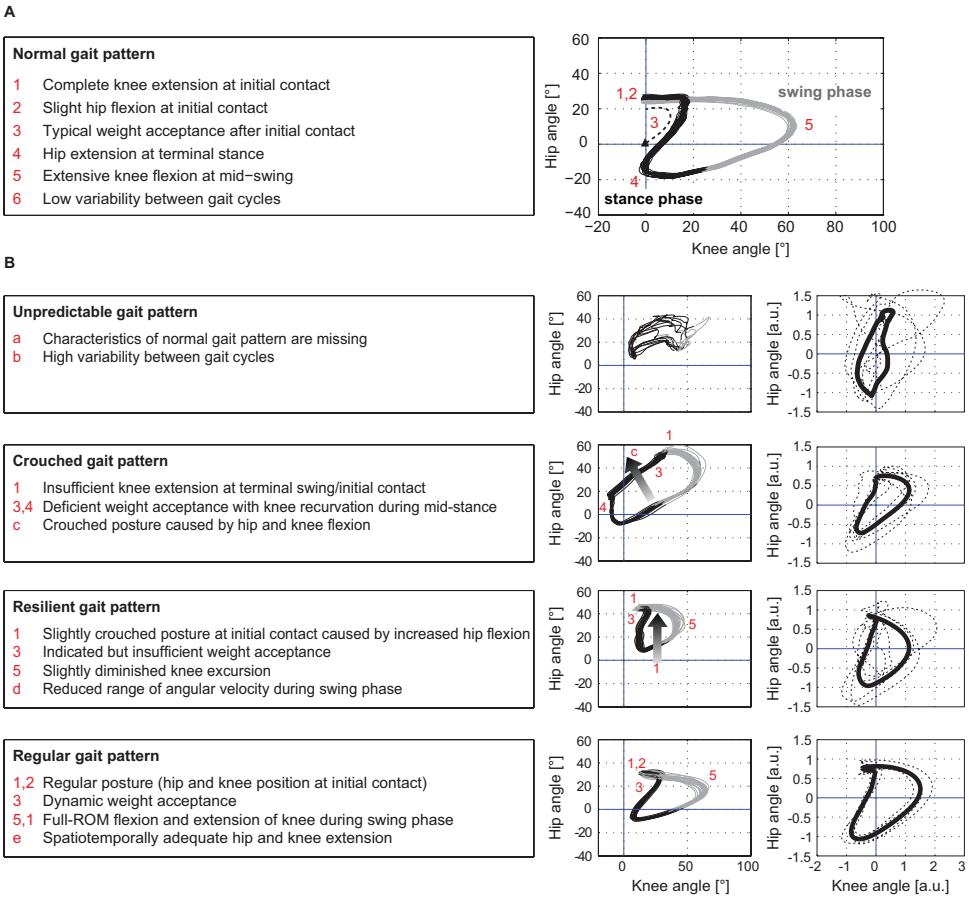

Figure 1.1 Hip-knee cyclograms of healthy controls and iSCI subjects. The hip-knee cyclogram of a healthy control subject with its typical characteristics is depicted in panel (**A**). iSCI subjects were classified into four groups of impairment, group 1 (unpredictable gait pattern) being the most affected group while group 4 (regular gait pattern) showed normal cyclograms (**B**). The criteria for each group are listed in the boxes on the left. The cyclograms in the left column show one representative example per group, the right column depicts the individual cyclograms of each iSCI subject within a group (dashed lines) and the group mean cyclogram (solid bold line) after translation of the cyclogram's centroid to origin (zero) and uniform scaling.

iSCI subjects showed one or more alterations of certain properties of the cyclogram and depending on the degree of deviation were classified into four groups of impairment (**Figure 1.1B**). The specific alterations of cyclogram characteristics are described in the boxes on the left. Accordingly, four iSCI subjects ended up in group 1 (unpredictable gait pattern), six iSCI subjects qualified for group 2 (crouched gait pattern), five iSCI subjects were classified into group 3 (resilient gait pattern), and finally four iSCI subjects exhibited a regular gait pattern (group 4). Correlation analysis between the cyclogram ranking and

preferred OG speed, hip ROM and knee ROM revealed a high correlation between preferred speed and cyclogram ranking (Spearman's ρ = 0.751; **Figure 1.2B**) while both hip- and knee ROM were relatively indifferent to the quality of the cyclogram (Spearman's ρ = 0.267 and 0.330, respectively; **Figure 1.2C**).

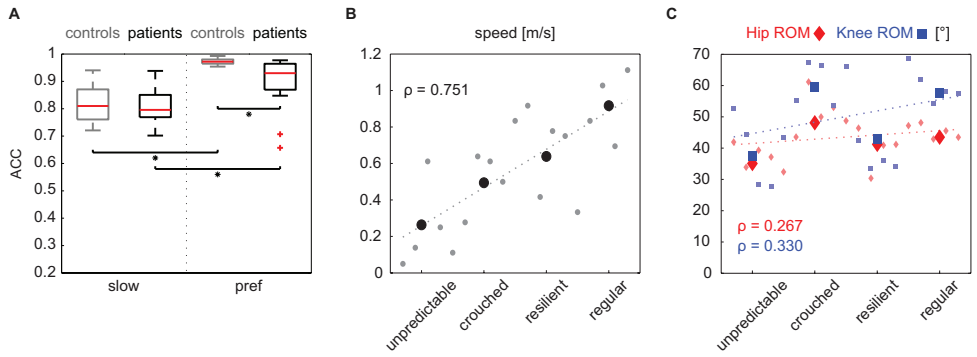

Figure 1.2 (**A**) The cycle-to-cycle shape consistency within a subject is quantified as the angular component of coefficient of correspondence (ACC). This value can attain values between 0 (no congruency between cycles) and 1 (complete shape congruency from cycle to cycle). Both groups increased their cyclogram consistency when changing from a slow to preferred walking speed. iSCI subjects only showed lower values at preferred walking speed. Statistical significance ($p < 0.0125$) is indicated by an asterisk. Panel (**B**) shows the correlation indicated by Spearman's rho of the cyclogram ranking to preferred OG walking speed and to hip- and knee ROMs (**C**). Little dots represent single values of individual subjects while the larger symbols represent the mean value per group.

Intralimb coordination

The Kruskal-Wallis test revealed significant group differences in non-normally distributed ACC (Chi-square: 59.59, $p < 0.001$). At the slow walking speed (0.5 km/h) the cyclograms of healthy subjects were similarly distorted and irregular as iSCI subjects' cyclograms (**Figure 1.3A**). In line with this, the post-hoc test revealed that the ACC did not differ between the two groups at the slow speed (Mann-Whitney U test: $p = 0.840$; **Figure 1.2A**). In contrast, control subjects normalized their cyclogram configuration to a very uniform shape between subjects when walking at preferred speed (**Figure 1.3A**). Likewise, the ACC was higher at preferred speed compared to the slow speed (Wilcoxon signed rank test: $p < 0.001$). iSCI subjects were also able to increase their ACC from slow to preferred speed (Wilcoxon signed rank test: $p = 0.005$), but their value was still significantly lower compared to healthy subjects (Mann-Whitney U

test: $p < 0.001$). In contrast to control subjects, iSCI subjects' cyclograms did not converge towards normal and were still very heteromorphic. The within-group cyclogram variability during a gait cycle was similar in healthy control subjects and in iSCI subjects at the slow walking speed (**Figure 1.3B**). The cumulative variability for 20 equal time bins was 3238.6 mm^2 in controls and 3149.9 mm^2 among iSCI subjects. However, at preferred walking speed, control subjects showed a remarkably lower variability than iSCI subjects. The cumulative variability at preferred speed for 20 time bins among control subjects was 650.9 mm^2 while it was even higher at preferred speed compared to the slow speed in iSCI subjects (4152.0 mm^2).

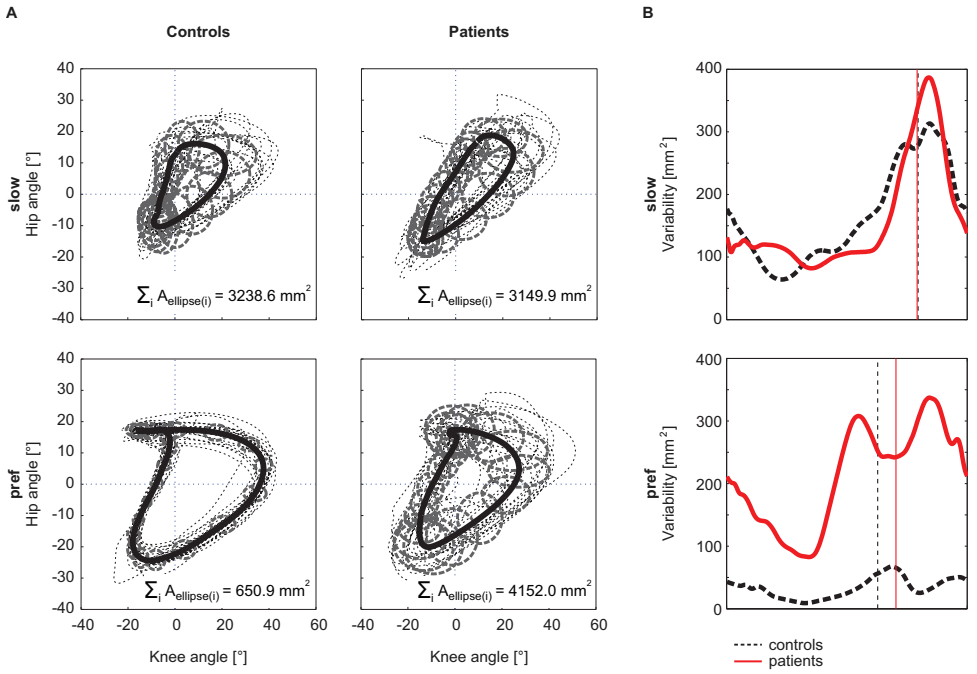

Figure 1.3 Within-group cyclogram variability. The variability of the cyclogram between subjects within a group was quantified by the cumulated elliptic area for 20 bins per gait cycle (**A**). The half axes of the ellipse correspond to the between-subject standard deviation of the hip- and knee angles, respectively. (**B**) shows the course of the variability at every time point of a gait cycle. The control group is represented by a black dashed line, iSCI group is depicted in red. The vertical lines mark the time point of toe-off.

The SSD, representing the amount of shape difference after uniform scaling and translation (**Table 1.2**), was smaller within the healthy control group (SSD = 6.44) compared to iSCI subjects (SSD = 32.96) at preferred speed, but showed no difference at the slow speed (healthy: SSD = 14.00, iSCI: SSD = 11.74;

Figure 1.4). The between-group shape difference was identical at the slow speed (SSD = 6.49) as at preferred speed (SSD = 6.46). Table 1.2 also shows the values of cyclogram shape comparison between each of the four groups of iSCI subjects compared to the control group. At preferred speed, the difference to normal shape according to the SSD coincided with the qualitative categorization of the cyclogram configuration.

Table 1.2 - Cyclogram shape difference.

Group comparison	SSD	
	slow	preferred
Within control group	14.00	6.44
Within iSCI group	11.74	32.96
Between controls and iSCI subjects	6.49	6.46
Between group 1 and controls	9.02	13.64
Between group 2 and controls	7.20	8.86
Between group 3 and controls	9.77	5.46
Between group 4 and controls	4.22	2.73

SSD = square root of sum of squared distances. The within-group SSD was calculated by comparing the cyclograms of subjects each by each and then calculating the mean value. The beween-groups SSD was calculated by comparing the mean cyclogram per group.

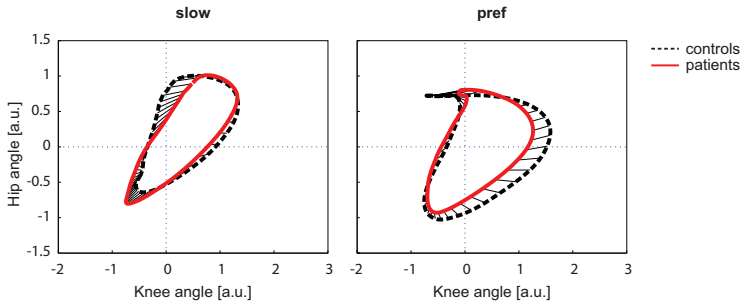

Figure 1.4. The square root of the sum of squared distances (SSD) calculated the difference in shape of two figures. The cyclograms are shown after translation of the centroid to origin (zero) and uniform scaling. The control group is represented by a black dashed line, iSCI group is depicted in red. The straight black lines indicate the deviation of the two figures. a.u. = arbitrary units.

1.5 Discussion

The kinematic analysis of walking pattern in human iSCI allows for categorization of lower-limb control during walking while these qualitative readouts of gait performance are complementary to measures of walking distance and speed. While the latter measures are able to quantify the capacity of walking the qualitative scoring provides additional information regarding intralimb motor control. The consideration of these combined outcomes will be meaningful to better target treatment interventions and improve the stratification of most suitable patients for clinical trials.

Modulation of intralimb coordination

Visual inspection and quantitative analysis of the cyclograms at a slow walking speed (i.e. 0.5 km/h) revealed that healthy control subjects exhibited similarly variable intralimb coordination as iSCI subjects. Speed increments in the two groups to preferred walking speed, however, induced distinct adaptations in cyclogram configuration. While effectively all control subjects gained a very regular and inter-subjectively uniform cyclogram at their preferred walking speed, iSCI subjects maintained considerable shape variability between subjects and their cyclograms remained different from the typical shape found in healthy subjects. The visually observed lack of cyclogram modulation in iSCI subjects was also made evident by the quantification of shape differences represented by the SSD. According to this value, the inter-subject shape difference within the iSCI group was bigger at preferred speed compared to the slow speed. The lack of shape assimilation is contrary to healthy subjects and might suggest that patients' impairments become more pronounced when walking at preferred speed. In iSCI subjects with most severe shape deformations (group 1 with the highest cyclogram impairments and the lowest walking speed) the increase in speed even induced an increase in shape deformity. This increase in shape deformity did not occur randomly as the reproducibility of this aberrant shape (i.e. ACC) increased at preferred walking speed, indicating that iSCI subjects have learned and consolidated an aberrant walking pattern in a rather abnormal manner.

Neural mechanisms

The lack of cyclogram modulation when increasing slow walking speed to preferred speed, at which locomotion is supposed to be more economic (Cotes and Meade 1960) may be associated with a limited access to supraspinal control. We deliberately refer to the term "supraspinal", including corticospinal as well as other descending motor tracts (e.g. rubrospinal or reticulospinal). Several aspects of locomotion, e.g. reciprocal activation of lower-limb muscles, appear to be primarily controlled at a spinal level and depend less on supraspinal efforts as revealed in preclinical studies in animals (Barbeau and Rossignol 1987, Duysens and Van de Crommert 1998). In humans, however, the correct spatiotemporal coordination of the lower-limb muscles and joints during locomotion (complex postural control and segmental interplay) seems to be more dependent on intact and sufficient supraspinal control (Kuhn 1950). Interestingly, in the present study, an individual iSCI subject was not able to normalize his or her cyclogram when increasing the walking speed from slow to preferred speed despite increasing supraspinal neural drive (Bachmann et al. 2013). However, those iSCI subjects with a higher preferred OG walking speed, probably reflecting greater access to supraspinal speed-driving centers, showed a closer-to-normal cyclogram. The distinct input on walking control can also be found in Parkinson's subjects, where the relation between step length and cadence with changes in speed is distorted (contrary to iSCI (Pepin et al. 2003)) while the hip-knee cyclogram retains a normal but small scaled shape (Morris et al. 1998, Morris et al. 2005). The distortion of cyclograms in iSCI subjects may not only originate from motor deficits, but may also be a consequence of impaired sensory feedback. Motor behavior is known to be affected in disorders associated with severe sensory impairment (Courtemanche et al. 1996, Manor and Li 2009). Studies with deafferented subjects particularly revealed that the interjoint coordination was distorted while performing an upper-limb task (Sainburg et al. 1993). Even though skilled upper-limb movements depend more strongly on voluntary control compared to lower-limb movements (MacLellan et al. 2013, Nakajima et al. 2000), a deterioration of peripheral sensory feedback is sufficient to disrupt complex interjoint limb movements (Sainburg et al. 1993).

Implications for treatment and clinical trials

The most widely used categorization scheme for spinal cord injury is the American Spinal Injury Association (ASIA) Impairment Scale (AIS). This scale is of rather low resolution and does not well distinguish patients upon walking abilities. In the present iSCI-subject sample the majority was classified as AIS D but ranged from AIS C/D to even AIS A (a subject with lesion level below T11). The categorization of iSCI subjects based on the cyclogram can complement the ASIA assessments and may serve several goals. From a therapist's point of view treatment interventions aiming at improving locomotion may become better tailored to the patients' walking impairment. Depending on the aim of training studies (e.g. improvement of quantitative measures and/or gait quality) different outcome measures should be chosen. Interventional studies may reveal that walking speed is improved while the gait quality remains impaired, or vice versa. Clinical trials investigating novel interventions (e.g. effect of drugs or cell transplantation) may have harmful or desired beneficial effects. By deploying the most sensitive assessment battery, differential effects may be discerned and mechanisms of action may be recognized.

Limitations

A sample size of 19 iSCI subjects is too low to be able to state whether the categorization based on the cyclogram quality is sufficient to stratify every iSCI subject. The categorization should be tested in a larger cohort, from which one could retrieve further quantitative measures that may serve as threshold values for future guidelines.

1.6 Conclusion

In clinical routines walking ability is captured by walking speed and distance covered, but the quality of walking is frequently ignored or reported according to subjective rater evaluation. Yet, the present study shows that the intralimb coordination represented by the hip-knee cyclogram reveals reliable and sensitive information on walking capacity after iSCI and may be used to stratify patients prior to clinical trial inclusion. Further, the cyclogram with its quantifiable parameters may provide additional insights into gait control across different neuromotor disorders beyond those assessed by time-distance measures.

Study 2

Domains of neural control of walking in human spinal cord injury

Lea Awai, Marc Bolliger, Adam R. Ferguson, Grégoire Courtine, Armin Curt

Neurology (submitted)

»»I would like to thank Barbara Huber, Werner Popp and Lorenzo Tanadini, who helped me with different aspects of this study. ««

2.1 Abstract

Measures of walking function based on time-distance parameters, although clinically meaningful for determining ambulatory capacity, provide limited information on changes in neural control after injury. In incomplete spinal cord injury (iSCI) disentangling different domains of neural control of walking may contribute to better target therapeutic interventions.

A comprehensive analysis of time-distance and kinematic parameters over a range of walking speeds combined with clinical measures was performed in 22 iSCI patients and 21 healthy controls.

Principal component analysis (PCA) applied on the multivariate set of gait data revealed that the largest variance was determined by parameters of walking speed, spinal cord integrity and intralimb coordination (PC1 47%), while gait-cycle parameters (PC2 22%) and ranges of hip/knee angles (PC3 8%) explained distinct dimensions of outcome. Although iSCI patients showed severe limitations in walking speed (~50% of controls) and altered intralimb coordination, they remained capable to modulate step length and timing of gait cycle according to the regained walking speeds. In contrast, active hip- and knee angle modulation was distinctly different from controls and inappropriately modulated with changes in walking speeds.

In iSCI distinct clusters of interrelated gait parameters can be discerned that may reflect distinct domains of neural control of walking. Data-driven analysis of kinematics may advance the evaluation of therapeutic interventions and accelerate the identification of targeted interventions to improve walking outcomes in iSCI.

2.2 Introduction

More than half of spinal cord injured patients exhibit incomplete injuries leading to varying degrees of functional impairment of the affected limbs (Wyndaele and Wyndaele 2006). The provision of patient-customized interventions (Mirnezami et al. 2012) for incomplete spinal cord injury (iSCI) is limited by the rather crude clinical tools currently used for assessing locomotion (e.g. motor scores, speed, distance). Detailed analysis of locomotion in iSCI patients serves two important aims. Firstly, the ability to score locomotor function allows the determination of changes in walking capacity and measure the effect of therapeutic interventions (Field-Fote 2001, Lucareli et al. 2011, Petersen et al. 2012, Thompson et al. 2013). Secondly, comprehensive assessment of walking beyond measures of capacity may provide insights into mechanisms underlying changes of neural control (Courtine et al. 2008, Rosenzweig et al. 2010).

The majority of studies on gait recovery after iSCI focus on quantitative measures of time and distance (10-meter walk test, 6-minute walk test), functional scores (e.g. walking index for spinal cord injury (WISCI) and the mobility sub-score of the spinal cord independence measure (SCIM III) (Ditunno et al. 2006, Furlan et al. 2011, van Hedel et al. 2006)) or a subjective rating of gait quality (Field-Fote et al. 2001). These investigations mainly assessed the temporal profiles of ambulatory capacity (Lorenz et al. 2012) and the impact of rehabilitation interventions on recovery (Dobkin et al. 2006, Lucareli et al. 2011). Few studies have used more detailed kinematic methodologies (e.g. quality of walking) to uncover alterations of iSCI walking (Gil-Agudo et al. 2011, Ivanenko et al. 2009, Nooijen et al. 2009, Pepin et al. 2003). The objective of the present study was to establish a comprehensive assessment framework in iSCI applying multivariate data analysis of motor function to i) reveal methods for distinguishing between changes in capacity and quality of walking, and ii) provide a novel approach for disentangling different domains of locomotor control in human SCI.

2.3 Materials and methods

Subjects

Inclusion criteria: iSCI patients aged 18 years and older, who were at least able to stand and walk without the assistance of another person. *Exclusion criteria*: Patients suffering from any other neurological disorder or pre-existing gait impairment were excluded. The study was approved by the Zurich Cantonal ethics committee. Participants provided written informed consent.

Experimental setup

Subjects walked barefooted overground along a straight 8 m walkway and on a treadmill at different walking speeds. Patients were allowed to use an assistive device for overground walking if needed and were allowed to hold handrails on the treadmill. Subjects first walked overground to assess their preferred walking speed. This value was used to subsequently determine the relative walking speeds on the treadmill: 50% (minimal), 100% (preferred), and 150% (maximal) of preferred speed. Additionally, the subjects walked at predefined treadmill speeds, starting at slow = 0.5 km/h, which was raised in increments of 0.5 km/h until the individual maximal walking speed (150% of preferred speed) was reached. If a patient could not reach this speed, the maximal walking speed they were able to walk was recorded instead.

For lower body kinematics, 8 infrared cameras (T10, Vicon motion systems Ltd., Oxford, UK) at 200 Hz and two synchronized digital high-speed video cameras (pilot series, Basler AG, Ahrensburg, D) at 100 Hz were used. Pressure sensors underneath the treadmill belt (Zebris FDM-T, zebris Medical GmbH, Isny im Allgäu, D) recorded force distributions at 120 Hz. 16 reflective markers (16 mm diameter) were placed on bony landmarks according to the Vicon Plug-in Gait lower-body model.

Outcome measures

Time-distance parameters

The following time-distance parameters were determined: preferred overground walking speed (preferred speed) [km/h], step length [cm], cadence [strides/min], stance phase [%], and single support phase [%] during treadmill walking. Initial foot contact defined gait cycle onset. One gait cycle ranged from initial contact of one foot to the subsequent initial contact of the same foot. Time-distance parameters were calculated by the Zebris WinFDM-T software.

Kinematic data

Kinematic data were processed offline using the Vicon Nexus Software and custom-written Matlab scripts (Matlab R2010b/R2013a, Mathworks Inc., Massachusetts, USA). Trajectories were smoothed and gaps interpolated using Woltring's cross-validatory quintic-spline routine with a mean squared error (MSE) of 10 mm^2. Continuous data from ~20 consecutive gait cycles was cut into individual gait cycles and time-normalized using linear interpolation. The maximal range of motion (ROM) of the hip- and knee angle, averaged over all gait cycles, and the resultant velocity vector (angular change per unit time) of these two angles at toe-off (angular velocity at toe-off (AngVel)) were calculated. To assess whether AngVel limits walking speed in patients, their data was compared to AngVel of controls at patients' maximal speed by interpolating data of the control group using a 3^{rd} degree polynomial least squares fit. Variable Δ values reflect the difference between minimal speed and preferred speed, providing a measure of how well subjects can modulate different features of gait with a doubling of walking speed (i.e. from 50% to 100% of preferred speed). To evaluate intralimb multi-segment coordination, combined hip-knee angle-angle plots, called cyclograms, were studied. The angular component of coefficient of correspondence (ACC) (Field-Fote and Tepavac 2002) was calculated to quantify the cycle-to-cycle cyclogram shape consistency. Patients were categorized into four groups of impairment based on specific features of the hip-knee cyclogram, as reported previously (Awai and Curt 2014). As a quantifiable measure of the cyclogram quality, the shape difference of patients' cyclograms was compared to a norm

cyclogram. The shape difference was calculated by the sum of squared distances (SSD) between two cyclograms (Awai and Curt 2014):

$$SSD_{j,k} = \sqrt{\sum_i \left(\alpha_{j,i} - \alpha_{k,i}\right)^2 + \left(\beta_{j,i} - \beta_{k,i}\right)^2}$$

where cyclogram *j* is compared to cyclogram *k* after uniform scaling and translation of the centroid to the origin while α and β represent hip and knee angles, respectively.

Clinical data

Lower-limb voluntary control was measured by trained examiners using the American Spinal Injury Association (ASIA) lower extremity motor score (LEMS). We evaluated the mean value of both legs (max. 25). Central motor and sensory pathway integrity was assessed by motor evoked potentials (MEPs) of the tibialis anterior and abductor hallucis muscles and somatosensory evoked potentials (SSEPs) were elicited from the tibialis posterior nerve. MEPs were elicited by transcranial magnetic stimulation of respective motor cortex areas via a figure-of-eight coil connected to a magnetic stimulator (The Magstim Company Ltd., Wales, UK). The evoked potentials were evaluated by taking into account both response latency and amplitude as reported previously (Curt and Dietz 1996), resulting in a 5-point impairment scale.

Statistical analysis

Statistical analyses were performed using SPSS Statistics 19 (IBM Corp., New York, USA) and Matlab.

Principal component analysis

A categorical principal component analysis (PCA) was performed including the entire set of data of all control and iSCI subjects in order to discern clusters of interrelated parameters of walking leveraging the extensive ensemble of gait-related variables (Pearson 1901). We retained the PCs according to the Scree plot (Cattell 1966) and PC overdetermination (at least 2 |factor loadings| ≥ 0.7). Variables with high

loadings on the same PC indicate a strong interrelationship. In the context of kinematic outcomes, PCs have been interpreted to reflect neurobiological "motor primitives" or discretely-organized "motor modules" of complex movements (Ivanenko et al. 2007). To examine the validity and robustness of the PC clusters, we used a bootstrapping procedure with 10'000 iterations on a random subset of 80% of subjects and cross validated the factor loadings considering Pearson's r, root mean square (RMS), coefficient of congruence (CC) and Cattell's S.

Pairwise comparisons

Spearman's rank correlation coefficient ρ (rho) was used to correlate a pair of single outcome measures. The comparison of two groups was performed by a two-tailed t-test for normally distributed data, and a Mann-Whitney U test or Wilcoxon signed-rank test for non-normally distributed independent or dependent samples, as appropriate. Bonferroni correction was applied (α/n).

2.4 Results

Subjects

Table 2.1 - Descriptive data of patients

ID	Age [years]	sex	Cause of SCI	Level of SCI	LEMS	Assistive device
01	73	m	Traumatic	C5	24.5	wheeler
02	24	m	Traumatic	C3	24.5	-
03	36	f	Disc prolapse	T7/8	16.0	crutches
04	47	f	Spinal ischemia	T9/10	24.0	-
05	30	m	Traumatic	L2	22.5	-
08	60	f	Spinal ischemia	T5	23.0	wheeler
09	48	f	Traumatic	T7	15.0	one stick
10	39	f	Spinal myelitis	C, T	19.0	wheeler
12	65	m	Hematoma	C6	24.0	-
13	23	m	Traumatic	C7	9.5	wheeler
15	78	m	Diverse	C3/4	22.5	wheeler
16	60	m	Spinal canal stenosis	T9/10	25.0	-
17	55	m	Cervical myelopathy	C5	19.5	-
18	63	f	Epidural abscess	T4	23.0	crutches
19	43	m	Traumatic	C2	24.0	two sticks
20	61	m	Disc prolapse	C2	25.0	-
21	40	m	Traumatic	C5	22.5	-
22	64	m	Spondylitis, abscess	T4	23.5	-
23	32	m	Traumatic	T11	8.0	crutches
24	36	m	Traumatic	L4/5	23.5	-
25	41	m	Traumatic	C7	24.0	-
26	48	f	Disc prolapse	T10	24.0	two sticks

LEMS = mean value of left and right lower extremity motor score (max = 25).

A total of 22 iSCI patients (15 males, 7 females; 48.3 ± 15.6 years, weight: 74.6 ± 13.4 kg, height: 171.6 ± 8.4 cm) and 21 healthy controls (8 males, 13 females; 38.4 ± 14.3 years, weight: 66.7 ± 12.1 kg, height: 172.2 ± 8.2 cm) participated in this study (**Table 2.1**).

Multivariate analysis

To reveal specific clusters of interrelated parameters within the multivariate set of data a PCA was applied on the 24 variables. Three patients were excluded from the analysis because of missing values. Plotting the transformed variables in the three-dimensional space made up by PCs 1-3 (**Figure 2.1A**) showed a close aggregation of control subjects and the wide dispersion of patients' data. The analysis uncovered 3 robustly reproducible PCs ($r \geq 0.98$, $RMS \leq 0.01$, $CC \geq 0.97$, Cattell's $S \geq 0.5$) that accounted for 76.7% of total variance in outcome, the first PC (PC1) alone accounting for almost 50% of the variance (**Figure 2.1B**). Examination of the constellation of variables with high factor loadings suggested that the emerging PCs reflected distinct domains of locomotor control. Variables with high loadings on PC1 were related to walking dynamics (walking speed, angular velocity), spinal cord integrity (i.e. MEP/SSEP) and intralimb coordination, while PC2 assembled step length and variables associated with the timing of gait cycle (reciprocal bilateral coordination of gait cycle phases). The third PC was predominantly characterized by measures of the hip- and knee angles.

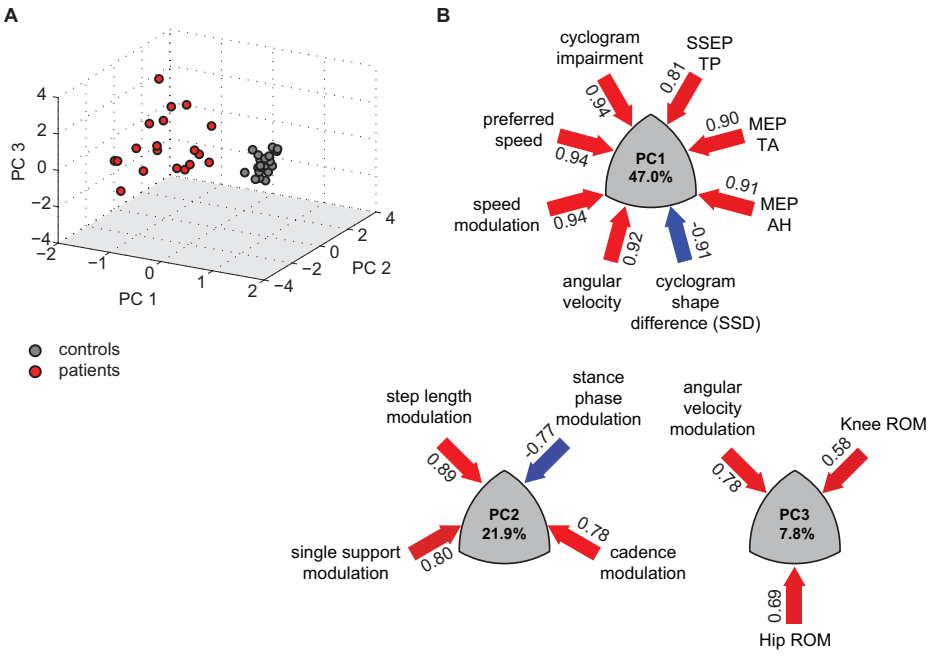

Figure 2.1 Multivariate analysis of gait-related parameters. Transformed data using principal component analysis (PCA) is plotted in the 3D space with PCs 1-3 as axes (**A**). In the present data set, PCs 1-3 explain 77% of the total variance. PCs show clustered

variance of multiple gait parameters with high loadings on the corresponding PC. Factor loadings are depicted in numbers next to the arrows whose color reflect magnitude and relationship of loading (positive relationship = red, negative = blue) (**B**). Parameter modulation (e.g. step length modulation) refers to the difference of the parameter (Δ value) between preferred and minimal walking speed (50% of preferred speed). PC = principal component, TA = tibialis anterior, TP = tibialis posterior, AH = abductor hallucis, MEP = motor evoked potential, SSEP = somatosensory evoked potential, ROM = range of motion.

Time-distance parameters

Patients showed a significant reduction in preferred walking speed (-50%) and a limited ability to increase speed (**Figure 2.2A**). While all controls could increase the walking speed to 150% (6.18 ± 0.79 km/h) 12 of 19 patients showed a restricted ability to increase their walking speed beyond preferred speed (2.85 ± 1.55 km/h). Even among the best walkers (preferred speed ≥ 3km/h) 3 of 5 patients could not attain velocities of 150% of preferred speed. Yet, within the range of achieved walking speeds no significant differences between controls and patients in the modulation of step length, cadence, single-support and stance phase were found (**Figures 2.2C** through **F**).

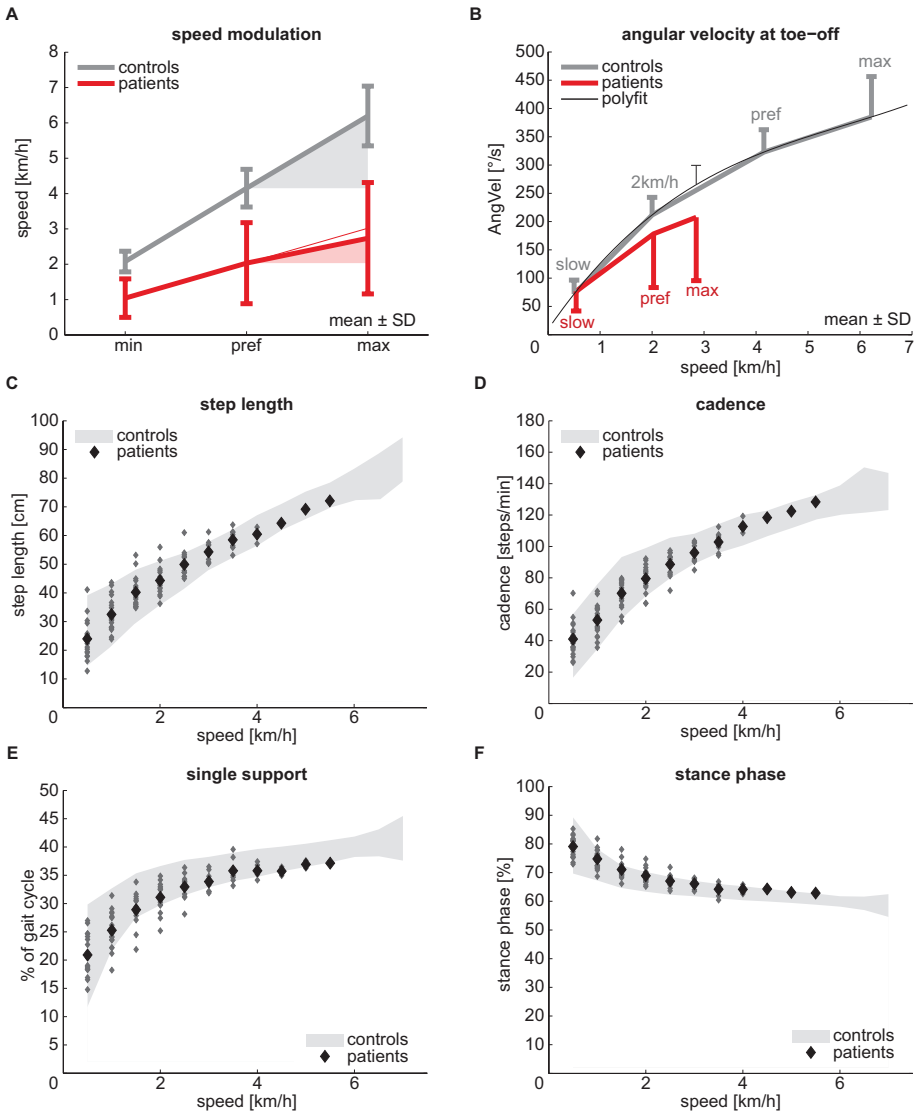

Figure 2.2 Speed modulation of time-distance parameters and angular velocity. (**A**) Absolute speed and speed modulation is limited in iSCI patients. While patients were able to comfortably reduce their preferred walking speeds (pref speed; 2.03 ± 1.15 km/h) to a minimal speed (min, 50% of preferred speed) they were limited in increasing their walking speed to 150% of their preferred speed (max); theoretical linear increase is indicated by the thin red line. Error bars indicate ± 1SD. (**B**) The diagram illustrates the modulation of the hip-knee angular velocity at toe-off. A 3rd degree polynomial fit (thin black line) was used to interpolate control subjects' data to obtain their angular velocity at patients' maximal speed. Error bars indicate 1SD. (**C** through **F**) Graphs illustrating the speed modulation of step length, cadence, single support and stance phase of control subjects (shaded gray area, ± 2SD interval) and patients (large dots = group mean values, small dots = individual patient's data) at different walking speeds ranging from 0.5 km/h to 7.0 km/h in the control group, and from 0.5 km/h to 5.5 km/h in the patient group. Within this speed range, the two groups did not differ. SD = standard deviation, AngVel = angular velocity at toe-off.

Kinematic data

The gait pattern of healthy controls and iSCI patients was studied both qualitatively and quantitatively considering specific characteristics of lower-limb coordination.

Gait pattern features were analyzed at 2 different walking speeds: slow (n = 21 at 0.5 km/h for controls; n = 19 at 0.5 km/h and n = 3 at 1.0 km/ for patients) and preferred speed (n = 19 for controls, n = 21 for patients). Patients at their preferred speed (mean 2.0 km/h) were also compared to controls at 2.0 km/h (n = 19).

Qualitative aspects of gait pattern

During walking, the hip-knee cyclogram exhibits a characteristic shape, which reflects gait-cycle dependent intralimb coordination. In comparison to healthy controls iSCI patients were unable to normalize their cyclogram at preferred speed compared to slow speed (**Figure 2.3A**). The cyclogram shape difference to normal, quantified by the SSD, confirms that control subjects converge towards a standard cyclogram shape when walking at preferred speed while patients show significantly less convergence (t-test: $p < 0.001$). Categorizing patients based on their cyclogram impairment resulted in five patients who were assigned to the group with the greatest impairment termed *unpredictable gait pattern*. Seven patients showed a *crouched gait pattern*. Five patients exhibited a *resilient gait pattern* and five patients qualified for having a *regular gait pattern*.

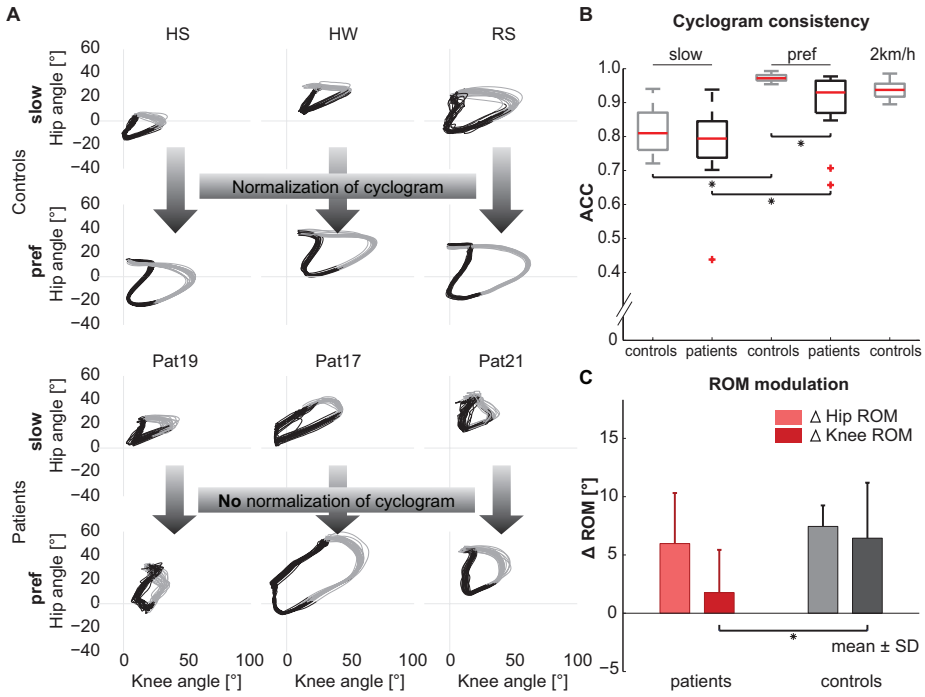

Figure 2.3 Speed modulation of kinematic measures. (**A**) Hip-knee cyclograms of control subjects (top 2 rows) and patients (bottom 2 rows) both at slow and at preferred (pref) walking speed. The cyclograms of 20 gait cycles are plotted, black color indicating stance phase, grey color indicating swing phase. At a fixed slow speed 29% of patients and 42% of controls expressed some degree of weight acceptance. At preferred speed 63% of patients showed some weight acceptance while 100% of controls did. (**B**) Distribution of the ACCs for both control subjects and patients at slow and preferred speed, respectively, and at 2km/h for control subjects. Panel (**C**) shows the amount of ROM increase (ΔROM) from minimal to preferred speed of hip and knee in patients and in control subjects. ACC = angular component of coefficient of correspondence (cyclogram consistency), ROM = range of motion, SD = standard deviation.

Modulatory capacity of speed

The median ACC of hip-knee cyclograms was indistinguishable between controls and patients at the slow and at a matched speed of ~2 km/h (**Figure 2.3B**) but was higher in controls than in patients at preferred speed (Mann-Whitney U test: $p = 0.394$, $p = 0.666$ and $p < 0.001$). The ACC was significantly higher at preferred speed compared to the slow speed in both groups (Wilcoxon signed rank test: $p < 0.001$).

Hip- and knee ROM were recorded at different speeds to reveal the modulatory capacity of joint control. At slow speed, the hip ROM of patients was larger than that of controls while the knee ROM did not differ between the two groups (t-test: $p = 0.005$ and $p = 0.961$). At preferred speed, hip ROM showed no

difference between groups, whereas knee ROM was larger in controls compared to patients (t-test: p= 0.317 and p = 0.001). At a comparable speed (2.0 km/h), patients differed from controls by showing a larger hip ROM (t-test: p < 0.001). Speed-dependent changes in hip ROM did not differ between patients and controls while the knee ΔROM was diminished in patients (t-test: p = 0.210 and p = 0.007; **Figure 2.3C**).

In controls, the increase of AngVel was significant both from slow to preferred and from preferred to maximal walking speed (paired t-test: p < 0.001 and p = 0.003; **Figure 2.2B**). In patients, the increase was only significant from slow to preferred speed, but not from preferred to maximal speed (paired t-test: p < 0.001 and p = 0.355). Comparing patients walking at their maximal speed (mean 2.85 km/h) to interpolated values at 2.85 km/h for controls revealed a difference between the groups (t-test: p = 0.026). However, no differences were found at the slow speed or at patients' preferred speed compared to controls at 2.0 km/h.

Spearman's ρ revealed a strong correlation between patients' preferred speed and measures related to the intralimb coordination (i.e. AngVel, cyclogram impairment and cyclogram shape difference) but no correlations to measures of spinal cord integrity, all of which load highly onto PC1 (**Figure 2.4A**). If LEMS and AngVel are respectively regarded as a static and dynamic measure of force exertion, correlation analysis reveals that dynamic force is more closely related to speed than a static measure. Hip- and knee ROMs are only weakly related to preferred speed (**Figures 2.4B**).

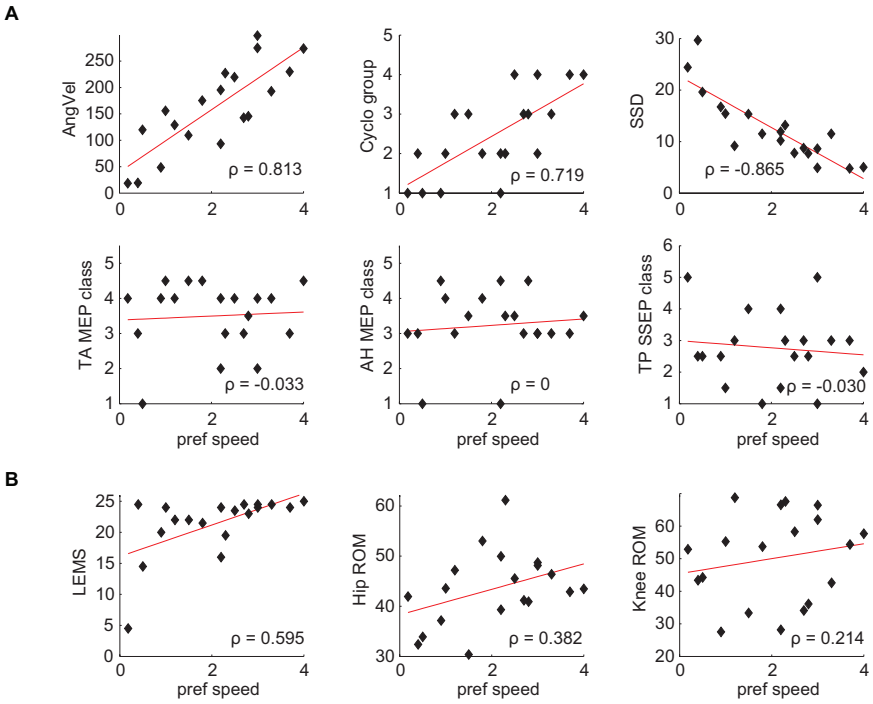

Figure 2.4 Pairwise comparisons. Patient data was analyzed with respect to preferred walking speed using Spearman's correlation coefficient. Panel (**A**) depicts the relation between preferred walking speed and parameters that showed high factor loadings on PC1. Cyclo group refers to the group of cyclogram impairment. The correlations between voluntary muscle force and ROMs (PC2) are illustrated in panel (**B**). Note that a linear fit was added to the graphs (red line) in order to illustrate trends even though Spearman's correlation analysis does not assume linearity of data. AngVel = angular velocity at toe-off, SSD = sum of squared distances (cyclogram shape difference), TA = tibialis anterior, TP = tibialis posterior, AH = abductor hallucis, MEP = motor evoked potential, SSEP = somatosensory evoked potential, LEMS = lower extremity motor score, ROM = range of motion.

2.5 Discussion

The present study applying a multivariate analysis approach allows disentangling the complexity of gait control in patients suffering from iSCI by providing distinguished clusters of outcome variables to describe gait. Through statistical data-integration across multiple outcome domains we achieved a more comprehensive view of changes in neural control of walking after iSCI (National Research Council (US)). Specific clusters were distinguishable within gait outcome that may be attributable to different domains of discretely-organized movement control and could be differently amendable by treatment interventions.

Characteristics of iSCI walking

PCA aggregated measures of walking speed, spinal cord integrity and features of the intralimb coordination onto PC1 that were therefore significantly involved in explaining data variance following SCI. Patients showed significant changes in their intralimb coordination (quantified by shape difference) and both their preferred and maximal walking speeds were severely reduced. However, patients remained able to reliably reduce their walking speed, which may even pose more challenges for balance control than walking at a preferred walking speed (Latt et al. 2008).

Factors with high loadings on PC2 comprised of those gait-cycle parameters (bilateral coordination of step cycles) that remained adequately modulated across a range of speeds in iSCI patients. This is in contrast to altered gait-cycle parameters observed in neurological disorders affecting supraspinal motor centers. In Parkinsonian patients, step length is greatly reduced (shuffling gait) while cadence can be increased to values that are even higher than in controls (Morris et al. 1998). Stroke patients typically show an asymmetric slow gait with decreased cadence (von Schroeder et al. 1995) and limited stride length (Nakamura et al. 1988).

PC3, explaining only little variance, assembled measures of active hip- and knee ROMs that showed rather low relation to walking performance while especially the knee ROM was most severely affected with impaired modulation across walking speeds.

Domains of neural control of iSCI walking

PCA revealed a clustered organization of gait parameters where PC1 explained the greatest variance in outcome and the high loadings of parameters related to the integrity of spinal pathways (MEP, SSEP) suggest that walking capacity is highly dependent on supraspinal input (cortical and subcortical) (Bachmann et al. 2013). However, spinal cord integrity was not immediately related to preferred speed as walking outcomes rather depend on complex interactions of supraspinal inputs that are fine-tuned by spinal networks receiving sensory feedback from the periphery to shape motor output. Spinal networks partially deprived of supraspinal input caused by SCI reorganize and functionally change over time (Beauparlant et al. 2013, Dietz 2010) where gait parameters are differently affected. PCs 1 and 2 are per definition orthogonal and therefore considered uncorrelated. Thus, features with high loadings on PC2, representing appropriate gait cycle modulation in iSCI while severely affected in stroke or Parkinson's patients, are influenced differently than PC1 factors. Therefore, PC1 and 2, although likely related to supraspinal input, reveal different levels of supraspinal dependency. The intact gait cycle control is in line with preserved temporal accuracy of skilled ankle movements in iSCI despite diminished absolute active ROM and movement velocity (Wirth et al. 2008). By contrast, stroke patients showed decreased movement accuracy both in the paretic and unaffected leg (van Hedel et al. 2010). These findings indicate that muscle weakness and movement accuracy are unrelated and the required supraspinal input for temporal movement accuracy (within the boundaries of preserved muscle strength) remains intact in iSCI while the gait pattern gets distorted by weakness and other confounders (e.g. muscle tone).

Hip-knee cyclograms (shape difference and quality impairment) provided a converging measure of gait differences in iSCI, normalizing towards preferred speed in controls but remaining altered in patients. With increasing walking speed controls more than patients revealed an increase in cyclogram consistency (ACC), suggesting a more economic walking probably also enhanced by biomechanical dynamics (Wuehr et al. 2013). The quality of the cyclogram seems to reflect the severity of impairment, as the shape difference (SSD) correlates with preferred walking speed, both highly loading onto PC1. A static measure of muscle force (LEMS) was less related to walking performance than AngVel, which reflects muscle

force converted to dynamic movements at toe-off, a phase of the gait cycle underlying great supraspinal influence (Schubert et al. 1997).

In humans and animal models there is evidence of task-specific sensory-motor integration within the spinal cord below the level of injury, independent of supraspinal control (Barbeau and Rossignol 1987, De Leon et al. 1998, Dietz et al. 1994). Preclinical studies in cats and rats have revealed that the spinal cord is effective at producing rhythmic motor output upon afferent input even in severe (i.e. complete) spinal cord lesions (Barbeau and Rossignol 1987, Courtine et al. 2009). Yet in humans, changes of motor output, i.e. to increase speed, strongly rely on supraspinal commands while afferent inputs alone (e.g. load, hip extension) from the lower limbs are less effective at driving independent walking (Dietz et al. 1994, Lunenburger et al. 2006).

Implications for interventions

Through more detailed outcome assessments patients may receive therapeutic interventions specifically tailored to their distinct impairment. It still remains open to what extent the quality of gait clinically matters (i.e. is it essential to relearn a normal cyclogram) and previous studies have failed to show whether an improvement in walking speed following training improves the overall gait quality or is rather due to increased efforts (e.g. higher force) without changes of intralimb coordination (Behrman et al. 2012).

Limitations

The number of subjects from this inherently heterogeneous group of patients was limited and therefore the generalization of results might be limited. Animal studies have revealed that voluntary changes of gait parameters, although immediately responding to supraspinal commands, are still influenced by sub-hierarchical (i.e. spinal) effects, such as facilitation or inhibition (Courtine et al. 2008, van den Brand et al.

2013). Therefore, discerning supraspinal and spinal neural control of locomotion especially in humans remains challenging.

2.6 Conclusion

Locomotor capacity in iSCI patients is well-assessed by measures of walking performance (speed) and gait-cycle parameters but should be complemented by gait-quality analysis. The modulation of human walking is critically dependent on supraspinal input and alterations of iSCI gait are distinct from patients suffering from brain disorders (e.g. Parkinson's disease, stroke). The limited modulation of joint angles and intralimb coordination during walking suggests less responsiveness to immediate supraspinal drive but strong modulation by the spinal cord. The distinction and understanding of the dynamic changes of neural control during recovery and rehabilitation interventions may contribute to improved outcome evaluation and advanced treatments for iSCI.

Study 3

Locomotor recovery in spinal cord injury – why do patients walk faster?

Lea Awai, Armin Curt

(Manuscript in preparation)

»» I would like to thank Barbara Huber and Monica Stüssi, who were involved in data acquisition. ««

3.1 Abstract

Recovery of locomotor function after disorders of the central nervous system is often assessed through walking speed. While improved speed is certainly an important factor that relates to recovery in incomplete spinal cord injury (iSCI), changes in walking speed do not inform on changes in gait quality or mechanisms underlying recovery.

Kinematic data of 16 subjects with an iSCI were repeatedly recorded during in-patient rehabilitation. The responsiveness of the individual parameters with respect to walking speed was assessed by linear regression analysis. Principal components analysis (PCA) was applied on a multivariate set of gait-related data in order to cluster parameters that share a common impact on recovery after iSCI.

Most gait-related parameters improved over time and were related to the recovery of walking speed, which increased from 1.17 ± 0.90 to 2.29 ± 1.51 km/h (96% increase). Multivariate analysis revealed that measures of walking speed, angular velocity, gait-cycle parameters and intralimb coordination similarly explained the variance (PC1 62.4%) of changes during recovery while measures of active knee- and ankle-joint ranges (PC2 15.8%) distinctly contributed to recovery. The consistency of intralimb coordination improved significantly while the shape remained deteriorated despite improvements in walking speed.

Linear regression analysis may not reveal the impact of a single gait parameter on the recovery of walking among mutually interacting factors. PCA offers an integrative evaluation across many parameters and may provide novel insights into complex interactions contributing to the recovery of walking. This approach may improve the appreciation of rehabilitation interventions and guide future clinical protocols in iSCI.

3.2 Introduction

The success of a treatment or rehabilitation programs is generally termed recovery. However, there is no uniform approach for the assessment of recovery. Often times functional recovery is assessed by clinical tests that evaluate the ability of a person to accomplish specific tasks representing activities of daily living (e.g., functional independence measure (FIM) (Kidd et al. 1995), Fugl-Meyer assessment (FMA) (Gladstone et al. 2002), spinal cord independence measure (SCIM-III) (van Hedel 2009)) and these functional assessments are specifically designed for a defined group of patients (e.g., stroke, multiple sclerosis, spinal cord injury). Locomotor recovery is frequently captured by the objective measure of walking speed (Severinsen et al. 2014, Thompson et al. 2013) that can be compared between different groups and disorders. Being able to walk from A to B within a certain time is functionally relevant to most people and can be easily assessed without the need for expensive equipment. However, monitoring walking speed alone is insufficient to reveal possible underlying mechanisms of recovery. The question is by what means do patients attain a faster walking speed? Possible explanations may include increased muscle strength (Kim et al. 2004, Petersen et al. 2012) or learning of new movement strategies (Buurke et al. 2008), some of which may rely on processes such as reorganization of neural circuits involving the formation of synaptic connections and signal conduction pathways at the level of the brain/brainstem and spinal cord (Raineteau and Schwab 2001, van den Brand et al. 2012). In addition to clinical tests electrophysiological recordings provide objective insights into the integrity of specific spinal pathways. Somatosensory- (SSEP) and motor evoked potentials (MEP) in humans were shown to remain relatively unchanged in functionally improving iSCI patients suggesting that mechanisms such as compensation and adaptation of movement strategies substantially contribute to functional recovery (Curt et al. 2008). A possible approach to reveal underlying mechanisms of recovery is a multivariate analysis of gait-related measures beyond the evaluation of responsiveness of single measures. Partial disruption of spinal pathways and diminished supraspinal input in incomplete spinal cord injury (iSCI) provide the opportunity to assess the capacity and plasticity of the human locomotor system to recover walking function. In the present study detailed kinematic analysis of ambulating iSCI subjects recorded at several

time points during rehabilitation served to disentangle the different contributions of gait parameters to the recovery of walking.

3.3 Materials and methods

Subjects

Patients undergoing in-patient rehabilitation due to iSCI were recruited for this study as soon as they were able to ambulate without the assistance of an additional person. Patients with comorbidities influencing or inhibiting gait were excluded. Reference data was obtained from 21 healthy control subjects with no neurological disorder or any other impairment affecting their gait. All subjects had to give written informed consent prior to participation. The study was approved by the ethics committee of the Canton of Zurich, Switzerland.

Protocol

iSCI subjects were recorded at least at two time points during recovery. Subjects were asked to walk barefooted overground along a straight 8 m walkway at their preferred walking speed. Several runs were recorded in order to obtain at least 10 gait cycles. Overground walking at preferred speed was chosen because subjects need to self-initiate and maintain walking (as opposed to treadmill walking) and it reveals a person's natural and inherent walking pattern. Patients were allowed to use an assistive device if needed.

Lower-limb kinematics were recorded using 8 infrared cameras (T10, Vicon motion systems Ltd., Oxford, UK) at 200 Hz and two synchronized high-speed digital video cameras (pilot series, Basler AG, Ahrensburg, D) at 100 Hz. 16 reflective markers (16 mm diameter) were placed on bony landmarks of the lower body according to the Vicon Plug-in Gait body model. Patients were allowed to rest whenever needed.

Outcome measures

One gait cycle ranged from initial contact of one foot to the subsequent initial contact of the same foot. Data were time-normalized to one gait cycle by linear interpolation and data of at least 10 gait cycles per subject and time point were analyzed. Evaluated parameters included preferred walking speed [km/h] and gait-cycle parameters: step length [cm], cadence [strides/min], stance phase [%], and single-support phase [%]. Kinematic data provided information on lower-body intralimb coordination (gait quality) by evaluating hip-knee cyclograms, where the knee angle (abscissa) was plotted against the hip angle (ordinate). Further parameters extracted from kinematic data were hip-knee angular velocity at toe-off (resultant velocity vector of hip and knee angular change per unit time), endpoint velocity at toe-off (velocity of the 2nd metacarpal marker in the sagittal plane), maximal hip-, knee-, and ankle range of motion (ROM) during a gait cycle, angular component of coefficient of correspondence (ACC) (Field-Fote and Tepavac 2002) as a measure for lower-limb pattern reproducibility. The hip-knee cyclogram shape difference was quantified by the square root of sum of squared distances (SSD) (Awai and Curt 2014) between the cyclogram (mean of all cycles) of a patient and the mean standard cyclogram (derived from control subjects). Foot clearance was defined as the maximal height above ground of the 2nd metacarpal marker during the first two thirds of swing phase [mm].

A greater SSD reflects greater shape difference from normal and therefore a higher degree of impairment. The same is true for the stance phase: the shorter the stance phase, the better the walking capacity. We therefore multiplied these two values by -1 in order to align all measures of progression. The recovery of a parameter was defined as its difference between the last time point and the first time point divided by the amount of days between the two time points. The rate of recovery (change per unit time) accounted for the different lengths of time intervals between the assessment dates.

Principal component analysis

Principal component analysis can be used to reduce the dimensionality and thus the complexity of a multivariate set of data and find specific clusters of mutually interacting factors that may explain a common behavior of outcome. In the present study PCA was applied on the correlation matrix of 14 different gait-related variables assessed at the first time point (early) and the last time point (late) that might or might not change during the course of rehabilitation. Variables with absolute factor loadings ≥ 0.8 on PCs were retained. A scree plot and over-determination of PCs (at least two variables with factor loadings ≥ 0.8) were used to estimate the number of PCs that should be considered to explain the data. The factor loadings were compared across time by Pearson's r to reveal the robustness of the obtained pattern. In order to compare whether different groups can be distinguished along the PC axes, a one-way ANOVA was applied and, if appropriate, a post-hoc Tukey's test was performed.

Statistical analysis

In order to evaluate the respective influence of different gait-related parameters on the outcome of walking speed, all parameters were normalized to have a mean value of 0 and standard deviation 1. This prevents an overestimation of big numbers (e.g. ROM, angular velocity) and, conversely, an underestimation of small values (e.g. ACC). The responsiveness to walking speed of 12 potentially predictive gait parameters was assessed using a linear regression model (Husted et al. 2000):

$$\Delta y = \beta_0 + \beta \Delta x_i$$

where $i = 1, \dots, n$; Δy describes the change of walking speed per unit time and Δx_i represents the change of a gait-related parameter per unit time. β_0 is the amount of change in Δy if there is no change in Δx_i and β indicates the average increase in Δy per unit change of Δx_i. Therefore, the β-values inform on how strongly changes in particular gait parameters are related to changes in walking speed (Δ speed). Pairwise correlations were performed using Spearman's non-parametric correlation coefficient rho and data points

approximated by a linear or a 2nd degree polynomial fit, as appropriate, in a least squares sense. To assess whether a parameter changed over time (from an early to a late time point), a paired t-test was used for normally distributed data and a non-parametric Wilcoxon signed rank test was used for non-normally distributed data. The α-value was Bonferroni corrected according to the number of tests performed.

3.4 Results

Subjects

16 patients (7 females, 9 males; age 51.2 ± 15.7 years; height 169.9 ± 8.6 cm; weight 67.1 ± 12.6 kg) met the inclusion and exclusion criteria and were evaluated for this study (**Table 3.1**). The kinematic data of 21 healthy control subjects (13 females, 8 males; age 38.4 ± 14.3 years; height: 172.2 ± 8.2 cm; weight: 66.7 ± 12.1 kg) with no neurological disorders and no walking impairments were used to compute the standard hip-knee cyclogram for the SSD calculation and to provide reference data.

Table 3.1 - Descriptive data of patients

ID	Age [years]	sex	Cause of SCI	Level of SCI	initial LEMS	initial speed km/h
01	73	m	Traumatic	C5	48	0.19
03	36	f	Disc prolapse	T7/8	32	1.12
04	47	f	Spinal ischemia	T9/10	45	2.54
05	30	m	Traumatic	L2	48	2.88
08	60	f	Spinal ischemia	T5	27	1.17
09	48	f	Traumatic	T7	30	0.86
10	39	f	Spinal myelitis	C, T	38	1.15
13	23	m	Traumatic	C7	19	0.13
30	36	m	Traumatic	T4	40	1.97
31	60	m	Traumatic	C3	48	1.50
32	47	m	Traumatic	C5	46	0.79
34	63	m	Tumor	T4	46	0.41
37	71	m	Ischemic	T11	43	0.11
39	76	f	Tumor	T1	37	0.20
40	58	m	Ischemic	T4	45	2.37
44	53	f	Traumatic	C4	48	1.27

SCI = spinal cord injury; C = cervical, T = thoracic, L = lumbar; LEMS = lower extremity motor score (max = 50).

Walking speed

Only one patient could not improve walking speed (-0.34 km/h) while all other patients showed increased walking speeds over time. The mean increase of the whole group was 1.12 ± 1.08 km/h (mean ± SD; paired t-test: $p < 0.001$). The initial walking speed of a patient was not related to the amount of gain in speed (Δ speed) during recovery (rho = 0.315).

Responsiveness of gait parameters

Most parameters improved from an early (74 ± 59 days post-incident; mean ± SD) to a late time point (216 ± 116 days). However, the knee and ankle ROMs and the cyclogram shape difference did not change over time. On average, the SSD only showed a trend towards decreased values (improved quality of intralimb coordination) from the first to the last time point of assessment (paired t-test: $p = 0.136$) while the cyclogram reproducibility increased during recovery (Wilcoxon signed rank test: $p = 0.006$).

Examining the contribution of changes in gait variables to changes in preferred walking speed by linear regression analysis showed that changes in walking speed were most closely accompanied by changes in hip ROM ($\beta = 1.17$), followed by cadence ($\beta = 1.10$), angular velocity at toe-off ($\beta = 1.07$), and step length ($\beta = 1.00$). Changes in the quality of intralimb coordination, quantified by the shape difference of the hip-knee cyclogram compared to normal ($\beta = 0.35$), the foot clearance ($\beta = 0.22$) and the cycle-to-cycle cyclogram consistency ($\beta = 0.09$) were least related on changes in preferred walking speed (**Figure 3.1**).

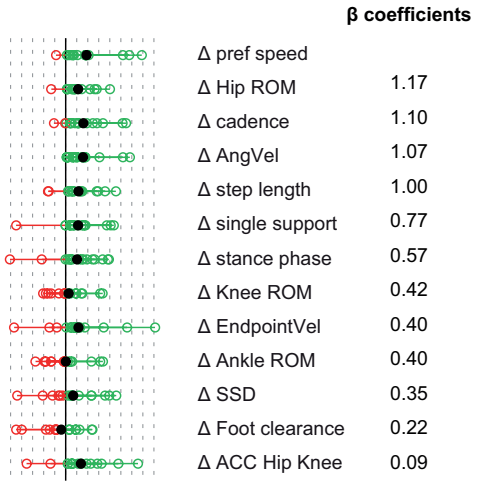

Figure 3.1 Responsiveness to change in speed. The stem plot illustrates delta values of parameters at the last time point minus the first time point of assessment divided by the amount of time (rate of change). Green circles represent positive changes and red circles negative changes. Black dot = mean. Note that a negative delta value for stance phase and a negative SSD (= shape difference to normal cyclogram) corresponds to improved walking. A linear regression analysis was performed consecutively with the 12 gait-related predictive parameters and preferred walking speed (pref speed) as the dependent variable in order to assess the responsiveness of the predictive variables on the 'gold standard' measure of recovery (walking speed). ROM = range of motion, AngVel = hip-knee angular velocity at toe-off, EndpointVel = velocity of the 2nd metatarsal joint marker at toe-off in the sagittal plane, SSD = square root of sum of squared distances, ACC = angular component of coefficient of correspondence.

Multivariate analysis

Principal component analysis applied on all variables at the first and the latest time point revealed that PC1 alone explained 62.5% of the total variance in data while the first two components collectively explained 78.2% of variance. The scree plot and PC over-determination suggested to retain the first two PCs. PC1 was highly loaded by gait-cycle parameters, preferred walking speed, angular velocity at toe-off, cyclogram shape difference, and cyclogram consistency (**Figure 3.2A**). PC2 only received high loadings from the knee- and ankle ROM. After segregating data into two groups based on early and late time points during recovery, ANOVA and post-hoc Tukey's test revealed that the data only showed group differences along PC1, suggesting that the variables with high factor loadings on PC1 explained recovery across time. When initial speed was selected as the grouping variable, the ANOVA and post-hoc Tukey's analyses yielded differences between slow walkers (≤ 1km/h) and both medium (≤ 2 km/h) and fast

walkers (≤ 3km/h) but not between medium and fast walkers (**Figure 3.2B**). A matching of the factor loadings on PC1 and PC2 across time points revealed a robust pattern over time with correlation coefficients of r = 0.933 and r = 0.910, respectively.

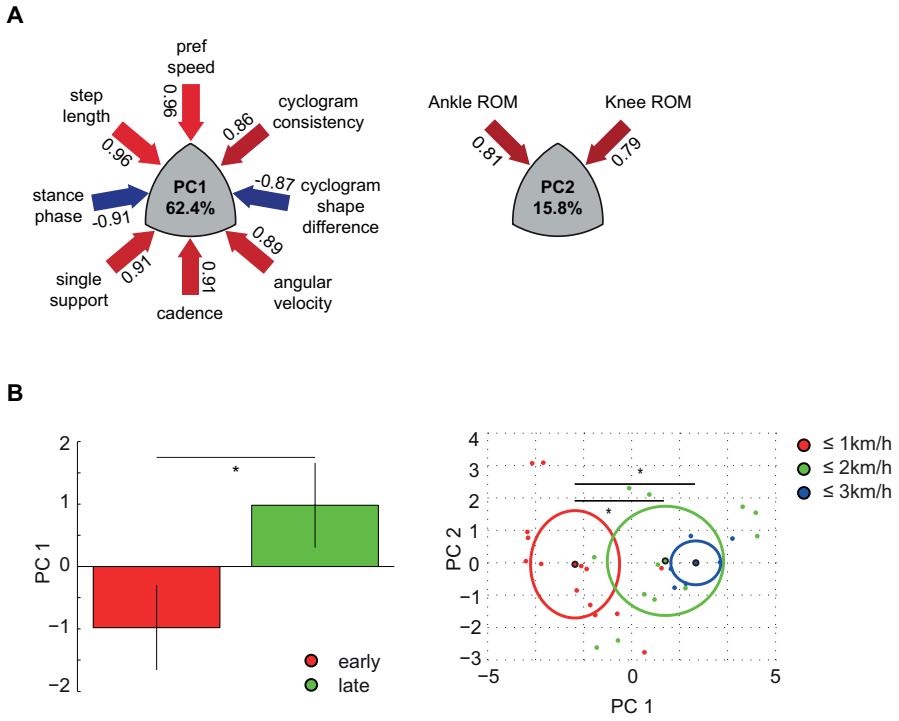

Figure 3.2 Principal component analysis applied on 14 gait-related parameters revealed that the first two PC's alone explained more than 75% of the variance in data (**A**). After grouping the data into an early and a late time point, group differences emerged along the PC1 axis but not the PC2 axis (not shown) (**B**). A segregation of the data according to the initial walking speed revealed that slow walkers (≤ 1km/h) differed from both medium (≤ 2km/h) and fast walkers (≤ 3km/h) with respect to PC1 but not PC2.

Speed dependence

The relation between speed and various parameters remained relatively consistent across time while it changed dramatically in knee- and ankle ROM. The SSD and ACC both showed a non-linear behavior with respect to preferred speed across time with far-from-normal values in slow walkers and plateauing in fast walkers (**Figures 3.3A, B**). The speed relation of step length (early: rho = 0.838, late: rho = 0.943, **Figure 3.3C**) and hip ROM (early: rho = 0.541, late: rho = 0.667, **Figure 3.3D**) both showed a similar and

adequate relation to walking speed at an early compared to a late time point, even though the relation was weaker in the hip ROM. The speed relation of the more distal joint ROMs was very weak at an early time point (knee: rho = 0.112, ankle: rho = -0.185) but improved at a late time point (knee: rho = 0.618, ankle: rho = 0.512) while remaining different from normal (**Figure 3.3E, F**).

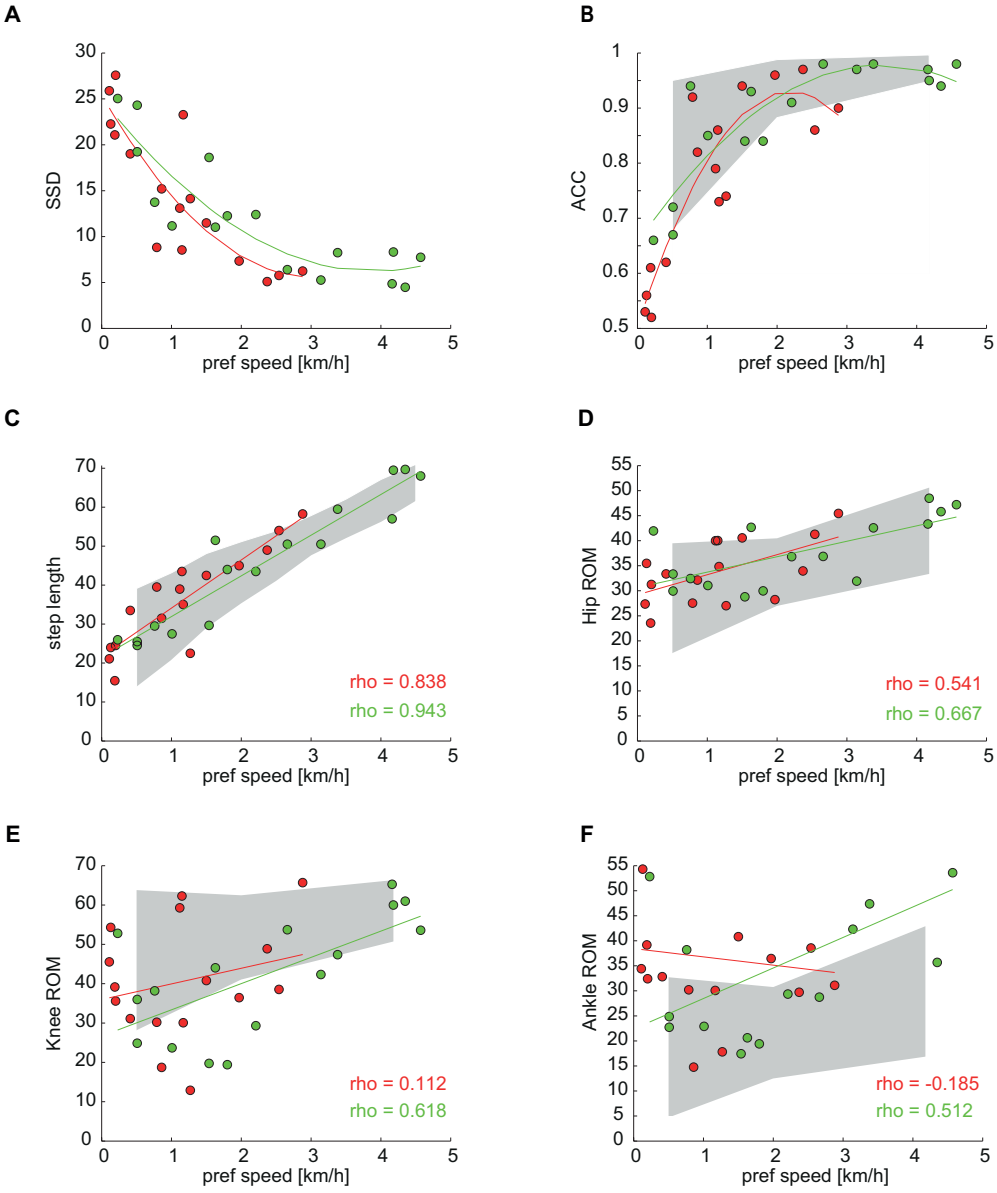

Figure 3.3 Speed dependence. The relation of various gait-related parameters was quantified by Spearman's correlation coefficient rho at an early (red) and a late (green) time point. The shaded gray area indicates the ± 2SD interval of healthy control subjects with respect to speed. SSD and ACC data (**A** and **B**) were fitted by a 2nd degree polynomial while the other graphs contain a linear fit (**C**

through **F**). SSD = square root of sum of squared distances, ACC = angular component of coefficient of correspondence, ROM = range of motion.

Patterns of intralimb recovery

With regard to gait quality patients behaved quite distinctively. In terms of cyclogram impairment, three patterns of recovery could be distinguished: 1) bilateral *recovery* of intralimb coordination (improved shape and consistency of cyclogram) over time, 2) *invariant* bilateral intralimb coordination despite higher walking speed, and 3) *dissociated* unilateral cyclogram recovery, with an improved cyclogram in one leg and an invariant or deteriorating cyclogram in the other leg (**Figure 3.4**).

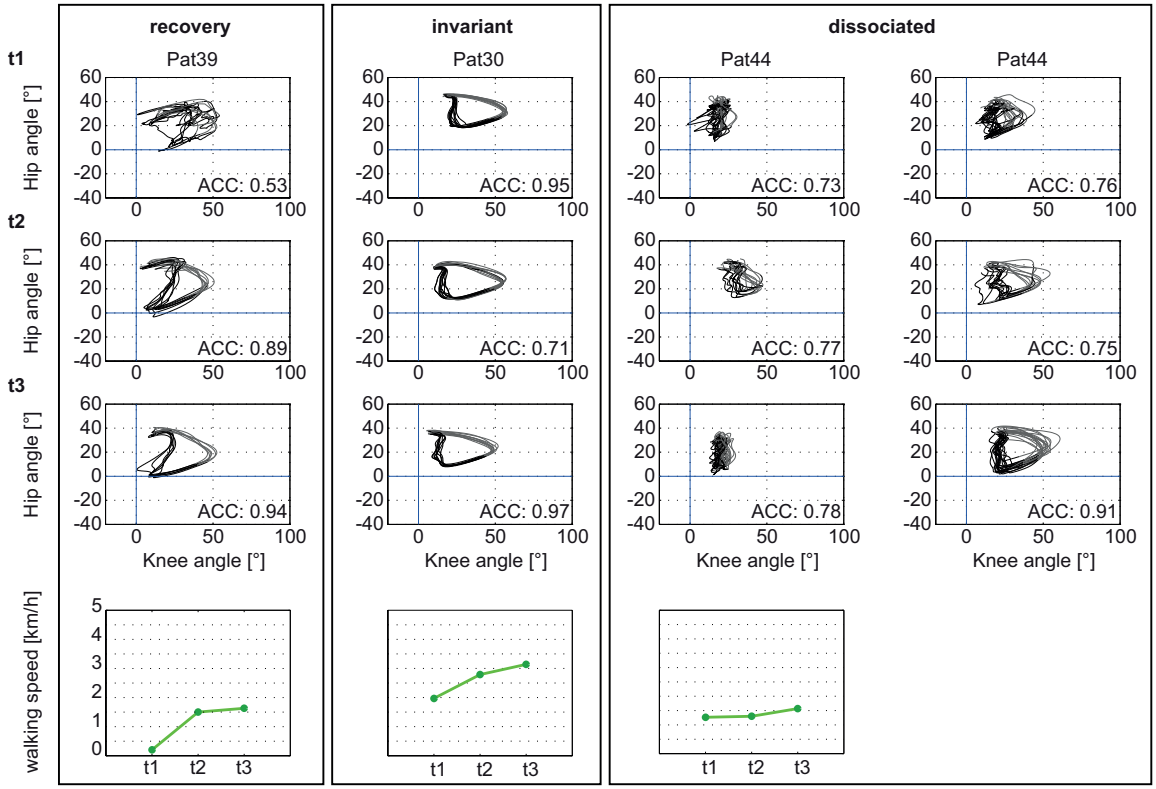

Figure 3.4 Patterns of intralimb recovery. Recordings at 3 time points during rehabilitation revealed 3 distinct patterns of intralimb recovery. *Recovery* and *invariant* patterns were revealed bilaterally while some patients showed a *dissociated*, unilateral pattern of recovery. The walking speed improved in all 3 categories. ACC = angular component of coefficient of correspondence.

3.5 Discussion

Recovery of walking function after iSCI underlies a complex process where many factors contribute to the increase in walking speed. Measures of responsiveness and correlation analyses are limited in explaining the intricate interactions of factors contributing to recovery. The application of a multivariate analysis (PCA) revealed that specific factors share a common impact on recovery that either showed a limited or high relation to changes in walking speed. The distinction of contributing factors of recovery compared to those measures that rather change as a consequence of improved walking speed might offer new insights for the evaluation and refinement of treatment interventions.

Responsiveness and speed dependence

Except for one subject all patients were able to increase their preferred walking speed. Changes in walking speed are known to affect gait parameters in healthy subjects and patients (Hanlon and Anderson 2006, Pepin et al. 2003). It is therefore important to note that the responsiveness to increased walking speed in iSCI patients may partially be attributable to recovery, but may also be a biomechanical consequence of increased walking speed. Interestingly, the initial walking speed was not indicative of the potential to improve walking speed but whether a patient was initially a slow or a fast walker determined the recovery capacity as revealed by PCA.

The relation to changes in speed (Δ speed) evaluated by linear regression analysis revealed that hip ROM was the most responsive variable and therefore showed stronger relation to speed improvements compared to the knee- and ankle ROMs. Δ speed was only weakly related to changes in the combined hip-knee coordination (SSD, ACC). Apparently, patients were able to increase hip ROM in accordance to an increase in speed and the relation between changes in these two parameters were close to normal. Gait-cycle parameters (e.g. step length) also showed regular interactions with changes in speed. Both variables of intralimb coordination were affected in slow walkers and approached normal values in fast

walkers even though the SSD showed no improvement across time while the ACC improved. The speed-relatedness of the SSD, ACC, step length and hip ROM remained relatively consistent across time (i.e., showed similar correlation coefficients) while it changed dramatically in the knee- and ankle ROMs. These findings indicate that distal limb joint angles are differently controlled than the hip joint (Dietz et al. 2002, Hicheur et al. 2006). Studies in animals and humans revealed that the control of lower limb movements also following iSCI is strongly modulated by afferent input from the hip (Dietz et al. 2002) and indicate that the neural control from the proximal to distal limb is not uniform. Furthermore distal joint angles may be impeded more strongly by confounders such as increases in muscle tone (eventually presenting as spasticity) and changes in mechanichal properties of the muscle-tendon compartments (i.e. joint contractures) (Krawetz and Nance 1996). The low responsiveness of intralimb coordination to speed may be due to the use of compensatory strategies in order to achieve the best performance (i.e. a stiff leg may allow a more reliable walking). These behaviors may be triggered or promoted by the reorganization of neuronal circuits following the deprivation of supraspinal inputs (Beauparlant et al. 2013, Calancie et al. 1996, Dietz et al. 2010, Hubli et al. 2011), which may be reflected in the altered intralimb coordination. Thus, even though the supraspinal input may be limited but still adequate to control faster stepping, this may not be sufficient to provide normal intralimb coordination.

Contributing factors of recovery

The present findings highlight the crucial importance of distinguishing between factors showing changes by simply responding to increased walking speed (i.e. responsiveness) and those parameters that actually contribute to recovery of walking function. A linear regression analysis has the disadvantage of requiring a dependent variable, while the responsiveness of different independent variables to this specific parameter is assessed. However, PCA does not require predefining a particular variable that is taken as a surrogate of recovery and may therefore be less affected by a selection bias. The clustering of parameters on PC1 suggests that they contribute to clinical recovery (i.e. the different gait parameters followed over time form an unbiased construct of recovery) in a particular, mutually interrelated way, which is not

necessarily paralleled by improvements across time. While gait-cycle parameters highly loaded onto PC1, suggesting a strong contribution to recovery they were also closely related to speed even at an early time point, suggesting that they may be little affected by the injury and increase due to improved walking speed. In contrast, variables related to the intralimb coordination (SSD, ACC) were impaired in the iSCI population and showed little responsiveness to changes in speed while being important at determining recovery, i.e., whether the intralimb coordination is normal or not influences the recovery of gait function even if it does not change across time. Hip ROM, on the other hand, showed the highest responsiveness to speed improvements but did not contribute to recovery as revealed by PCA. Thus, whether parameters are well modulated by patients or impaired due to the underlying injury while unrelated to speed and invariant across time may intricately affect recovery. Obviously, if the parameters identified by PCA actually underlie true recovery (i.e., improve over time) or whether they merely change over time as a consequence of increased speed cannot be elucidated by PCA alone. These distinct findings suggest that an improvement or a high responsiveness to walking speed does not coincide with recovery of walking function.

Limitations

Major drawbacks of the present study were the irregular visit time points and the varying number of visits. The inpatient rehabilitation schedule was often packed with therapies, leaving no vacancy for the rather time-consuming gait analysis. Sometimes appointments were cancelled at short notice due to sudden conflicting events or because patients were too tired to participate or had other reasons for cancellation. We tried to overcome this problem by looking at the first and the last time point of assessment and by quantifying the changes over time by dividing the parameters by the respective time intervals so that we could study the rate of change of the various parameters. Also, we only included patients who were able to walk independently and therefore already regained large parts of their locomotor capacity. We therefore might have missed the interesting phase when most plasticity takes place within the sensory-motor system.

3.6 Conclusion

Regression analysis may reveal the responsiveness of gait parameters to increased walking speed while the complex process of recovery may only be correctly assessed by multivariate analysis followed by detailed post-hoc analysis of complementary outcome measures including gait-cycle parameters and intralimb coordination while the former is well controlled even at an early stage of recovery while the latter may remain impaired throughout rehabilitation. These distinct findings are crucial for the conduct and evaluation of future interventional studies.

Study 4

Extensive plasticity of the human spinal cord

Lea Awai, Armin Curt

Journal of Neurotrauma (submitted)

»» I would like to thank Reto Sutter, who helped me with the MRI data. ««

4.1 Abstract

Although the central nervous system has a limited capacity for regeneration after acute brain and spinal cord injuries, it can reveal extensive morphological changes. Occasionally the formation of an extensive syrinx in the spinal cord can be observed causing no or only limited signs of functional impairment. This creates a unique condition to evaluate the mismatch between substantial morphological changes and functional outcomes.

7 patients with holocord syringomyelia affecting the cervical cord following chronic traumatic thoracic/lumbar spinal cord injury (19 - 34 years after injury) or of non-traumatic origin were identified and anatomical syrinx dimensions (length, syrinx-to-neural tissue ratio) were determined using sagittal and axial MRI scans. Motor- and sensory-pathway integrity were evaluated using electrophysiological assessments (motor (MEP), sensory (dSSEP) and contact-heat (dCHEP) evoked potentials; nerve conduction studies (NCS)) and specifically compared to clinical measures of upper limb strength and grasping performance including 3-D motion analysis.

Despite extensive anatomical changes of the cervical cord (on average 26% reduction of cross-sectional spinal cord area and intrusion of almost the entire cervical spinal cord) a clinically relevant impairment of upper limb motor function was absent while only subtle sensory deficits could be detected. dCHEPs revealed the highest sensitivity by disclosing impairments of spinothalamic pathways.

Comparable to the brain extensive anatomical changes of the spinal cord can occur with only subtle functional impairment. Obviously, the time scale of very slowly emerging morphological alterations is essential to permit an enormous capacity for plasticity of the spinal cord.

4.2 Introduction

There is no universally accepted and unanimous definition of neural plasticity and involved mechanisms are manifold. Analogous to the brain different aspects of neural plasticity can be discerned at the spinal level. Structural changes on a microscopic level involving neural repair (e.g. remyelination of axons) (Kato et al. 2000) and restorative processes (e.g. axonal sprouting and reorganization of neural circuits) (Carmichael and Chesselet 2002, Courtine et al. 2008, van den Brand et al. 2012) may be revealed by neurophysiological recordings assessing conductivity of specific pathways and reflex circuits along the neuraxis (Curt and Ellaway 2012, Hubli et al. 2012) while changes in function are captured by specific measures of activity and multimodal profiles of body function. Ultimately, clinical recovery likely results from multiple mechanisms also including compensatory mechanisms independent of neural repair (e.g. muscle-strength increase by means of improved neuro-muscular performance and learning of new movement strategies) (Buurke et al. 2008). On a macroscopic scale neural plasticity in terms of morphological alterations as revealed by magnetic resonance imaging (MRI) is frequently associated with tumor or cystic formations. Interestingly, in very slowly progressing disorders such as the growth of benign brain tumors or the development of a hydrocephalus, patients can appear asymptomatic for a long time despite striking anatomical alterations (Desmurget et al. 2007, Onizuka et al. 2001). Accordingly, in the spinal cord, the formation of a tumor or syringomyelia occasionally occurs without specific symptoms (i.e. unspecific symptoms such as tingling sensation, pain and muscle weakness are reported) (Emery et al. 1998, Schurch et al. 1996, Zager et al. 1990). The most extensive form of syringomyelia is termed holocord syringomyelia, affecting almost the whole spinal cord in the axial plane, which can be found in association with congenital neural malformations (e.g. Arnold Chiari) (Emery et al. 1998) or as a late sequel of spinal cord injury (SCI) (Schurch et al. 1996, Vernon et al. 1982). In rare cases, the etiology remains unknown and the holocord syrinx forms without apparent preceding incident. The holocord syrinx may eventually be discovered when causing symptoms or, coincidentally, while examining unrelated disorders. At this stage, the syrinx may already cover a large volume of spinal cord, forcing neural tissue to the margins of the remaining space. These morphological changes not only involve adjustments within the neural tissue,

but also require associated adjustments of vascular and connective tissue. In the present study clinical, electrophysiological and kinematic measures were collected to assess the specific susceptibility of particular sensory and motor spinal tracts and to evaluate the capacity of the spinal cord to compensate for extensive morphological changes.

4.3 Materials and methods

Subjects

Inclusion criteria: Patients diagnosed with holocord syringomyelia of the cervical spine, aged 18 years or older were included. *Exclusion criteria*: Patients with any disorder other than thoracic or lumbar SCI affecting motor function were excluded. For kinematic analyses healthy control subjects were recruited. Additionally, healthy age- and gender-matched control subjects were recruited to compare spinal MRI data. The study was approved by the ethics committee of the Canton of Zurich. Participants provided written informed consent.

Neuroimaging

Anatomical data were obtained from magnetic resonance images (MRI) acquired by a 3T Magnetom Verio Scanner (Siemens Healthcare, Erlangen, Germany) with a 16-channel receive head and neck coil. The patients were scanned with a clinical MRI protocol of the cervical spine, containing the following sequences: 1) Sagittal T2-weighted turbo spin-echo sequence (repetition time 3760 ms; echo time 87 ms; number of slices 20; slice thickness 2.5 mm; matrix 288 x 384; field-of-view 220 mm x 220 mm); 2) transverse T2-weighted turbo spin-echo sequence (repetition time 3120 ms; echo time 93 ms; number of slices 26; slice thickness 3 mm; matrix 256 x 320; field-of-view 160 mm x 160 mm). This data was compared to T2-weighted images of healthy control subjects that were secondarily reconstructed into the transverse plane from sagittal sequences (repetition time 3760 ms; echo time 87 ms; number of slices 20; slice thickness 2.5 mm; matrix 288 x 384; field-of-view 220 mm x 100 mm) using Jim 6.0 (Xinapse systems, Aldwincle, UK). In patients, the extent of the holocord syrinx was evaluated by the absolute length (most rostral to most caudal vertebral segment with a syrinx in the sagittal MRI), relative length (length of syrinx in % of total cord length between vertebral levels C0 and T12/L1), and the syrinx-to-spinal cord ratio (cross-sectional syrinx area in % of total cord area obtained from axial anatomical MRIs at the level

of maximal syrinx diameter). At these levels the cross-sectional area of remaining spinal cord tissue (total spinal cord area minus syrinx area) was compared to the spinal cord cross-sectional area of age- and gender-matched healthy control subjects at the same spinal level. Spinal cord cross-sectional areas were calculated as the mean of the areas at the level of greatest syrinx diameter (bottle neck), one slice rostral and one slice caudal to that level using Jim 6.0, as reported previously (Horsfield et al. 2010). In one patient the cross-sectional syrinx area was assessed from spinal level T2 because of flow artifacts in the cervical MRI.

Neurophysiology

The integrity of the corticospinal pathway was assessed via motor evoked potentials (MEPs), elicited by a magnetic stimulator (The Magstim Company Ltd., Wales, UK) via a figure-of-eight coil placed over the motor cortex and derived from pre-activated muscles on the contralateral side of the body. If possible, the MEP was recorded from the abductor digiti minimi (ADM) muscle. Only in Pat35 the abductor pollicis brevis (APB) was taken due to a pre-existing sulcus ulnaris syndrome. In order to exclude peripheral nerve damage, nerve conduction studies (NCS) including F-wave recordings of the ulnar nerve (median nerve in Pat35) were performed. Sensory pathways, i.e. dorsal columns and spinothalamic tract, were assessed by testing light touch and pinprick sensation and by more elaborate dermatomal somatosensory evoked potentials (dSSEPs) and contact heat evoked potentials (dCHEPs) (Kramer et al. 2010, Ulrich et al. 2013), respectively, elicited in dermatomes C4, C6, and C8. All evoked potentials (EPs) were evaluated by means of amplitude and latency compared to standard values and were rated as abolished (no EP response), impaired (reliable response but pathological findings of latency and/or amplitude) and normal response (Curt and Dietz 1997, Curt and Dietz 1999, Kuhn et al. 2012).

Functional outcome measures

Clinical outcome measures such as the upper and lower extremity motor scores (UEMS, LEMS), the spinal cord independence measure III (SCIM-III), and the graded redefined assessment of strength, sensibility and prehension (GRASSP) (Kalsi-Ryan et al. 2012) were used to assess different levels of functional abilities in patients. For UEMS and LEMS the left and right sides were added to give a total score. The SCIM-III sub-items *self-care*, *mobility inside* and *mobility outside* were considered for evaluation of patients' functional state during activities of daily living and divided into those relying predominantly on upper limb function and those relying more on lower limb function. Scores were indicated as percentage of maximally possible score corresponding to that of an able-bodied person. The four domains of GRASSP were evaluated accordingly. Additionally, a specific reaching task was performed using the dominant arm/hand while recording kinematics. Kinematic data acquisition was performed at 200 Hz using a 3-D motion capture system (Vicon motion systems Ltd., Oxford, UK) recording the movements of passive reflective markers placed on the scapula, the acromion, the lateral humeral epicondyle, the head of the ulna and radius, the head of the 1st, 2nd and 5th metacarpus, and the tips of each finger of the dominant hand. Subjects started from a resting position, where their hand passively lay on their lap, and were asked to reach forward towards an object of the size of a walnut on a stick. They had to grasp the object, bring it to their mouth, bite and hold it there while moving their hand back to resting position. This movement mimicked reaching for and eating a piece of food. 10 trials per person were recorded and analyzed. For analysis, the reaching movement was split into three sub-movements: *reaching*, *retract-to-mouth*, and *back-to-start*. Success rate, movement speed, movement variability, and hand-path ratio (HPR) (Kamper et al. 2002, Zimmerli et al. 2012) were chosen as quantifiable readouts. Retrieval was classified as successful if all of the following conditions were met: only a one-time contact of the object while grasping (no regrasping/correction movement), the subject did not drop the object, and the object touched the mouth only once. Success rate was evaluated as percentage of successfully retrieved objects during 10 trials. Movement speed was calculated as the speed of the endpoint (marker on 2nd metacarpus) during the *reaching* and *retract-to-mouth* sub-movements. Movement variability was calculated as the elliptic area of

the endpoint in the sagittal plane where the half axes correspond to the standard deviation of the endpoint position in the horizontal and vertical axes. *Reaching* and *retract-to-mouth* sub-movements were time-normalized and variability was calculated for 10 trials at equal bins. HPR was calculated as the ratio of the direct path between start and end position and the actual path of the 2nd metacarpal marker during the *reaching* and *retract-to-mouth* sub-movements. This readout is a measure for movement linearity of hand motion and was calculated as the mean of 10 trials.

Statistical analysis

The cross-sectional spinal cord area was compared between the two groups by a two-sample t-test. An ANOVA was used to examine differences between patients and healthy controls with regard to the kinematic data assessing movement speed and variability of the reaching movement, and HPR. Post-hoc Tukey's test was applied if ANOVA revealed significant differences. The success rate was compared between the groups using a Chi-Square test. Bonferroni correction was applied to account for multiple testing.

4.4 Results

Subjects

7 patients (6 males, 1 female; 45.4 ± 8.1 years) with a diagnosed holocord syringomyelia were included in this study (**Table 4.1**). 4 of the patients suffered from chronic traumatic thoracic/lumbar SCI (19 - 34 years prior to study inclusion) that affected only their lower limbs. 1 patient showed a Chiari malformation while in 2 patients no associated disorder could be identified (termed idiopathic holocord syrinx). For the reaching task we evaluated 7 healthy control subjects (4 males, 3 females; 25.1 ± 2.6 years), while a second group of 7 age and gender-matched subjects served as controls for the evaluation of spinal cord cross-sectional area (6 males, 1 female; 45.1 ± 7.7 years).

Table 4.1 - Descriptive data of patients

Patient ID	Age [years]	Sex	Extent of syrinx	Preexisting disorder	Onset of SCI
09	48	f	BS – T10/11	traumatic SCI (T7)	- 26 years
28	36	m	BS – T4/5	none	n/a
35	51	m	BS – T10/11	traumatic SCI (T3/4)	- 29 years
36	48	m	C3/4 – T9/10	none	n/a
38	50	m	BS – L1/2	traumatic SCI (cauda)	- 34 years
41	32	m	C1 – T10	Chiari malformation	n/a
43	53	m	C0 – T12	traumatic SCI (T5)	- 19 years

Indication of the extent of the syrinx refers to the vertebral levels or intervertebral spaces. The onset of SCI refers to the incidence of the traumatic SCI prior to participation in the present study. BS = brain stem, n/a = not applicable.

Neuroimaging

All patients showed an extensive syrinx (**Table 4.2**) in the cervical spinal cord that in mean occupied about 84% of the total cord length (**Figure 4.1A, F**), and about 54% of the spinal cord cross-sectional area

at the level of the largest syrinx diameter (**Figure 4.1B, D**). For the whole group the remaining neural-tissue area at the level of maximal syrinx diameter was significantly less (74%) in patients (59.7 ± 12.9 mm^2) compared to the corresponding spinal cord area in healthy, age-matched controls (80.2 ± 16.8 mm^2, t-test: p = 0.025; **Figure 4.1C, E**).

Table 4.2 - Characteristics of Holocord Syrinx

Patient ID	Relative length of syrinx	Relative syrinx area at max. diameter (vertebral level)	Neural-tissue area at max. diameter [mm^2]	Spinal-cord area in healthy controls [mm^2]
09	90 %	74 % (C2/3)	45.2	59.0
28	60 %	44 % (T2)	51.6	76.0
35	90 %	80 % (C2)	42.1	88.5
36	70 %	35 % (C7)	69.0	87.0
38	100 %	49 % (C2)	71.1	75.5
41	80 %	34 % (C6)	70.9	74.0
43	95 %	60 % (C2)	67.9	96.0
total	84 ± 14 %	54 ± 18 %	59.7 ± 12.9	80.2 ± 16.8

The relative length of syrinx refers to the extent of the syrinx in relation to the total length of spinal cord between vertebral level C0 and the distal end of conus medullaris. The relative area at maximal diameter describes the cross-sectional area of the syrinx in relation to the total area of the spinal cord (Figure 4.1B,D). Neural-tissue area was assessed after subtraction of the CSF area of the syrinx from the surrounding tissue area (outer rim of the spinal cord). Spinal-cord areas were retrieved from age- and gender-matched control subjects.

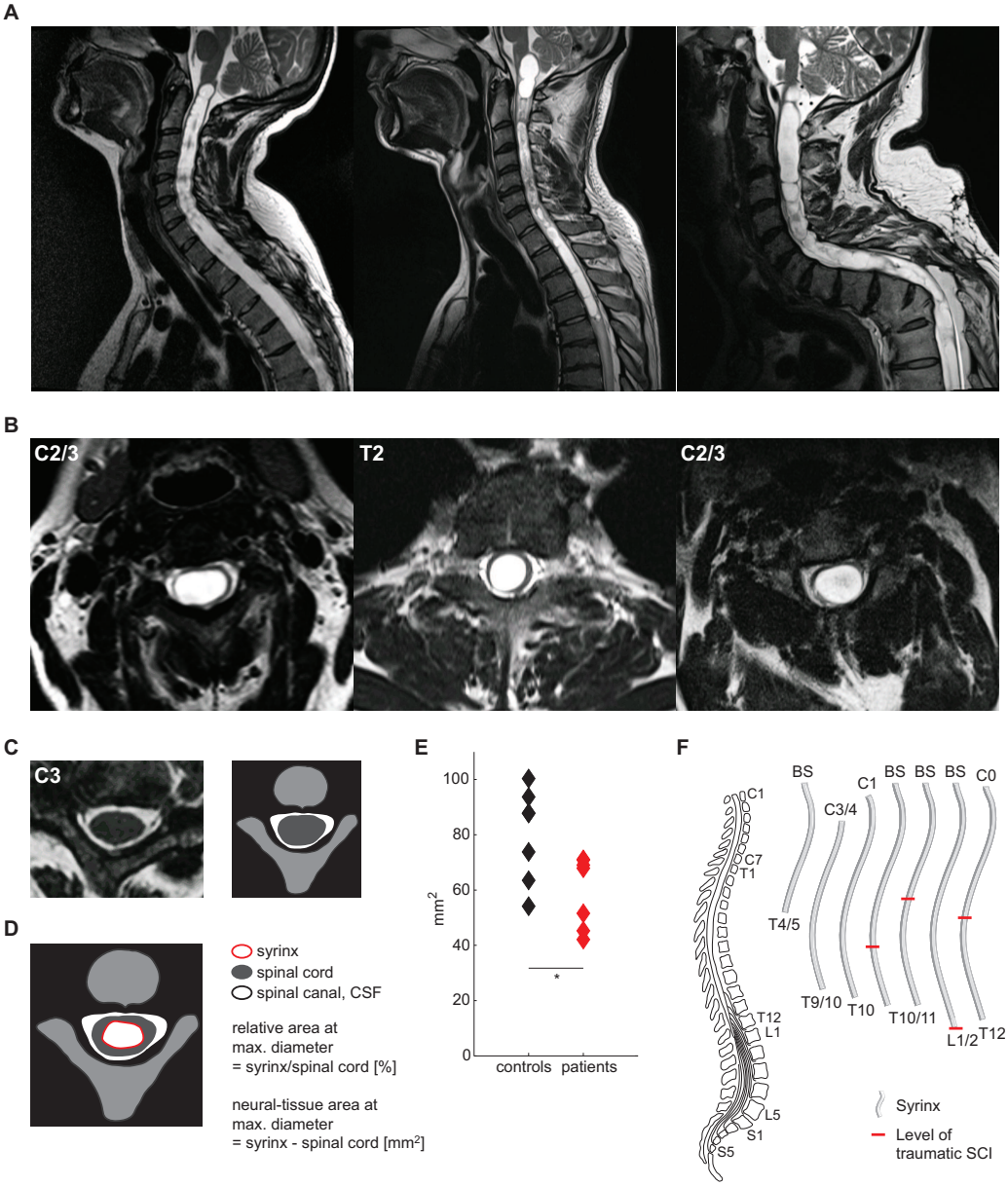

Figure 4.1 Sagittal and axial scans of the holocord syrinx. The top panel (**A**) shows the sagittal T2-weighted scans of 3 patient examples. The cerebrospinal fluid (CSF) of the holocord syrinx in the T2-weighted images appears bright and neural tissue appears in dark gray. Panel (**B**) shows the axial images of the same patients at the level of largest syrinx diameter (labeled with cervical (C) and thoracic (T) segments). (**C**) A T2-weighted image of a healthy control subject at level C3 is shown on the left and a schematic drawing of a healthy axial spinal cord section on the right. The schematic drawing in (**D**) illustrates the syrinx parameters derived from axial MR images. The spinal cord cross-sectional areas at corresponding levels in healthy controls and in patients are illustrated in (**E**). Panel (**F**) depicts the extent of the syrinxes and the level of lesion (red bars) in the 4 patients with SCI.

Clinical scores

The mean UEMS of patients was 49.86 ± 0.38 (99.7% of maximal value (50)), comparable to the strength domain of the GRASSP (94.9%), which showed almost normal qualitative and quantitative grasping (99.4% and 98.3%, respectively). Only sensibility was impaired to a greater extent (71.7%). LEMS was 50 (100%) in all patients without SCI and 15.25 ± 17.61 (30.5%) in patients with SCI (Figure 4.2A). In the sub-items of the SCIM-III predominantly depending on upper limb function patients attained 98.2% of maximal score. Items depending on both upper- and lower extremity function were scored 81% while those of lower extremity reached 68%. Patients without SCI reached 100% both in the *mobility inside* and *mobility outside* categories while patients with SCI reached 77.5% in the *mobility inside* and 43.3% in the *mobility outside* sub-items.

Neurophysiology

Electrophysiological data showed different sensitivities in detecting impairment **(Figure 4.2B)** depending on the distinct pathways that were assessed **(Figure 4.2C)**. The NCS yielded normal results in all patients. Likewise, all of the assessed MEPs of the upper limbs showed normal values. The assessment of sensory pathways showed distinct findings revealing differently affected dSSEPs and dCHEPs **(Figure 4.2D)**. 4 of 7 patients showed normal dSSEPs from all assessed dermatomes, 2 patients showed at least one dermatome with normal dSSEPs, and one patient showed altered dSSEPs from every dermatome. However, there was no patient with normal dCHEPs derived from all of the measured dermatomes and 3 patients revealed pathological dCHEPs in all dermatomes. Clinical testing of light touch and pinprick sensations revealed a similar picture but of poorer resolution and sensitivity. Light touch sensation was impaired in one patient while pinprick sensation was impaired in two patients and abolished in one.

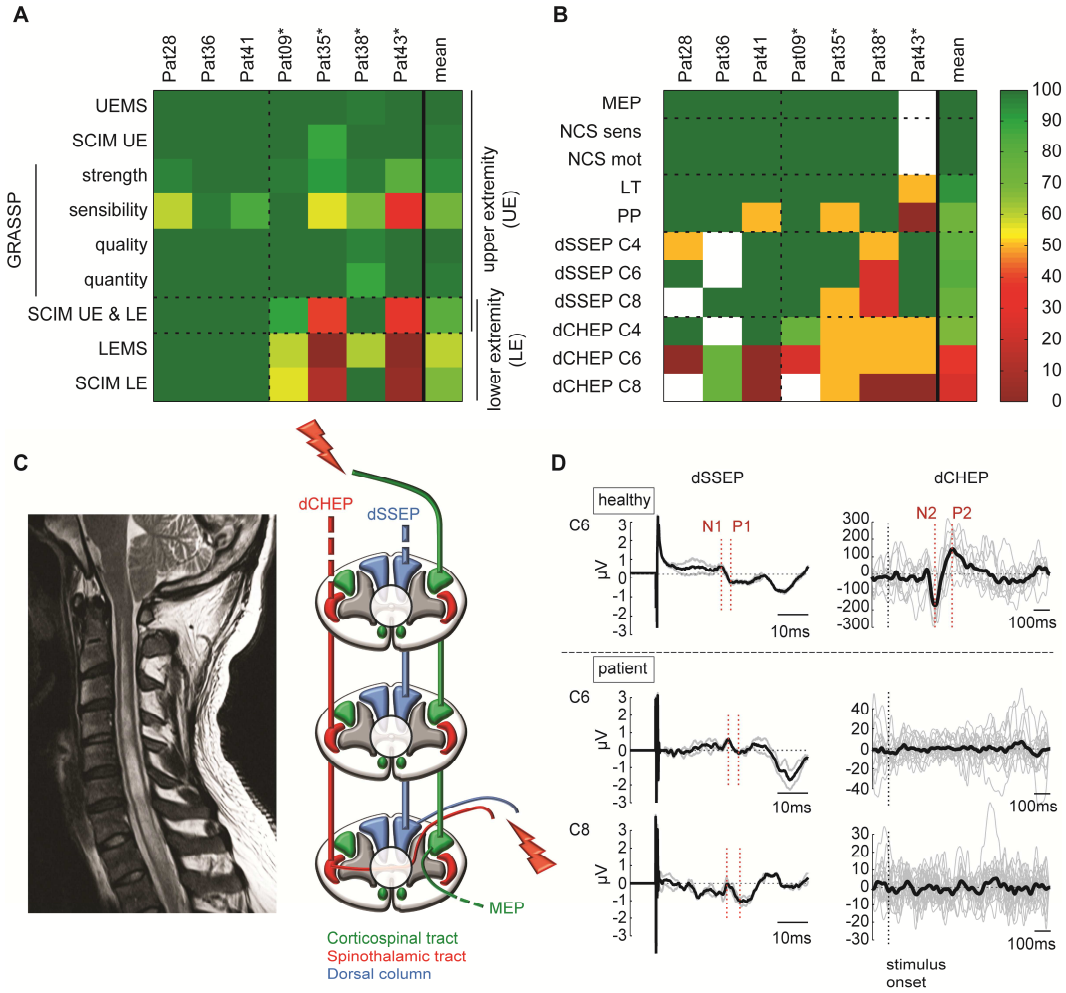

Figure 4.2 Clinical scores and electrophysiological data. Clinical scores are illustrated in (**A**) and electrophysiological data are presented in (**B**). The values are color-coded, red corresponds to low values while green indicates high values. Percentages were calculated as ratios of maximal values (i.e. control values) or coded as normal, impaired or abolished EP recordings (0%, 50% and 100%). Missing values are colored white. Patients with a preexisting spinal cord injury are marked with an asterisk. (**C**) A sagittal MRI of the cervical spinal cord of a patient (Pat41) is shown. The schematic drawing on the right shows motor and sensory pathways, which may be differentially affected by the holocord syrinx indicated by the shaded white circle in the middle of the spinal cord cross-section. The top panel in (**D**) shows sensory evoked potentials of a healthy subject derived from level C6, below are the evoked potentials elicited at levels C6 and C8 of Pat41. Patient's dSSEPs, assessing dorsal-column integrity, were normal while CHEPs of the same dermatomes, revealing spinothalamic tract function, were abolished.

Kinematic analysis

Kinematic analysis revealed that upper limb motor function was barely affected by the extensive holocord syrinx. Only one patient showed some deviations at performing the reaching task revealed by slightly

deteriorated kinematics (**Figure 4.3B**) when compared to healthy control (**Figure 4.3A**). On average patients showed upper limb movements comparable to controls (**Figure 4.3C**). ANOVA revealed no difference in kinematic measures between groups ($F = 1.7$, $p = 0.174$). The movement variability (**Figure 4.3D**) in both groups tended to be smaller during the *reaching* sub-movement compared to the *retract-to-mouth* movement (**Figure 4.3E**). Interestingly, healthy control subjects had a trend of greater endpoint variability than patients, though the difference was not statistically significant. The success rate was 100% in both groups. HPR did not differ between healthy controls and patients while the movement velocity tended to be higher in controls, both during *reaching* and *retract-to-mouth* sub-movement, though lacking statistical significance (**Figure 4.3F**).

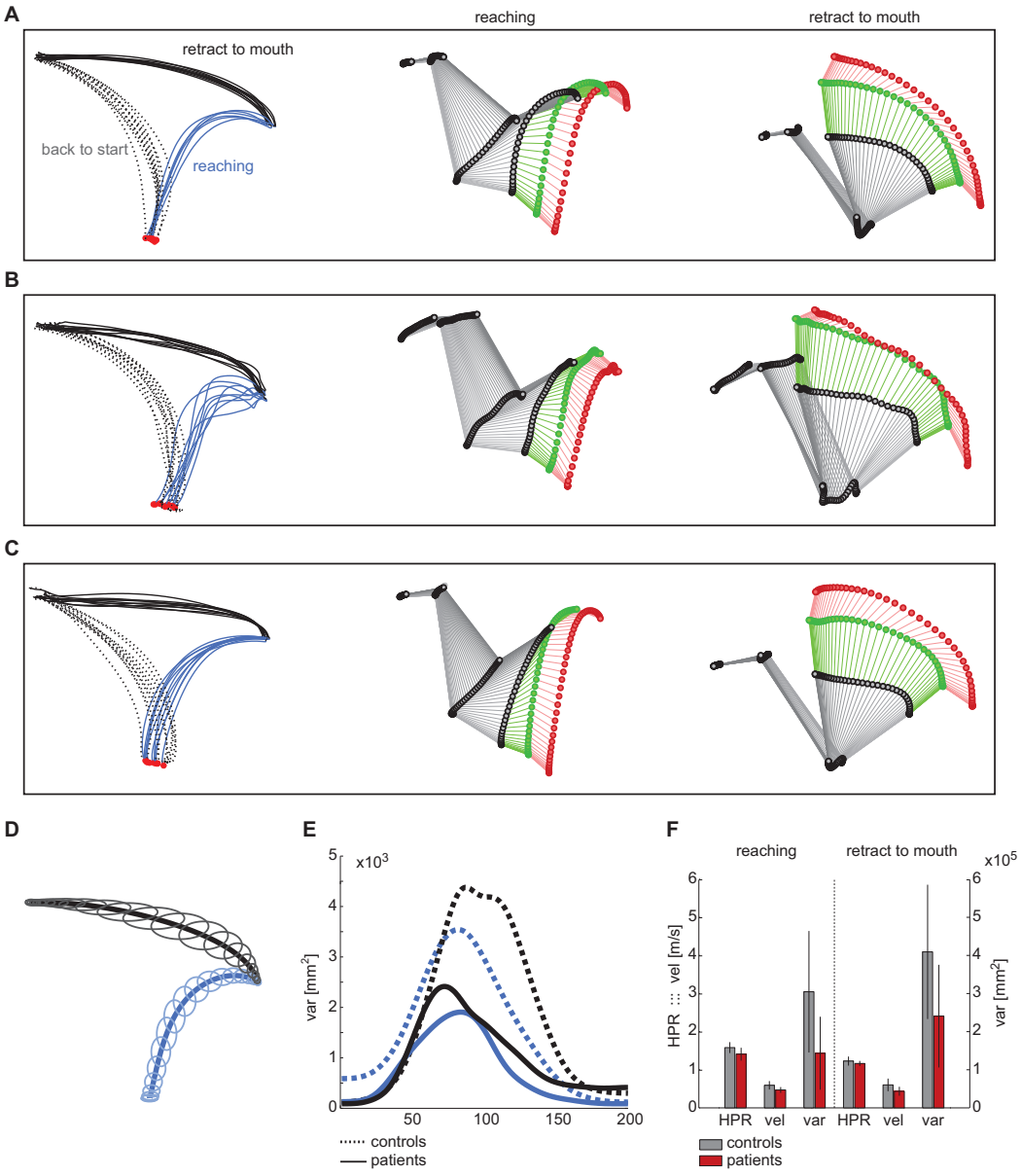

Figure 4.3 Reaching kinematics and performance. (**A**) The endpoint trajectories of 10 trials of a healthy control subject are shown in the top panel. Movement onset is marked by a red dot. The reaching movement was divided into the three sub-movements *reaching* (blue line), *retract-to-mouth* (black solid line), and *back-to-start* (dashed black line). The patient who performed worst in the reaching task (**B**) and an average patient example (**C**) are shown. Endpoint variability was calculated as the area of an ellipse where the half axes correspond to the standard deviation of the endpoint in horizontal and vertical direction (**D**). The variability of both groups for the *reaching* and *retract-to-mouth* sub-movements is plotted in (**E**). The kinematic readouts HPR, endpoint-movement velocity, and endpoint variability did not statistically differ between patients and healthy controls (**F**).

4.5 Discussion

The present findings in patients with holocord syringomyelia show that, despite extensive morphological alterations, spinal cord plasticity may still allow for normal limb movements. This impressive plasticity of the spinal cord is particularly startling considering the diminished amount of cross-sectional neural tissue area and major deformations of the spinal cord anatomy. While previous studies mainly focused on reporting specific symptoms of developing syringomyelia, this is the first study in holocord syringomyelia to address the capacity of specific spinal pathways to cope with extensive morphological changes and, despite these pathological alterations, to enable normal complex upper limb movements. The findings reveal that, comparable to the brain, the spinal cord has a high capacity to overcome large-scale morphological changes in slowly emerging space-consuming abnormalities (Desmurget et al. 2007, Feuillet et al. 2007).

Distinct manifestation of motor and sensory deficits

Clinical scores assessing upper limb function in these patients with holocord syringomyelia revealed only minimal deficits in terms of muscle strength, quality and success of movement while sensation was particularly affected. In accordance with clinical motor testing the electrophysiological assessments of motor pathways (MEP addressing corticospinal-tract conductivity, NCS evaluating α-motoneuron damage) showed unsuspicious findings. This is in contrast to findings in traumatic incomplete SCI where lesions of the cervical cord (including Central Cord Syndrome with circumscribed lesions of the central gray matter) show altered neurophysiological recordings and lead to obvious motor impairments of the upper limbs (Curt and Dietz 1996a, Curt and Dietz 1996b, Roth et al. 1990, Ulrich et al. 2013). However, sensory assessments (clinical and electrophysiological) provided a higher sensitivity to disclose the vulnerability of specific fiber tracts (Masur et al. 1992). Segmental sensory function assessed by dSSEPs (to examine dorsal column-medial lemniscal pathway integrity) and by dCHEPs (to reveal lateral spinothalamic-tract function propagating information on pain and temperature) was significantly

affected (Haefeli et al. 2013, Kramer et al. 2012) revealing considerable impairments in dCHEPs while dSSEPs were normal in half of the patients. The reason for the differing sensitivity of EPs may lie within the anatomy of spinal tracts (i.e. lateral spinothalamic tract decussating on the spinal level of entry) affected by the centrally located syrinx and a higher vulnerability of pain-conducting fibers (i.e. thinly myelinated Aδ- and unmyelinated C-fibers).

Upper limb function and kinematic measures

Kinematic data confirmed the preservation of gross upper limb motor function and only when looking at specific parameters of arm-/hand movements, a few trends became visible. The movement velocity tended to be higher in control subjects, which might be partly because of their lower mean age. Since MEP amplitudes and latencies were not impaired in patients and muscle strength was not reduced, the decrease in movement speed may also be attributed to the alteration in sensibility. During closed-loop control of targeted arm-/hand movements, timely and appropriate sensory information is required for correct movement execution. Accordingly, deterioration of somatosensory information was shown to have detrimental effects on motor control in patients with proprioceptive deficits (Gordon et al. 1995, Sainburg et al. 1993). However, the higher variability by tendency of the endpoint trajectory during the *retract-to-mouth* movement in controls was rather surprising. A possible explanation may be the higher movement velocity, which leads to higher endpoint variability in target-aimed movements (Meyer et al. 1988). Generally, the movements showed great spatial inter-subject variability in terms of endpoint trajectory both in patients and controls, which is in contrast to small spatial lower limb endpoint variability during walking (Winter 1992). The latter movement is probably less dependent on voluntary supraspinal control but more on sensory-motor integration on a spinal level.

Spinal cord plasticity

In patients with acutely (i.e. rapidly) progressing syringomyelia associated symptoms are typically unspecific and diverse, ranging from increasing pain symptoms to changes in sensation and eventual muscle weakness, which may emerge very rapidly (McIlroy and Richardson 1965, Milhorat et al. 2003, Muhn et al. 2002, Zager et al. 1990). Any secondary neurological deteriorations following SCI call for further investigations (Schurch et al. 1996, Vernon et al. 1982). In most studies there was no reliable relation between clinical findings and neither diameter and length nor level of the syrinx as measured by MRI (Emery et al. 1998, Grant et al. 1987, Jabbari et al. 1990, Schurch et al. 1996). The present study in highly chronic and slowly developing syringomyelia confirms this missing relation between the extent of a syrinx and clinical measures, which is probably most convincing in these presented cases with a holocord syrinx. Interestingly, even the reduction in remaining neural-tissue area by as much as 26% and involvement of the whole cervical cord area was not related to the clinical conditions. Obviously, a change in cross-sectional spinal cord area is not a valuable marker for potential axonal damage but may serve as an indicator for the extent of morphological changes. The objective of this study was to reveal the discrepancies between morphological changes and neural function by taking the extreme example of holocord syrinx. Comparable discrepancies can be observed in compressive spinal disorders such as chronic calcified disc protrusions and extramedullary spinal tumors where, despite massive space occupying conditions with enormous thinning of the cord, patients may also present themselves with minor and unspecific symptoms (Chamberlain and Tredway 2011, Gezen et al. 2000). Common to all these disorders is that they develop on a very slow time scale that likely spans over several years. In the presented 4 cases with post-traumatic holocord syrinx following thoracic or lumbar SCI the mean latency between incident of SCI and inclusion into this study ranged between 19 and 34 years. The underlying mechanisms enabling morphological plasticity while preserving complex function are not well understood. Obviously, a well-coordinated adjustment of neural and glial tissue as well as vascular and connective tissue is required. If and to what extent some of the underlying mechanisms may be in

principle comparable to reparative changes (i.e. are there common elements of spinal plasticity after acute trauma and slowly developing morphological changes?) is unclear.

Limitations

This study is clearly limited by the relatively small number of subjects with holocord syringomyelia available to us. The intention of this study was not to investigate the etiology and progression of the disorder, nor was it intended to serve as a basis on which to make decisions regarding surgical intervention.

4.6 Conclusion

Analogous to the brain, extensive morphological alterations of the spinal cord may develop with only minor and unspecific clinical symptoms. While upper- and lower limb function appeared unimpaired specific sensory assessments were most sensitive to reveal distinct alterations. In slowly progressing disorders spinal cord plasticity can overcome large-scale morphological changes enabling unimpaired functioning on a behavioral level.

Appendix

Corticospinal tract plasticity after spinal cord injury supports greater recovery in humans and monkeys than rats

Lucia Friedli, Ephron S. Rosenzweig, Quentin Barraud, Martin Schubert, Nadia Dominici, Lea Awai, Jessica L. Nielson, Pavel Musienko, Hui Zhong, Sharon Zudnowski, Roland R. Roy, EMSCI Study Group, M.S. Beattie, J.C. Bresnahan, Adam R. Ferguson, Armin Curt, V. Reggie Edgerton, Mark H. Tuszynski, and Grégoire Courtine

Manuscript in preparation

A.1 Abstract

Incomplete spinal cord injury in experimental animals and humans is accompanied by spontaneous improvement in function. However, this recovery is thought to be superior in less complex mammalian species. To test this assumption, we compared the impact of a lateral cervical hemisection in rats, monkeys, and humans. Standardized assessments of kinematics and muscle activity revealed that monkeys and humans showed greater recovery than rats, both for locomotion and, even more strikingly, hand function. In rats and monkeys, functional improvements correlated with multi-level plasticity of bilateral corticospinal projections, but only monkeys exhibited substantial growth and sprouting of corticospinal axons in sub-lesional spinal segments. Motor cortex stimulation in humans suggested similar plasticity of corticospinal projections. Our results show that corticospinal tract plasticity is a fundamental mechanism of recovery after spinal cord injury. The bilateral architecture of the primate corticospinal system augments the efficacy of this mechanism, providing a target for therapeutic development.

A.2 Introduction

Despite the regenerative failure of severed axons after spinal cord injury (SCI) (Lu et al. 2012), it is well established that partial lesions of the adult mammalian spinal cord often are associated with various degrees of spontaneous functional recovery, both in experimental animals (Courtine et al. 2005, Courtine et al. 2008, Rosenzweig et al. 2010, Weidner et al. 2001) and humans (Levi et al. 1996, Curt et al. 2008). In fact, nearly half of injured individuals regain significant levels of control of arm and leg movements after a few months of recovery post-SCI (Fawcett et al. 2007). Notwithstanding these recurring clinical observations, there is a consensus that spontaneous recovery of function is limited in humans compared to common experimental species, such as rodents, after similar severities of SCI (Dietz and Curt 2006). This assumption had a strong impact on translational SCI research, often casting doubt on the clinical relevance of therapeutic interventions that are nearly exclusively developed and tested in rodent models of SCI (Dietz 2010). However, this important issue has never been experimentally addressed conclusively. Here, we aimed to examine the assumption that spontaneous restoration of function after partial SCI is greater in rodents compared to nonhuman primates and humans, and sought to provide mechanistic insights that could account for putative inter-species differences in the extent of functional recovery post-SCI.

To circumvent the problem of heterogeneous and uncharacterized damage in humans, we selected a specific type of SCI that produces a distinguishable functional deficit termed Brown-Séquard syndrome (Brown-Sequard 1868). This syndrome results from a unilateral SCI and is clinically characterized by the complete loss of motor function on the ipsilesional side and deficits in pain and temperature sensation on the contralesional side (Brown-Sequard 1868). Lateral spinal cord hemisections accurately mimic Brown-Séquard syndrome in experimental animals (Courtine et al. 2008, Filli et al. 2011, Rosenzweig et al. 2010), and thus are frequently used for developing therapeutic strategies. Although the prevalence of Brown-Séquard syndromes is low, extensive functional recovery has been documented in the individuals showing well-defined hemiplegia in the sub-acute phase of SCI (Brown-Sequard 1868, Dlouhy et al. 2013, Little and

Halar 1985, Roth et al. 1991). Spontaneous restoration of motor functions after a lateralized SCI in humans compared to experimental animals and the translational mechanisms underlying this recovery across mammals remain poorly characterized.

To address this issue comprehensively, we first leveraged the database of the European multicenter study about SCI (EMSCI) to conduct an epidemiologic analysis of the recovery profile among more than 400 individuals with varying degrees of lateralized spinal cord damage. We then modeled this type of lesion in rats and monkeys to compare the degree of spontaneous improvement across species, and identify possible mechanisms underlying differing spontaneous recovery in rats, monkeys, and humans (Rosenzweig et al. 2010). Our combined results reveal that the emergence of spinal cord decussating corticospinal fibers and bilateral motor cortex projections during primate evolution (Rosenzweig et al. 2009) support greater spontaneous recovery of locomotion and hand function in monkeys and humans compared to rats. These new findings stress the need to develop novel experimental models and specific therapeutic strategies to take full advantage of this unique anatomical substrate for recovery after SCI in humans.

A.3 Materials and methods

Experimental animal models and human subjects

EMSCI database

Recovery of upper and lower limb function were analyzed in a total of 437 individuals who suffered a cervical SCI. All individuals were included in the EMSCI database (www.emsci.org). For each subject, we computed a laterality index that quantified the extent of asymmetry in functional deficits at 2 weeks post-SCI. This index was derived from the international standards for neurological classification of spinal cord injury (ISNCSCI), which combine both sensory (pinprick) and motoric (motor score) evaluations. Pinprick scores, which primarily evaluate the integrity of the spinally decussating spinothalamic tract, contributed to the contralateral sensory score. Motor scores were calculated, for each limb and side, as the combined ASIA motor scores of all the segments below the lesion. The segments C2 to T1 contributed to upper limb motor scores, while segments T2 and below contributed to lower limb motor scores. Sensory and motor scores were summed to generate a sensorimotor score for each limb and side. The laterality index was computed as the difference between left and right sensorimotor scores divided by their sum. Consequently, a value equal to 0 would correspond to perfectly symmetrical deficits. Instead, a value equal to 1 would correspond to a pure Brown-Séquard syndrome. Functional recovery was computed as the relative increase in sensorimotor scores for each limb and side at 6 or 12 months compared to evaluations carried out at 2 weeks post-SCI.

Human subjects

We monitored recovery of motor functions in individuals who presented distinct lateralized sensorimotor deficits classified as Brown-Séquard syndrome. Three patients, one male and two females, met this criterion. The male suffered a traumatic SCI at the C5 level that led to complete paralysis on one side of the body. He showed a laterality index of 0.82 **(Figure A.1)**. The two additional subjects had experienced an ischemic injury at thoracic level Th5, and a disc prolapse at Th8, which led to laterality

index of 0.65 and 0.50, respectively. These two patients had deficits restricted to the legs. The patients had not suffered from any other neurological disorder or pre-existing gait impairment. All patients followed a conventional SCI rehabilitation program. Recovery of complex motor functions was compared to the same recordings performed in a total of 33 healthy human subjects. The Zurich Cantonal ethics committee approved all aspects of the study. All participants provided written informed consent.

Monkeys

A total of 14 male rhesus monkeys (Macaca mulatta) aged 5 -18 years (mean 9.6 ± 4.1 years) were studied. No effects of age were observed on any of the variables reported herein. All surgical and experimental procedures in these experiments were carried out using the principles outlined by Laboratory Animal Care (National Institutes of Health Publication 85-23, revised 1985) and were approved by the Institutional Animal Care and Use Committee (IACUC).

Rats

A total of 30 female adult rats (Lewis) were studied (~220 g body weight). Animals were housed individually on a 12 h light/dark cycle, with access to food and water *ad libitum*. Temperature (22 ± 1 °C) and humidity (40 - 60 %) in the animal facilities were maintained constant in accordance to Swiss regulations for animal housing. The Veterinarian Office of the Cantons of Zurich and Vaud, Switzerland approved all aspects of the study.

Experimental surgical procedures

EMG electrodes

All surgical procedures used have been described previously (Courtine et al. 2009, Musienko et al. 2011, Rosenzweig et al. 2010). Under aseptic conditions and general anesthesia (1-2.5% Attane Isoflurane, Piramal Healthcare Limited, Mumbai, India), both rats and monkeys received bipolar intramuscular EMG

electrodes (AS632, Cooner Wire, Chatsworth, CA, USA) into selected hindlimb and forelimb muscles. The electrodes were connected to a head-mounted connector in rats, and an implanted recording system in monkeys (Konigsberg Instruments, Pasadena, CA, USA). In subsets of rats and monkeys, the following muscles were implanted: soleus and tibialis anterior for both hindlimbs; the biceps brachii, triceps brachii, extensor digitorum communis and flexor digitorum profundis of the ipsilesional forelimb. The ipsilesional pollicis brevis profundus also was implanted in monkeys. The proper location of EMG electrodes was verified post-mortem. Analgesia and antibiotics were provided post-surgically under monitoring of certified veterinaries.

Cortical electrodes

A subset of rats (n = 8) was implanted with an epidural monopolar electrode over the hindlimb area of the contralesional motor cortex to deliver stimulation. A reference electrode was positioned near the shoulder girdle (van den Brand et al. 2012).

Lesion

After completion of pre-injury behavioral recordings, a second surgery was performed. A partial laminectomy followed by a lateral hemisection of the spinal cord was made at the C7 spinal segment. In both rats and monkeys, a surgical micro-knife was mounted on a stereotaxic arm, positioned at the spinal midline and midway between the C5 and C6 dorsal laminae. This rostrocaudal position corresponds to the C7 spinal cord segment, as previously described (Rosenzweig et al. 2010). A micro-scissor was used several times to cut all the entire grey and white matters lateral to the inserted micro-knife. For all the experimental subjects, the segment containing the lesion was reconstructed using continuous series of Nissl stained sections. The lesion area was delimited for each section, and the area of maximum damage projected into a plane to obtain a reconstruction of the lesion extent (**Figure A.2d,e**).

Behavioral testing tasks

Locomotion

Rats, monkeys, and humans were tested on a motorized treadmill over a range of speeds. A Plexiglas enclosure was used to maintain the rats and monkeys in position while enabling kinematic recordings of the stepping performance. Food reward was used for positive reinforcement. The more comfortable speed to obtain consistent stepping patterns over the entire course of the recovery was selected for further analysis. This corresponded to 9 cm/s in rats, 0.47 m/s in monkeys, and 4 km/h in humans. A total of 10 consecutive steps were recorded and extracted for further analysis. To evaluate skilled locomotion, rats (n=9) and human subjects (n=3 patients; n=4 healthy control subjects) were instructed to walk along a horizontal ladder with evenly spaced rungs. Ten successive trials along the ladder were performed.

Hand function

To examine manual dexterity, a skilled motor task thought to reflect the functional integrity of corticospinal projections to the hand musculature was used. Rats and monkeys were trained over several subsequent sessions to retrieve food rewards from a stick until they reached a stable performance. Monkeys and human subjects were instructed to retrieve a grape, while the rats were presented with a 2 mm piece of chocolate. Monkeys and human subjects were seated. Rats were standing quadrupedally. The subjects were requested to perform 10 trials, and the number of successful food retrievals was recorded for each session.

Time points

Both rats and monkeys were recorded prior to the lesion, and at regular intervals post-lesion until 2 or 6 months post-injury, respectively. At this stage, both rats and monkeys had reached a plateau, i.e., when no or limited improvements occur (Courtine et al. 2008, Rosenzweig et al. 2010). To compare rats, monkeys, and humans at comparable time-points, we focused the analysis on three salient time-points: pre-lesion, early, and chronic. Early corresponded to the time when the subjects could locomote on the treadmill despite paralysis of the ipsilesional limbs, and could reach the food reward with the ipsilesional limb, but

failed to retrieve the item. In humans, recordings at chronic time-points were obtained between 8 and 12 months post-SCI.

Data acquisition and analysis

Kinematics and electromyographic recordings

Bilateral leg or unilateral arm kinematics were recorded using 12 infrared motion capture cameras (200 Hz; Vicon) in rats and humans, and 4 TV cameras (100 Hz, Basler Vision Technologies) for monkeys. Reflective markers were attached to the shaved skin of rats and humans overlying leg or arm landmarks for locomotion and hand function assessment, respectively. Reflective painting was used for monkeys. The landmarks for the legs were the iliac crest, greater trochanter, knee joint, malleolus, fifth metatarsal, and outside tip of the fifth or fourth digit. The landmarks for the arm were the anterior border of the scapula, head of the humerus, elbow joint, distal head of the ulna, metacarpo-phalangeal joint, and outside tip of the third digit. The body was modeled as an interconnected chain of rigid segments, and joint angles generated accordingly. In humans, bipolar surface electrodes (1 cm diameter, electrode separation of 1 cm) connected to a wireless transmitter (Myon) were placed over leg (medial gastrocnemius, soleus, tibialis anterior) and arm (biceps brachii, triceps brachii, extensor digitorum communis and flexor digitorum superficialis) during locomotor and hand function assessments, respectively. A ground electrode was placed on the wrist. In all the species, signals were sampled at 2 kHz, amplified, band-pass filtered (10-1000 Hz), stored, and synchronized on-line (Vicon Nexus) or off-line (SIMI) for kinematic analysis.

Electrophysiological recordings

In rats, access of the motor cortex to leg motoneurons was tested under fully awake conditions while the animals were suspended in a harness. Five trains of stimuli (0.2 ms, 10 ms pulse length, 300 Hz, 0.5-1.5 mA) and 5 single pulses (0.2 ms, 0.5-1.5 mA) were delivered through the chronically implanted cortical electrode. The same rats were tested prior to the lesion and weekly after the lesion for 2 months.

Stimulation bouts were separated by 90 sec. In humans, transcranial magnetic stimulation (TMS) was applied over the leg area of the motor cortex. The coil was positioned over the location eliciting the largest possible responses in the leg muscles, which corresponded to Cz (Schubert et al. 1997). After establishing the positioning of the coil, a recruitment curve was performed until reaching 100% of the output. In both rats and humans, peak-to-peak amplitude and latency of evoked responses were computed from EMG recordings from the left and right TA muscles.

Gait data analysis

A minimum of 10 step cycles was extracted from a continuous bout of stepping on the treadmill for each experimental condition and subject. A total of 99 parameters quantifying gait and kinematic features were computed for each limb and gait cycle according to methods described in detail previously (Courtine et al. 2008, Courtine et al. 2009, Dominici et al. 2012, Musienko et al. 2011). These parameters provide a comprehensive quantification of gait pattern characteristics ranging from general features of locomotion to fine details of individual limb motion. For the ladder, 20 step cycles were extracted for analysis. Additional parameters related to the positioning of the foot with respect to the successive rungs of the ladder were calculated to assess the precision of foot placement during gait (Dominici et al. 2012). A PC analysis was applied on all computed parameters with two objectives: (i) assess the degree of locomotor recovery compared to pre-lesion or healthy subjects (Dominici et al. 2012), and (ii) extract, for each limb and species, the most relevant parameters to account for lesion-induced changes in ipsilesional and contralesional leg movements (Beauparlant et al. 2013). For each species, all computed parameters were centered and reduced to obtain dimensionless values ranging from -1 to 1. PC analysis was applied on the normalized parameters for each species and for all species combined. Averaged scores for each limb and conditions were extracted and the relative degree of functional recovery was measured as the 3-D distance between pre- and postlesion (early and chronic) data points in the space created by PC1-3 (Dominici et al. 2012). Parameters with high factor loadings ($|value| > 0.5$) on PC1 and PC2 were extracted and regrouped into functional clusters (Beauparlant et al. 2013).

Hand function data analysis

For each species and time-point, kinematic and EMG data were extracted from 5 representative reaching movements. The trajectory of the hand was segregated into the different phases of the movement: start, reach, grasp, retrieval, and end. To compute the consistency of limb endpoint trajectories, we applied a PC analysis on the 3- D coordinates of the hand marker during the reach phases of all trials. The consistency of limb endpoint trajectories was calculated as the percent of variance explained by the first PC. The degree of co-contraction between proximal and distal pairs of antagonist muscles was measured as the percentage of overlapping area between two EMG traces (Winter 1990). EMG signals were rectified and filtered with a 4_{th} order zero-phase shift Butterworth filter with a cut-off frequency of 30 Hz. The co-contraction Index between pairs of antagonist muscles (EMG1, EMG2) during reaching and grasping was computed as follows:

$$\text{Cocontraction Index} = 2 * \frac{\int \min[\text{EMG1}(t), \text{EMG2}(t)]dt}{\int \text{EMG1}(t)dt + \int \text{EMG2}(t)dt}$$

where EMG1 and EMG2 are the EMG activity of flexor and extensor muscles normalized to the maximum value observed during the movement, while min denotes the minimum between the activity of both muscles at time t.

Anatomical procedures

Tracing

Rats and monkeys underwent anterograde tracing of corticospinal projections from both left and right motor cortexes using tracers. All animals were anesthetized deeply as reported above. In monkeys biotinylated dextran amine (BDA; 10% solution in H_20; 10,000 molecular weight; 150nl/site; Molecular Probes) was injected into 127 sites spanning the arm, trunk, and leg regions of the right motor cortex. Dextran-conjugated Alexa488 (D-A488) was injected using the same methods into the corresponding

coordinates in the left motor cortex. Seven weeks later, monkeys were anesthetized deeply and perfused transcardially with a 4% solution of paraformaldehyde. For rats, BDA (10% solution in H_20; 10,000 molecular weight; 500nl /site) was injected into 10 sites spanning the forelimb, trunk, and hindlimb regions of the right or left motor cortex. Three weeks later, rats were anesthetized by an intraperitoneal injection of 0.5 ml sodium pentobarbital (50 mg/mL) and perfused transcardially with approximately 80 ml Ringer's solution containing 100'000 IU/L heparin (Roche) and 0.25% $NaNO_2$ followed by 300 ml of cold 4% phosphate buffered paraformaldehyde, pH 7.4, containing 5% sucrose.

Tissue processing

The spinal cord dura was removed and the spinal cord was cut in the transverse plane into blocks, using the nerve roots as a guide for the spinal levels. The block containing the lesion was sectioned in the horizontal plane on a freezing microtome or a cryostat set at 30 µm intervals. Analogous blocks were obtained from the intact animals. Blocks containing segments C3-C6 and C8-T2 were sectioned in the transverse plane on a freezing microtome or a cryostat set at 40 µm. Cut tissue sections were stored at -20°C for monkeys and at 4°C for rats in cryoprotectant (25% glycerin, 30% ethylene glycol in 0.5 M phosphate buffer). Lesion extent was assessed using a 30-µm-thick horizontal section stained for Nissl substance. Transverse sections from the tissue blocks immediately rostral and caudal to the lesion block (segments C3-C4 and C8-T1) were selected for analysis of corticospinal tract and 5-HT fiber density. Our standard protocols were used to detect traced corticospinal fibers (Rosenzweig et al. 2010, van den Brand et al. 2012) and 5-HT fibers using goat anti-5-HT antibodies for monkeys (Immunostar; 1:10,000 in TBS-X) and rabbit anti-5-HT antibodies for rats (Sigma Aldrich; 1:5000 in blocking solution containing 4% NGS).

Quantification

Image capture and manipulation were performed as described previously (Rosenzweig et al. 2010, van den Brand et al. 2012). For corticospinal fiber density quantification each of 3 sections for monkeys and 5 sections for rats were randomly selected per animal. The fiber density of the gray matter were obtained

using confocal stacks per animal acquired with standard imaging settings and analyzed using custom-written Matlab (MathWorks) scripts according to previously described methods (van den Brand et al. 2012). Additionally, the number of labeled axons crossing the spinal cord midline was counted manually in each section used for the fiber density analysis. For 5-HT quantification of monkey sections, Stereo Investigator was used to outline lateral motor pools under low magnification and generate optical fractionator sampling sites. With a 100x objective, intersections of 5-HT-labeled axons with the inclusion lines of these sampling sites were marked. For rats, the same regions were quantified using the same methods as described for corticospinal tract axons. Serial reconstructions of some CST axons were performed as described previously for both monkey and rat sections below the level of injury (Rosenzweig et al. 2010, van den Brand et al. 2012). All the evaluations were performed by an investigator who was blind to experimental conditions.

Syndromic analysis

To evaluate the effect of species on the integrated syndromic outcome after SCI (Ferguson et al. 2013), we harnessed non-linear principal components analysis (NLPCA). This method uses a combination of optimal scaling and variance-maximization procedures to detect coherent patterns in data involving linear or non-linear relationships (Linting et al. 2007). We performed separate NLPCA extractions for rat-monkey and rat-human data using variable subsets that allowed direct cross-species comparisons. Datasets from kinematics, food-retrieval success, and anatomical measures were manually curated and combined into a single large dataset for monkeys and rats. Treadmill and ladder locomotion kinematics and neurophysiological measures were combined from human and rat data. Bivariate correlation matrices were created for each combination of outcomes. Syndromic analysis was performed in SPSS Categories v.1.9, to generate syndromic variables (PC1-2) specific to either rat-monkey or rat-human comparisons. PC1 is the shared variance (%) of all measures as they move together in a multivariate space, with each measure loading (weighted arrows) onto PC1 based on their respective correlation to the entire syndrome (PC1, **Figure A.13c, d**).

Statistics analysis

All data are reported as mean values ± s.e.m. Statistical evaluations were performed using one-way ANOVA for neuromorphological evaluations, one-way repeated-measures ANOVA for functional assessments, and unpaired two-tailed t-tests for syndromic analysis. Tukey's post-hoc test was applied when appropriate.

A.4 Results

Functional recovery correlates with SCI laterality

We implemented the international standards for neurological classification of spinal cord injury (ISNCSCI) to conduct a repeated prospective assessment of functional recovery during 1 year after a cervical SCI in 437 humans (**Figure A.1a**). To determine the relative degree of SCI laterality, we developed a laterality index that ranged from 0 (symmetric injury equally affecting both sides of the body) to 1 (asymmetric injury primarily affecting one side of the body) based on the relative difference between left and right sensorimotor scores evaluated at 2 weeks post-SCI (see Methods). More than 80% of analyzed individuals showed laterality values below 0.4 (**Figure A.1b**), indicating bilateral and symmetrical functional impairment. Only 4 out of the 437 studied subjects exhibited clinically a pure Brown-Séquard syndrome with predominant unilateral motor deficits and crossed spinothalamic impairment (**Figure A.1b**). Magnetic resonance imaging in these individuals revealed white matter sparing on one side of the spinal cord, as expected based on functional deficits (**Figure A.1a** and **Figure A.2f**).

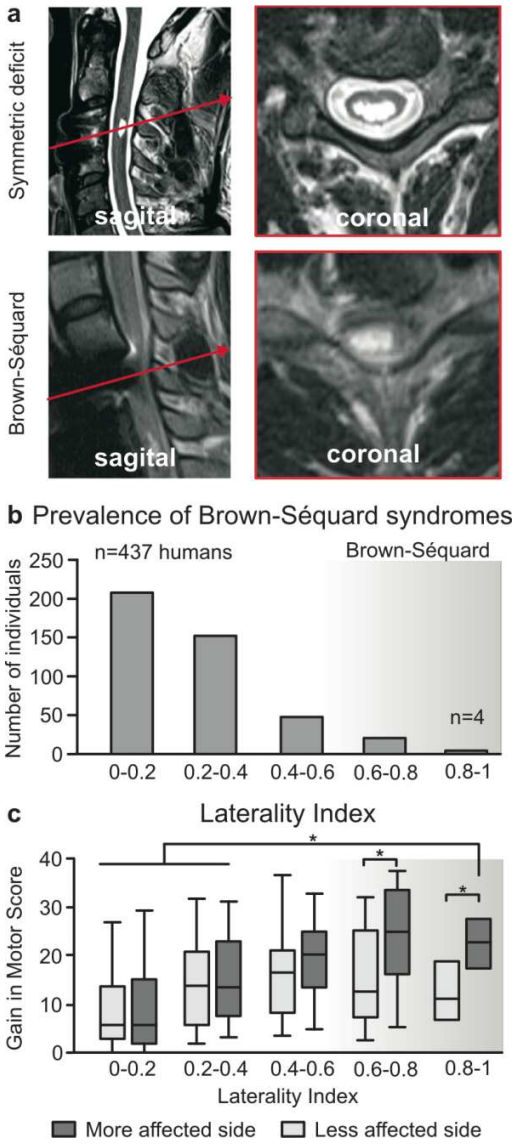

Figure A.1: Functional recovery gradually increases with SCI laterality in humans. (a) Visualization of spinal cord damage through MRI in two individuals with symmetric (left) and lateralized motor impairments. **(b)** SCI Laterality was defined as the relative difference between motor scores of the left and right sides, termed laterality index. The histogram plot reports the distribution of this laterality index across a population of 437 individuals with a cervical SCI (EM-SCI platform). The shaded area indicates individuals clinically classified with a Brown-Séquard syndrome. **(c)** Histogram plots reporting, for each range of laterality index, the mean gain in upper and lower motor scores in the chronic compared to sub-acute stage of SCI. The horizontal bars report the median. The upper and lower bars correspond to the 75% and 25% percentile of data, while the error bars correspond to the 90% and 10% percentile of the data. * indicates significant differences at $p < 0.05$ compared to non-marked conditions.

We sought to assess whether the initial degree of laterality post-injury influenced the extent of recovery in the chronic stage of SCI following conventional rehabilitation. To this aim, we computed the relative gains in left and right motor scores between early (2 weeks) and late (6 to 12 months) time-points post-SCI. We found that improvements of motor function gradually increased with SCI laterality ($p < 0.0001$; **Figure A.1c**). Individuals with a laterality index above 0.5 (n = 25 individuals, 5.7%), who were clinically classified with a Brown-Séquard syndrome, regained extensive bilateral motor capacities.

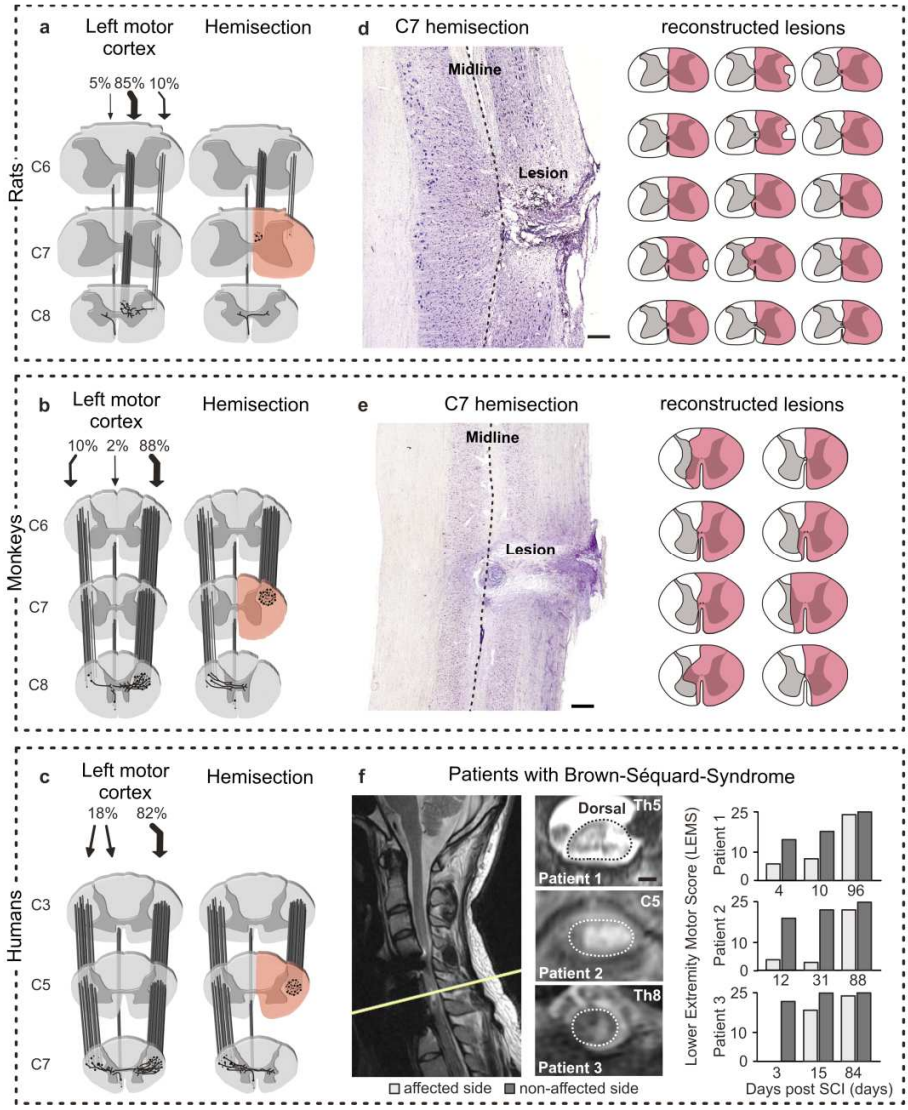

Figure A.2: Clinical cases and experimental models of Brown-Séquard syndrome. (a-c) Schematic representation of motor cortex axonal projections in the spinal cord white and grey matter of rats, monkeys, and humans before injury (or healthy), and after a lateral hemisection SCI. **(d-e)** Representative Nissl staining of a longitudinal section of the hemisected spinal cord in rats and

monkeys. For each experimental animal, the extent of the injured area was measured using camera lucida reconstructions. The surface of maximal damage per quarter of spinal cord was calculated to generate a measure of spared tissue. Scale bar: 300 µm and 1 mm for rats and monkeys, respectively. **(f)** MRI pictures through the transverse plane obtained in the 3 spinal-cord-injured individuals who participated in the longitudinal study. The level of the lesion is indicated in each MRI. Histogram plots report, for each individual, changes in left and right lower extremity motor scores (LEMS) over the course of the recovery.

Clinical cases and experimental models of Brown-Séquard syndrome

We next aimed to establish a direct comparison between rats, monkeys, and humans on the extent of spontaneous recovery of locomotion and hand function after a Brown-Séquard syndrome. For this purpose, we monitored changes in functional capacities in 3 individuals with a Brown-Séquard syndrome; one male with a traumatic cervical SCI (C5, laterality = 0.86), and two females with a SCI at the thoracic level (Th5 and Th8, laterality = 0.65 and 0.50, respectively), who all presented distinct unilateral motor impairments in the early stage of SCI (**Figure A.2f**). All the human subjects followed a conventional rehabilitation program. To compare recovery profiles across species, we placed a C7 lateral hemisection lesion in 15 rats and 8 rhesus monkeys (**Figure A.2d,e**). This lesion replicates a Brown-Séquard syndrome in animal models (Rosenzweig et al. 2010, Filli et al. 2011). Four out of the 8 monkeys were included in previous reports (Nout et al. 2012a, Nout et al. 2012b, Rosenzweig et al. 2010) and have undergone new analyses that are the subject of the present study. The hemisection resulted in flaccid ipsilateral hemiplegia for approximately 3 days in rats and 2 weeks in monkeys. After this period, both rats and monkeys were trained to step on a treadmill and to retrieve objects with their hand 3 times per week for 20 minutes per task. Recovery of locomotion and hand function of rats, monkeys, and humans was evaluated at early and chronic time-points under standardized conditions using similar kinematics and electromyography (EMG) measures across species.

Greater recovery of locomotor function in monkeys and humans compared to rats

In early post-injury stages, hemisected rats and monkeys essentially dragged their ipsilesional leg on the treadmill. We recorded high level of EMG activity in ankle flexors due to stretching of the paw, and near absent EMG activity in ankle extensors (**Figure A.3a, b**). Because hemiplegic human subjects could not step independently, we utilized the gait orthosis Lokomat to rhythmically move the left and right legs along pre-defined foot trajectories (**Figure A.3c**). Despite stepping-like movements, ipsilesional ankle muscles showed quiescent EMG activity while contralesional muscles exhibited robust and alternating EMG bursts (**Figure A.3a-c**). In the chronic stage of SCI, rats, monkeys, and humans with Brown Séquard syndromes regained plantar stepping movements on the ipsilesional leg with alternating recruitment of ankle muscles, although specific features of motor function remained clearly impaired (**Figure A.3a-c**).

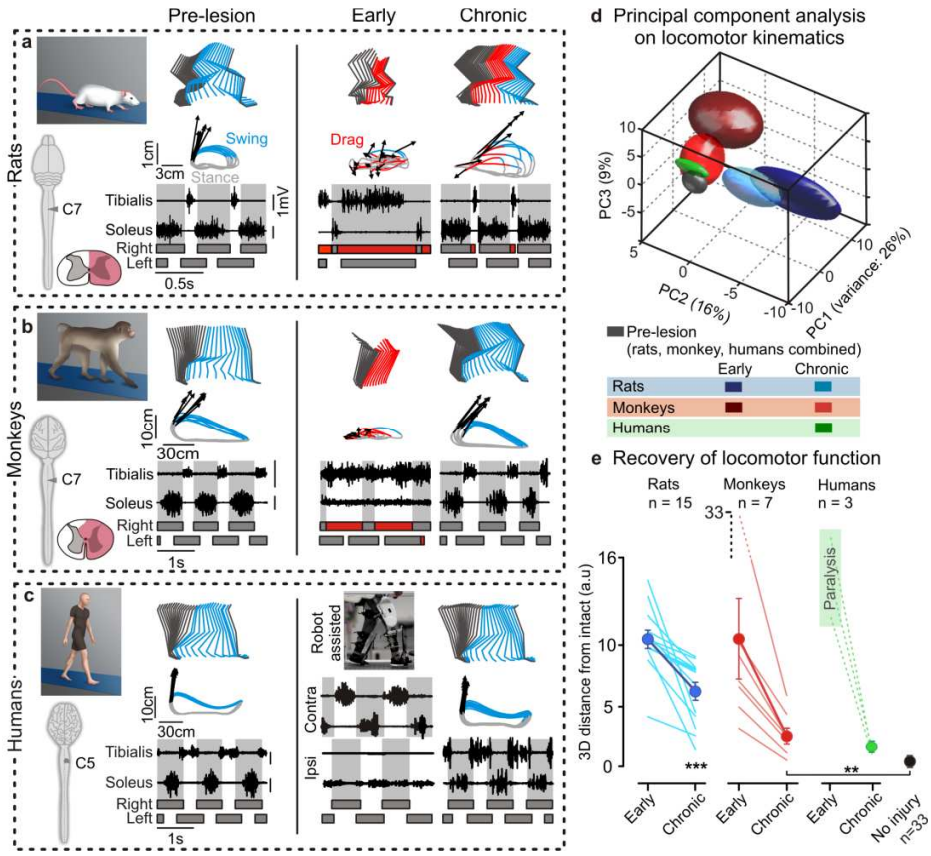

Figure A.3: Monkeys and humans show superior recovery of locomotion than rats. (a-c) Stick diagram decomposition of lower limb motion during stance (black) and swing (blue) together with successive limb endpoint trajectories during locomotion on a treadmill. The vectors indicate the direction and amplitude of foot acceleration of swing onset. The concurrent EMG activity recorded in the soleus and tibialis anterior muscles is shown at the bottom. The shared areas indicate the duration of the stance phases. Representative data are shown for rats, monkeys, and humans before the injury (or healthy), and at early and chronic time-points post-SCI. To monitor bilateral EMG activity in the hemiplegic patient at early time-points, we used the gait orthosis Lokomat that moved both legs in a rhythmic and alternated fashion. **(d)** PC analysis was applied on dimensionless variables (n = 99) characterizing locomotion kinematics of rats, monkeys, and humans. Least-squares spheres are traced to emphasize time- and specie-dependent gait recovery. **(e)** Individual (lines) and averaged (+/- s.e.m.) 3D distance between non-injured data points, and those measured at the early and late time-points (a.u., arbitrary units). **, *** denote conditions that were significantly different at $p < 0.01$ and $p < 0.001$, respectively.

We sought to quantify these residual deficits with objective, multifactorial measures. We first computed a larger number of kinematic parameters (n = 103,) to generate a comprehensive quantification of bilateral gait features (Courtine et al. 2009). We subjected these measurements to a principal component (PC) analysis (Dominici et al. 2012) that identified the most relevant parameters to characterize alteration of

ipsilesional versus contralesional leg movements (**Figure A.4a-c**). This multi-factorial analysis demonstrated that a Brown-Séquard syndrome alters the same components of bilateral locomotor control across species. However, analysis of pre-injury versus post-injury changes in gait parameters indicated that **5** rats retained significantly more pronounced deficits in the chronic stage of SCI compared to monkeys and humans ($p < 0.05$ for most comparisons with monkeys and humans, **Figure A.4d**). For example, all the studied species exhibited a significantly longer swing phase duration on the ipsilesional leg compared to the contralesional leg ($p < 0.05$, **Figure A.4d, top**). Prolonged swing duration is well-documented in hemi-paretic subjects with unilateral SCI (Courtine et al. 2005) or stroke (Chen et al. 2005). However, this asymmetry was markedly superior in rats (36%) compared to monkeys (25%, $p < 0.05$), and even more compared to humans (5%, $p < 0.05$).

To directly compare gait recovery between rats, monkeys, and humans, we normalized all the computed parameters related to the ipsilesional leg to pre-lesion (or healthy) values for each species, and applied a PC analysis on all the combined variables. In the PC space (**Figure A.3d**), the differences between gait patterns are proportional to the distance between the data points. We thus quantified recovery as the 3-D distance between post- and pre-lesion (or healthy) values in the PC space (Dominici et al. 2012). Rats exhibited significantly larger distances to pre-lesion data points at the chronic stage of the injury compared to monkeys and humans ($p < 0.05$, **Figure A.3e**). This analysis revealed that monkeys and humans showed a greater recovery of gait compared to rats after a Brown-Séquard syndrome.

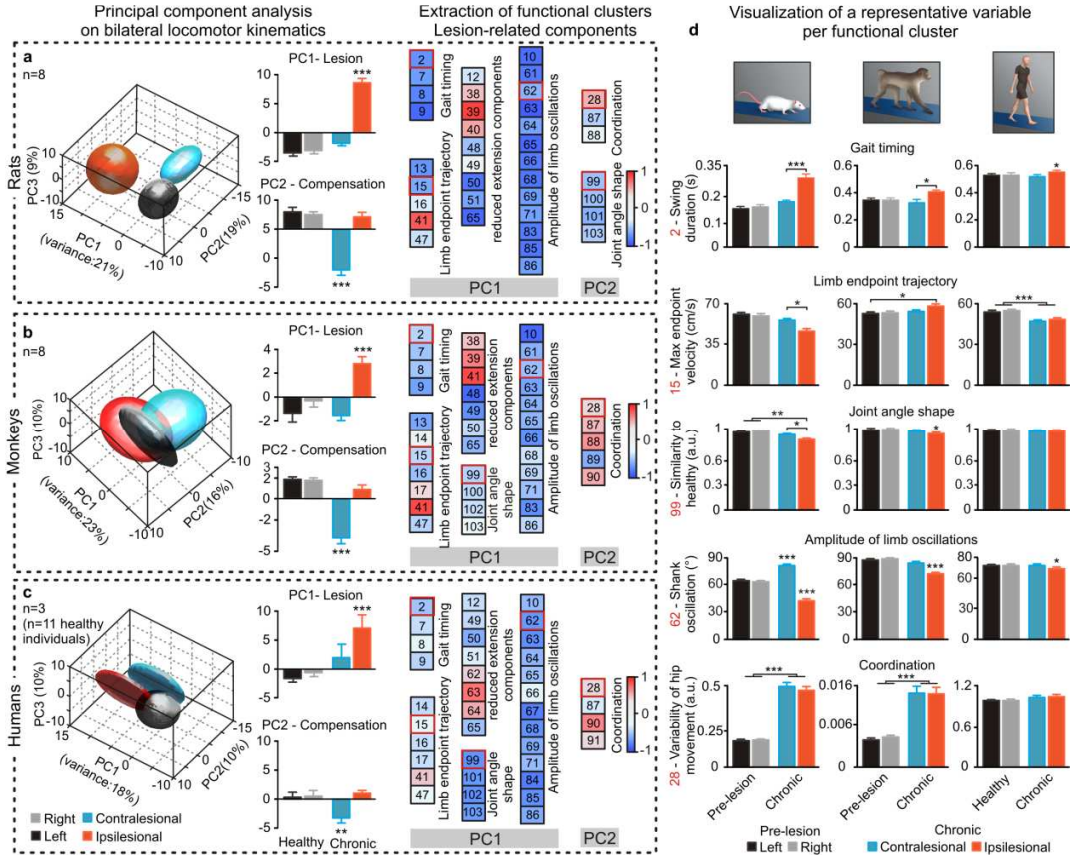

Figure A.4: Kinematic patterns underlying deficit and compensation during basic locomotion in rats, monkeys, and humans. **(a-c)** A PCA was applied on all the kinematic parameters measured for the left and right leg before the injury (or healthy), and in the chronic stage of the SCI. The complete overlap between left and right leg related clusters before the injury revealed the high degree of similitude between kinematic patterns of both legs in rats, monkeys, and humans. In the chronic stage, clusters corresponding to the contralesional and ipsilesional legs moved in opposite directions, indicating side-specific alteration of gait patterns. Histogram plots report the mean values of scores for the left and right legs before the injury (or healthy), and in the chronic stage of the lesion. For each species, PC1 and PC2 distinguished the ipsilesional and contralesional legs, respectively. We extracted the factor loadings for PC1 and PC2, and regrouped them into functional clusters that we named for clarity. The numbers refer to individual parameters (not detailed) that were calculated in the exact same manner in rats, monkeys, and humans. Strikingly, the same list of parameters loaded on PC1 and PC2 in rats, monkeys, and humans, although the analyses were conducted independently for each species. **(d)** To document gait features using more conventional representations, the histogram plots report the mean values of parameters with high factor loadings, which are framed in red in the clusters. These parameters are shown for the left and right legs before the injury (or healthy), and in the chronic stage of the lesion.*,**,*** denote statistical differences with $p < 0.05$, $p < 0.01$, and $p < 0.001$, respectively. Error bars, s.e.m.

Difference in gait control recovery was even more striking during more challenging conditions such as traversing a horizontal ladder. Rats failed to position their ipsilesional hindpaw onto the regularly spaced

rungs of the ladder ($p < 0.0001$, **Figure A.5a**). In contrast, the 3 spinal-cord-injured humans showed 100% success on this challenging task without prior practice (**Figure A.5b**). Humans performed well on the horizontal ladder task despite the use of distinct gait strategies compared to healthy subjects ($p < 0.01$, **Figure A.5c, d**). Monkeys were not tested on this task.

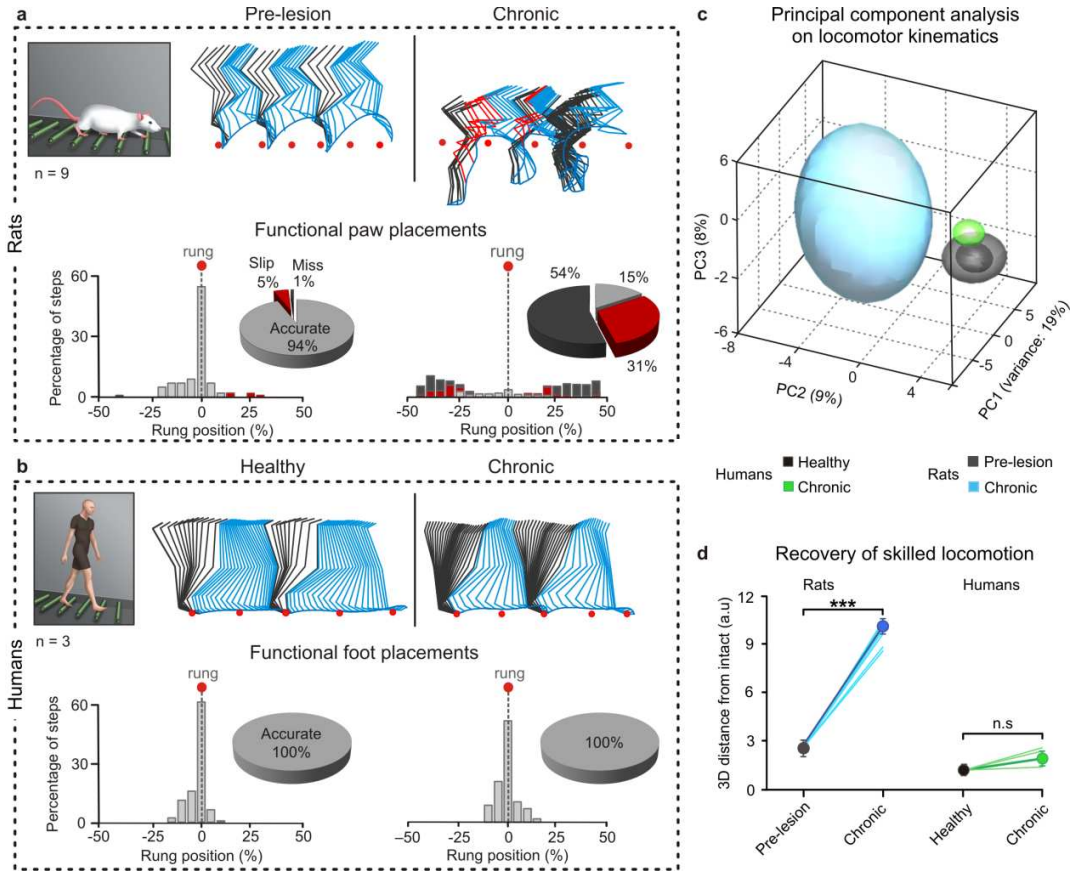

Figure A.5: Humans recovered the ability to walking along a horizontal ladder, but not rats. (a-b) Stick diagram decomposition of lower limb motion during stance (black) and swing (blue) during a continuous sequence of locomotion along the equally spaced rung (red) of a horizontal ladder. Functional foot placement was measured as the relative positioning of the ipsilesional foot with respect to two successive rung positions (red dots). The number of occurrence per 5% bin is reported together with the percentage of accurate, slipped, and missed placements. **(c)** PC analysis was applied on all the kinematic parameters (n=105) measured for the ipsilesional leg before the injury (or healthy), and in the chronic stage of the SCI. **(d)** Individual (lines) and averaged 3D distance between non-injured data points, and those measured at late time-points. *** denote conditions that were significantly different at $p < 0.001$, respectively. Error bars, s.e.m.

Extensive recovery of hand function in monkeys and humans, but not in rats

Non-injured rats, monkeys, and humans deployed similar motor control strategies to retrieve food items with the hand, which involved reciprocal activation of extensor and flexor digit muscles to open the hand during reaching, and close the hand during retrieval (**Figure A.6** and **Figure A.7**). The lesion resulted in loss of detectable function and muscle activity in the ipsilesional hand immediately post-injury ($p < 0.001$, **Figure A.6**). Over time, monkeys regained the capacity to recruit extensor and flexor digit muscles reciprocally ($p < 0.01$, **Figure A.6b** and **Figure A.7e, h)**, with parallel recovery of object retrieval ($p < 0.01$, **Figure A.6e**). The improved performance in monkeys was often accompanied by a change in reward retrieval strategy, including grasping between the fingers and the palm of the hand in a subset of monkeys (Nout et al. 2012a). In contrast, all of the 15 hemisected rats failed to retrieve any item with digits of the forelimb over time (**Figure A.6a, d**). Rats exhibited highly variable hand trajectories ($p < 0.01$) and disorganized activation of proximal and distal muscles ($p < 0.01$, **Figure A.6a** and **Figure A.7d, g)**. Notably, the human subject with a cervical Brown- Séquard syndrome, who had completely lost ipsilesional hand function during the first 2-3 weeks post-injury (**Figure A.6f**), exhibited complete recovery on this task (**Figure A.6c**). He was able to perform fine manipulations with the digits that were associated with an almost complete recovery of clinical motor scores (**Figure A.6f**). Well-timed recruitment of proximal and digits muscles were associated with highly reproducible hand trajectories during execution of the retrieval task in this human subject (**Figure A.7c, f, i**).

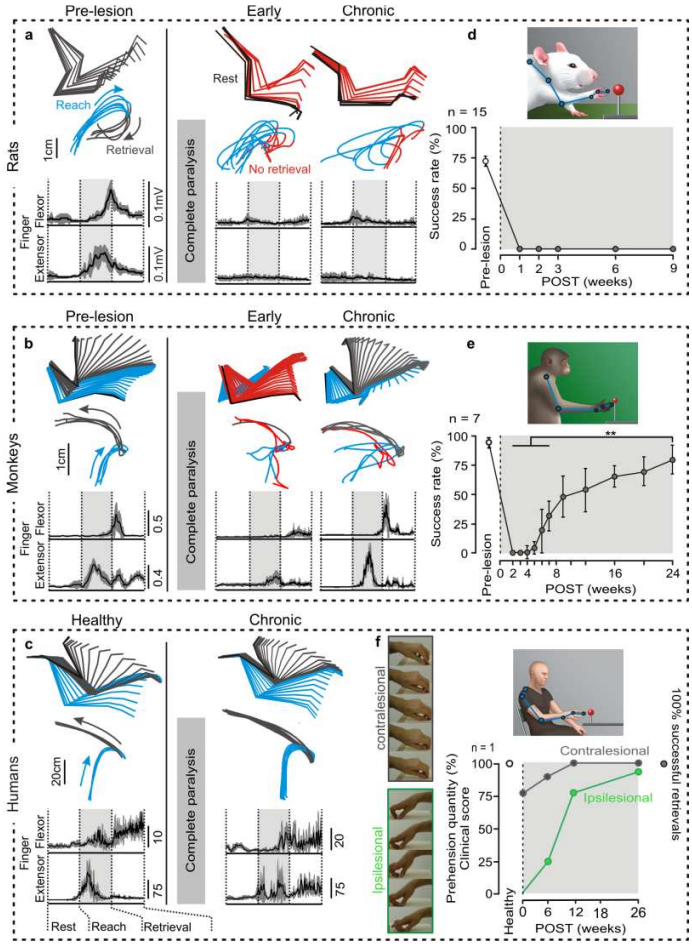

Figure A.6: Monkeys and humans show superior recovery of hand function than rats. (a-c) Stick diagram decomposition of upper limb motion during reach (blue) and retrieval (black) together with successive limb endpoint trajectories during retrieval. The averaged (+/- s.e.m.) EMG activity recorded from the extensor digitorum communis and flexor digitorum profundus is shown during successive retrievals before the injury (or healthy), and at early and chronic time-points post-SCI in rats, monkeys, and humans. **(d, e)** Mean success in hand use reported as a percent of successful food retrieval trials (+/- s.e.m.) in rats and monkeys. **(f)** The human subject with cervical SCI showed 100% in the retrieval task. The plot instead shows recovery of bilateral prehension quantity, which corresponds to evaluation of refined hand movements under time constraints. A vertically ordered sequence of pictures is displayed during retrieval of a coin with the ipsilesional and contralesional hand. ** denote conditions that were significantly different at $p < 0.01$.

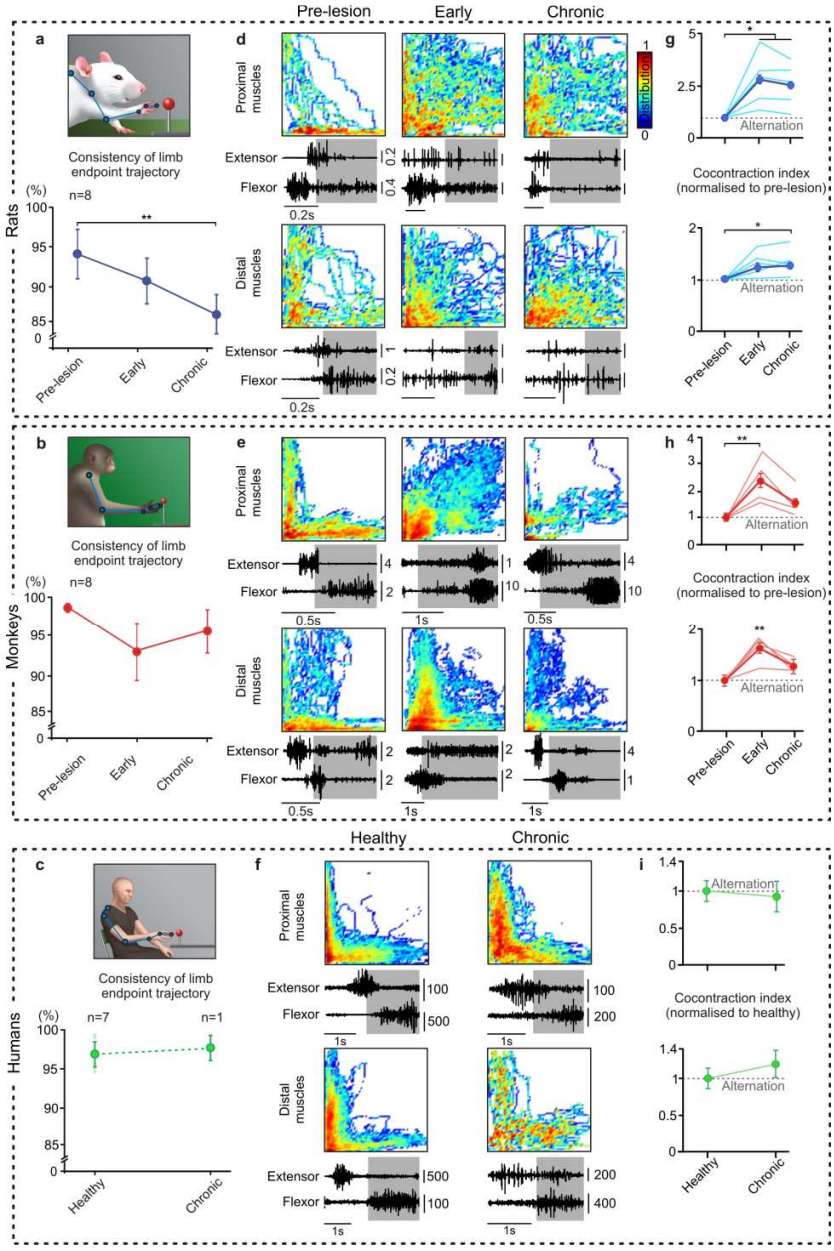

Figure A.7: Recovery of hand kinematic and muscle activation patterns. (a-c) The consistency of reaching movement was measured as the percent of explained variance by PC1 when applying a PC analysis on 10 successive 3D reaching trajectories. **(d-f)** Representative example of recruitment pattern for proximal and distal pairs of antagonist muscles during a reach. The empty and shaded areas correspond to the reach and grasp phases, respectively. The color-coded plots show, for each pair of antagonistic muscles, the probability of co-activation. A L-shaped pattern indicates reciprocal activation between antagonist muscles, while a filled pattern highlights a high degree of co-activation. **(g-i)** Plots reporting the normalized values of the co-contraction index computed for proximal and distal antagonistic muscle pairs before the SCI (or healthy) and in the chronic stage. * denote conditions that were significantly different at $p < 0.05$, ** at $p > 0.01$, respectively. Error bars, s.e.m.

Extensive plasticity of axonal projections from the left and right motor cortex

Monkeys and humans showed significantly greater motor recovery than rats after a Brown- Séquard syndrome. Differences in recovery were especially pronounced for skilled motor tasks that are believed to rely on corticospinal tract (CST) contribution (Kinoshita et al. 2012, Lemon 2008, Nishimura et al. 2007). We thus hypothesized that corticospinal axonal plasticity is a mechanism underlying recovery, as suggested previously (Rosenzweig et al. 2010). To test this hypothesis, we labeled the axonal projections from the left and right motor cortex with injections of anterograde tracers. We compared lesion-induced reorganization of bilateral CST patterns in rats and monkeys sacrificed at sub-acute (n = 8 rats and 3 monkeys) or chronic (n = 7 rats and 8 monkeys) time-points post-SCI.

In rats, the vast majority of CST fibers decussated at the level of pyramids, extended rostrocaudally in the dorsal column (**Figure A.2a**), and projected contralaterally in the dorsal and intermediate laminae of spinal segments (**Figure A.8a, c**). Consequently, the C7 hemisection interrupted nearly all the crossed axonal projections from the contralesional motor cortex. We found a small yet significant increase in the density of CST fibers at C8 in chronically injured rats compared to sub-acutely injured rats ($p < 0.05$, **Figure A.8c, e**). Serial reconstructions revealed that these axonal structures arose from the ventral component of the CST, which contains ipsilaterally projecting CST fibers spared by the SCI (Weidner et al. 2001) (**Figure A.8i**). In contrast to rats, but similar to humans, intact monkeys have extensive bilateral axonal projections from motor cortex to cervical spinal segments (Rosenzweig et al. 2009) (**Figure A.2b**). Consequently, a complete C7 hemisection lesion in primates spares a substantial number of corticospinal axons, which originate from the spinal cord contralateral to the lesion and decussate across the spinal cord midline below the lesion (Rosenzweig et al. 2010) (**Figure A.8j**). These axons innervate the intermediate and ventral laminae of the spinal cord (**Figure A.8d, f**). At the C8 level, below the injury, we found a significant increase in the number of midline crossing CST axons in monkeys after chronic compared to sub-acute injury ($p < 0.05$, **Figure A.8f**), which was not present in rats (**Figure A.8e**). These axons exhibited a significantly increased density in the ventral horn of spinal segments containing motor

pools innervating the hand ($p < 0.05$, **Figure A.8d, f**). This sprouting reconstituted a large proportion of pre-injury CST fiber density in monkeys, which contrasted with the near complete depletion of CST fibers observed in chronic compared to non-injured rats ($p < 0.0001$, **Figure A.8e**). In both rats and monkeys, sub-lesional CST axons in chronically injured animals established synapses, as they co-localized with synaptophysin (**Figure A.8k, l**).

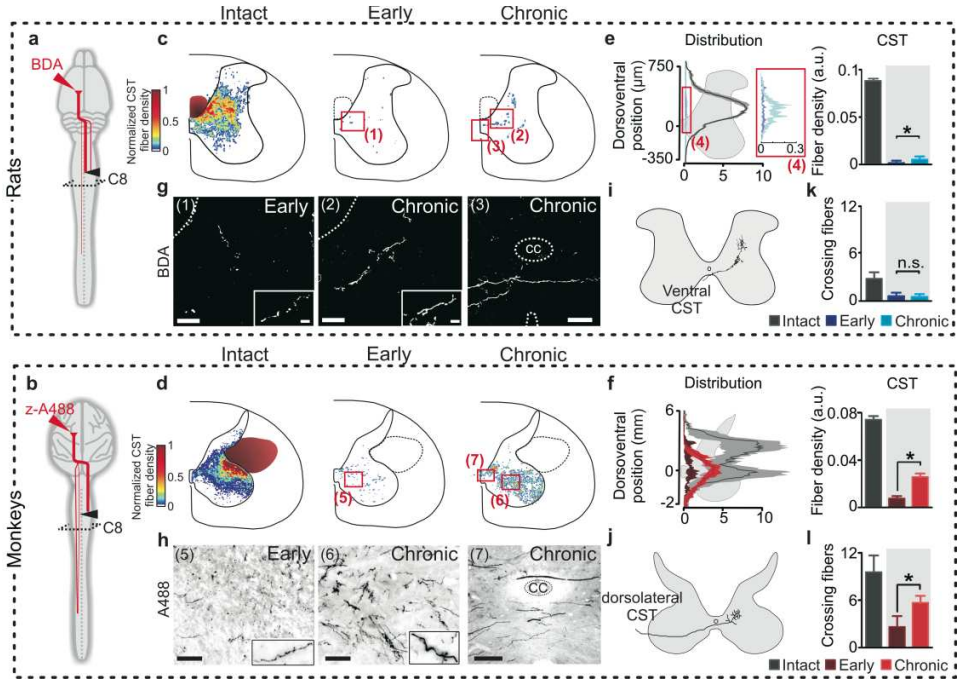

Figure A.8: Monkeys show superior plasticity of sub-lesional CST fibers than rats. (a, b) Diagram illustrating anatomical experiments and analyzed regions in rats and monkeys. **(c, d)** Heat maps, (**e, f**) fiber density distribution and graphs showing ipsilesional CST axon density at C8 below the injury, in intact animals, and at early and chronic time-points post-SCI (a.u., arbitrary units). **(g, h)** Representative photographs taken from highlighted areas (red numbers) showing compensatory sprouting of spared CST axons in sub-lesional segments. Cc, central canal. (**i, j**) Serial reconstruction of a single axon, demonstrating that CST fibers originated from the left contralesional ventral CST in rats, and from the left contralesional dorsolateral columns in monkeys. In both species, CST fibers crossed the spinal cord midline below the SCI, but the number of fibers was substantially larger in monkeys than rats, as illustrated in the photographs. **(k, l)** Histogram plots reporting the averaged number of CST fibers crossing the spinal cord mid-line per analyzed C8 section. Scale bar, 40μm (insets: 10μm) for rats and 100 μm for monkeys. Error bars, s.e.m.

Analysis of CST axon density at C5-C6, above the lesion, also revealed substantial structural plasticity. Both rats and monkeys exhibited increases of CST axon density in C5-C6 segments at chronic compared to sub-acute time points ($p < 0.05$ in rats; $p = 0.10$ in monkeys; **Figure A.9**).

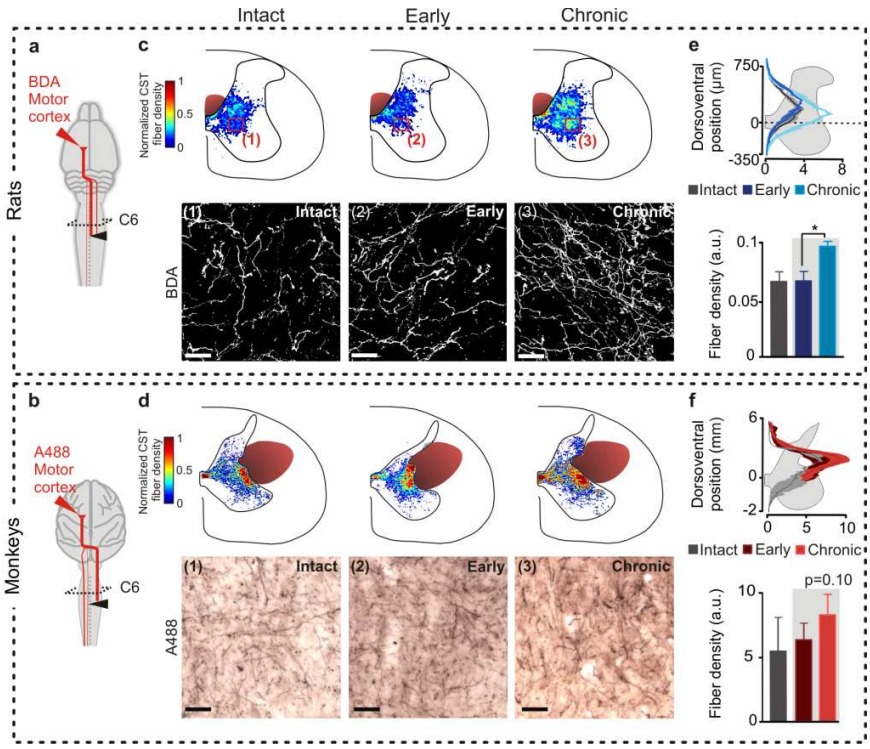

Figure A.9: Plasticity of contralesionally originating CST fibers above the SCI. (a, b) Diagram illustrating anatomical experiments and analyzed regions in rats and monkeys. **(c, d)** Heat maps of CST fiber density in the ipsilesional C6 segment, together with representative photographs of CST fibers in rats and monkeys. **(e, f)** CST fiber density distribution and histogram plots reporting the averaged density of CST fibers in the analyzed C6 segment. Scale bar, 30 μm and 100 μm for rats and monkeys, respectively. * denote significant difference at $p < 0.05$. Error bars, s.e.m.

We also detected a significant increase in the density of axons originating from the motor cortex ipsilateral to the spinal cord lesion (right) (**Figure A.10**). In both rats and monkeys, axons originating from the right motor cortex decussate at the pyramids and then re-cross the spinal cord midline below the injury, where they exhibited significantly increased density in animals sacrificed at chronic compared to early time-points ($p < 0.05$, **Figure A.10e, f**). Importantly, remodeling of spared axons did not occur in all axonal projections to the spinal cord: the density or distribution of serotonergic axons in cervical

segments caudal to the lesion did not change in either rats or monkeys (**Figure A.11**). These combined anatomical evaluations showed that both rats and monkeys exhibited multi-level plasticity of the CST in the chronic stage of hemisection, but the degree of CST plasticity in sub-lesional spinal segments was greater by several orders of magnitude in monkeys compared to rats.

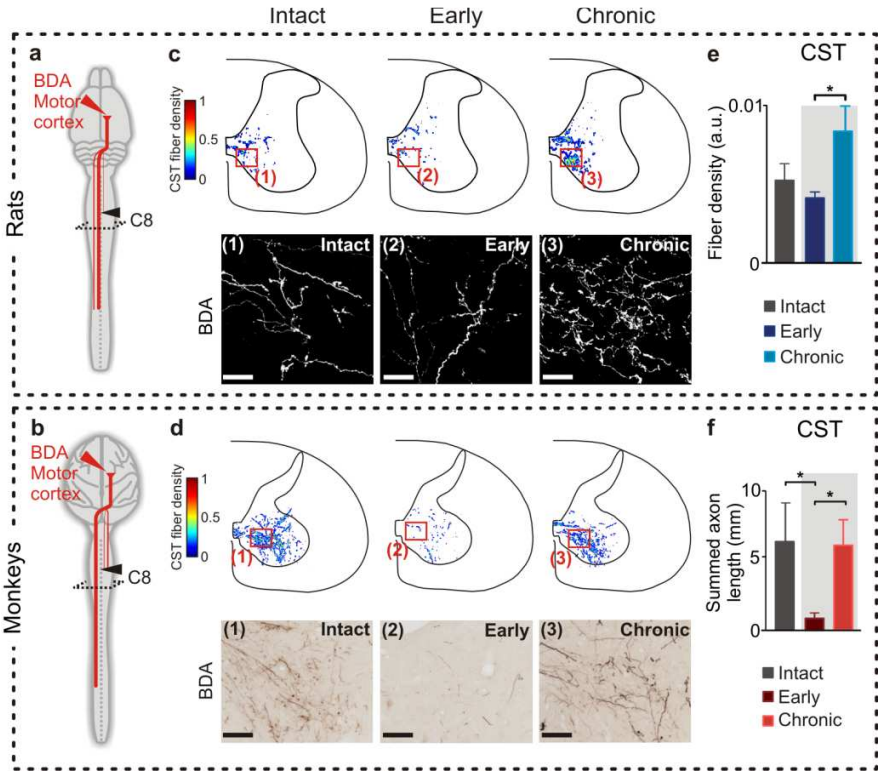

Figure A.10: Plasticity of ipsilesionally originating CST fibers below the injury (a, b) Diagram illustrating anatomical experiments and analyzed regions in rats and monkeys. **(c, d)** Heat maps of CST fiber density in the ipsilesional C8 segment, together with representative photographs of CST fibers in rats and monkeys. **(e, f)** Histogram plots reporting the averaged density of CST fibers in the ipsilesional hemicord of the C8 segment. Scale bar, 30 μm and 100 μm for rats and monkeys, respectively. * denote significant difference at $p < 0.05$. Error bars, s.e.m.

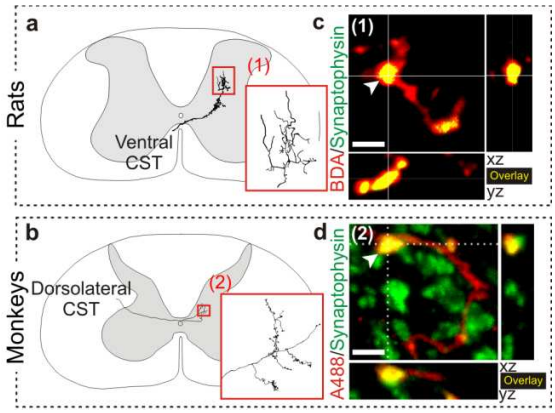

Figure A.11: CST fibers form button-like structures below the SCI. (a, b) Serial reconstruction of CST fibers originating from the contralesional motor cortex in the C8 segment of rats and monkeys with chronic hemisection SCI. **(c, d)** Representative photographs showing 3D co-localization of BDA and synaptophysin in rats, and D-A488, and synaptophysin in monkeys, which demonstrate the presence of synaptic terminals in the sub-lesional CST fibers. Scale bar, 4 μm and 2 μm for rats and monkeys, respectively. * denote significant difference at $p < 0.05$. Error bars, s.e.m.

Recovery of cortical access to lower extremity motor pools in humans, but not in rats

To evaluate whether a similar reorganization of motor cortex axonal projections occurs in humans, we monitored the recovery of motor evoked potentials in the left and right leg muscles in response to transcranial magnetic stimulation applied over the leg area of the motor cortex. To establish translational comparisons, we delivered electrical stimulations in awake rats through a chronically implanted electrode over the motor cortex (van den Brand et al. 2012). In non-injured rats and humans, the stimulation evoked bilateral motor responses in leg muscles with reproducible latencies (**Figure A.12a-d**). Both rats and humans with a Brown-Séquard syndrome exhibited a complete suppression of motor evoked potentials in leg muscles ipsilateral to the lesion at early time-points ($p < 0.001$, **Figure A.12c, d**), and a significant reduction in the motor evoked potential amplitude in muscles contralateral to the lesion ($p < 0.01$, **Figure A.12e, f**). The loss of motor evoked potentials in leg muscles ipsilateral to the lesion in rats was permanent ($p < 0.001$, **Figure A.12c, e**). In contrast, all 3 human subjects with Brown-Séquard syndrome, who exhibited no or minimal responses in ipsilesional leg muscles in the first 2 weeks post-injury,

showed a significant recovery of motor evoked potentials in the leg muscles ipsilateral to the lesion ($p < 0.05$, **Figure A.12d-f**). The latencies of these responses were significantly prolonged on the ipsilesional side (18.6 +/- 1.23ms) compared to the contralesional side (16.3 +/- 1.59, $p < 0.05$, **Figure A.12d**).

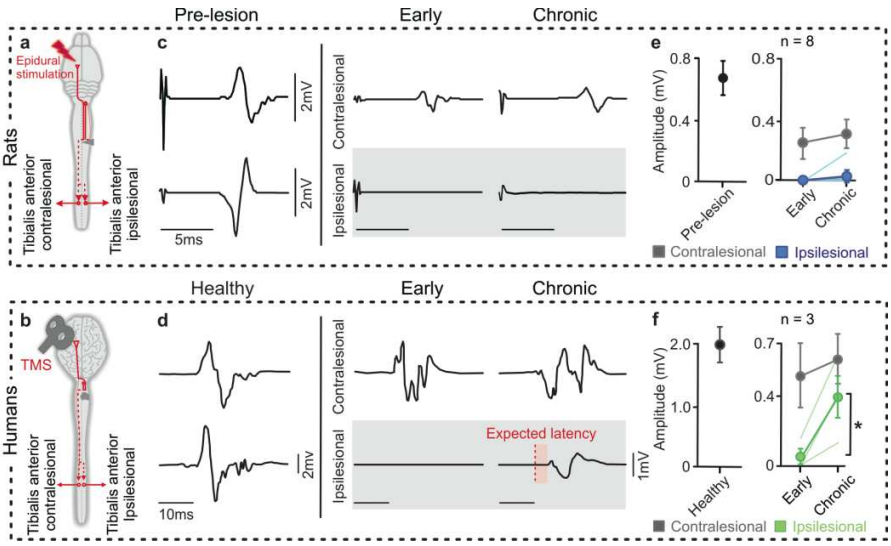

Figure A.12: Humans show recovery of cortically evoked motor potentials in ipsilesional leg muscles, but not rats. Diagrams illustrating electrophysiological experiments in **(a)** rats and **(b)** humans. **(c, d)** Representative traces (means of 10 repetitions) of cortically evoked motor potentials recorded in the left and right tibialis anterior pre-lesion (or healthy), and at early and chronic time-points post-SCI. The shaded area indicates the side of the injury. The doted line reports the expected latency of motor evoked potentials based on contralesional recordings. **(e, f)** Plots reporting the mean values of the amplitude of cortically evoked motor potentials in contralesional and ipsilesional tibialis anterior muscles. Thin lines represent individual data. * denotes significant differences at $p < 0.05$. Error bars, s.e.m.

Multi-level plasticity of motor cortex axonal projections augments functional recovery

We finally conducted an integrated syndromic assessment using non-linear principal components analysis (Linting et al. 2007) (NLPCA) to explore mechanistic relationships between anatomical and functional parameters (Ferguson et al. 2013). We performed separate NLPCA extractions for rat-monkey and rat-human data using subsets of variables that were collected in both species, allowing direct cross-species comparisons (**Figure A.13**). In both analyses, the first PC accounted for more than 50% of the

total variance. Extraction of PC loadings demonstrated that, in all the studied species, the degree of anatomical and functional plasticity among left and right motor cortex axonal projections significantly correlated with increased recovery of locomotion, and even more extensively, hand function (**Figure A.13c, d**). However, analysis of individual PC scores revealed that this mechanism of recovery was remarkably more efficient in monkeys ($p < 0.001$, **Figure A.13**) and humans ($p < 0.01$, **Figure A.13f**) compared to rats.

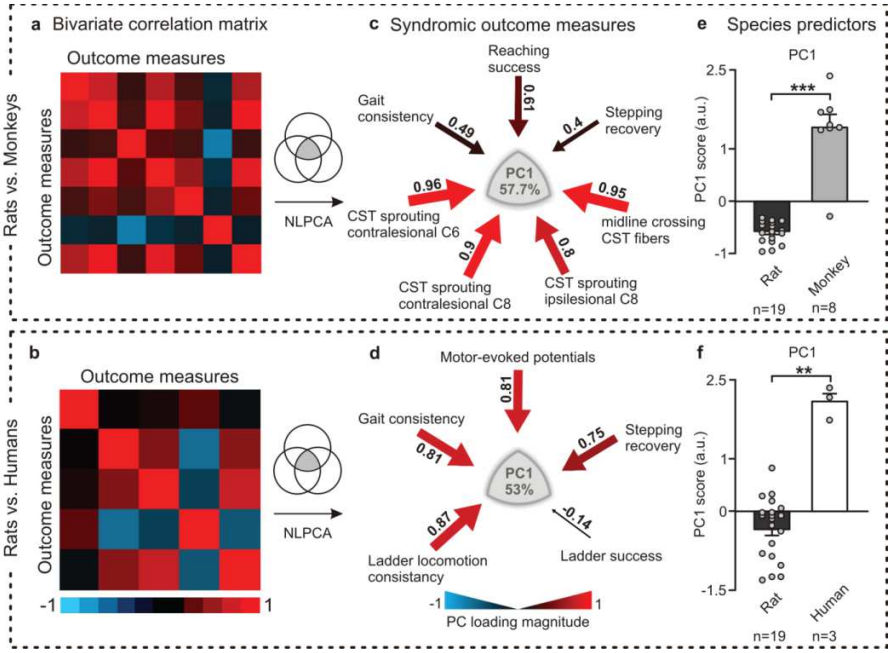

Figure A.13: Syndromic analysis establishing relationships between plasticity of motor cortex axonal projections and functional recovery. (a, b) Bivariate correlation matrix showing robust correlations between the subset of parameters show in (b). **(c, d)** A categorical PCA was applied on all the parameters measured in rats and monkeys, and in rats and humans. PC1 accounted for a large amount of variance, which is reported in the respective panel. Color- and size-coded arrows indicate the direction (red, positive correlation) and amplitude of factor loadings of the represented anatomical, electrophysiological, and functional parameters. Ipsilesional and contralesional refer to the origin of the CST. Correlation coefficients are also reported. The rat vs. monkey analysis indicated that the degree of multi-level remodeling of the left and right CST significantly correlated with the extent of recovery of locomotion and hand function, both in rats and monkeys. The rat vs. human analysis revealed robust correlations between the recovery of motor-evoked potentials in leg muscles, and the recovery of basic and skilled locomotion, both in rats and humans. **(e, f)** Histogram plots reporting the mean (+ s.e.m.) values of scores on PC1 for both analyses. Each dot represents individual data. **, *** denotes significant differences between the studied species ($p < 0.01$, $p < 0.001$). Both analyses revealed a significant enhancement in recovery in both monkeys and humans, compared to rats.

A.5 Discussion

We conducted the first comprehensive comparison of spontaneous functional recovery in rats, monkeys, and humans after similar types of spinal cord lesions. We demonstrate that, contrary to the general consensus, monkeys and humans show greater spontaneous recovery of gait, and even more strikingly, hand function compared to rats. Anatomical, electrophysiological and statistical analyses revealed that substantial, multi-level reorganization of bilateral corticospinal tract projections above and below the lesion was associated with enhanced recovery in monkeys and probably humans compared to rats.

Extensive functional improvements after lateral hemisection SCI have been reported in both humans (Brown-Sequard 1868, Dlouhy et al. 2013, Little and Halar 1985, Roth et al. 1991) and experimental animals (Filli et al. 2011, Nout et al. 2012a, Nout et al. 2012b, Rosenzweig et al. 2010) but potential differences in the extent of recovery across mammals have never been investigated conclusively. To address this issue, we implemented the first standardized kinematics and electromyography methodologies across multiple behavioral paradigms in rats, monkeys, and humans. Using multifactorial analysis, we uncovered qualitatively similar patterns of deficits in lower limb movements in all the studied species. However, the impairment of lower limb control during locomotion in the chronic condition remained significantly more pronounced in rats compared to monkeys and humans. Even more strikingly, only higher mammals regained the capacity to activate digit muscles reciprocally to retrieve objects with their hands. These results have two important implications for translational SCI research. First, they show that multifaceted and quantitative information can be collected in rats, monkeys, and humans during natural behavioral tasks to establish translational metrics that allow a meaningful and objective comparison of motor functional recovery across species (Ferguson et al. 2011). Second, these results demonstrate that recovery of locomotion and hand function is greater in monkeys compared to rats after the same SCI. To circumvent the intrinsically variable and undefined nature of spinal cord damage in humans, we focused our analyses on individuals exhibiting a Brown-Séquard syndrome, which leads to characteristic sensorimotor deficits. Due to the naturally low incidence of Brown-Séquard

syndrome in humans, we only could conduct detailed assessment of motor recovery in 3 patients, including one with a cervical SCI. Despite these inherent limitations, our results suggest that functional recovery is much greater in humans compared to rodents, and potentially, monkeys. Our epidemiologic analysis conducted in 437 individuals with a cervical SCI reinforce the validity of these conclusions, showing extensive recovery of upper and lower limb functions in individuals with Brown-Séquard syndrome.

The development of the corticospinal tract during evolution has enabled higher primates to perform incrementally more complex motor tasks (Lemon and Griffiths 2005). Three salient features characterize the adaptions of the corticospinal tract during primate evolution. First, the rapidly increasing number of axons triggered a migration of the corticospinal tract from the dorsal column to dorsolateral funiculi (Kuypers 1964). Second, the pattern of corticospinal projections became increasingly bilateral, with a substantial number of axons decussating extensively across the spinal cord midline (Rosenzweig et al. 2009). Third, the appearance of direct cortical projections onto motoneurons correlated with the emergence of precision grip between the thumb and the index fingers (Kinoshita et al. 2012, Lemon 2008). These evolutionary adaptations in the architecture and properties of the primate corticospinal tract have provided significant advantages for recovery after SCI (Oudega and Perez 2012), especially after lateralized injuries. In contrast to rats, a substantial number of corticospinal tract fibers originating from the contralesional motor cortex are spared after a lateral hemisection SCI in monkeys (Rosenzweig et al. 2010) and assumingly humans (Lemon an Griffiths 2005) (**Figure A.2a-c**). We observed a substantial growth and sprouting of these spared corticospinal fibers across the sub-lesional spinal cord midline of chronically injured monkeys. This anatomical remodeling reconstituted a substantial number of original motor cortex axonal projections into the ventral horn of spinal segments containing hand muscle motoneurons. Recovery of cortically evoked motor potentials with increased latencies in ipsilesional leg muscles suggested similar reorganization of motor cortex axonal projections in humans. Along the same line, post-mortem anatomical analyses (Fishman 1987) and electrophysiological recordings (Curt et al. 1998, Thomas and Gorassini 2005) provided indirect evidence suggesting that sprouting of spared

corticospinal fibers contributes significantly to functional recovery after SCI in humans. Importantly, both rats and monkeys showed ubiquitous sprouting of ipsilesional and contralesional corticospinal axons below and above the lesion. This multi-level, bilateral corticospinal tract plasticity suggests that the dramatic difference between rats and monkeys in the amount of corticospinal axons below the injury was in part due to the lack of spared contralesional motor cortex originating fibers in rats.

Other descending tracts appear more resistant to anatomical reorganization post-SCI (Courtine et al. 2008), especially in cervical segments (Courtine et al. 2008, Filli et al. 2011). For example, we did not observe significant changes in the projection patterns of serotonergic pathways in cervical segments of both rats and monkeys, which contrasted with the robust reorganization of serotonergic fibers observed in the brain (Hawthorne et al. 2011) and in thoracic segments (Mullner et al. 2008) after injury. These results highlight a surprisingly high degree of specific sprouting and growth of spared corticospinal tract axons into cervical segments of mammals after SCI (Steward et al. 2008). Multifactorial analysis conducted on a large number of variables extracted from our cohort of 8 monkeys and 15 rats established robust relationships between multi-level reorganization of bilateral corticospinal tracts and functional recovery, in particular for fine motor tasks. The same multifactorial analysis applied to data collected in both rats and humans uncovered significant correlations between recovery of motor cortex access to sub-lesional motoneurons and improved restoration of function. These results indicate that, as previously proposed (Oudega and Perez 2012, Rosenzweig et al. 2010) but not tested directly across multiple species, corticospinal tract reorganization is a fundamental mechanism of recovery after SCI in mammals. However, due to the bilateral projection patterns of corticospinal axons in higher mammals, and probably, the more advanced contribution of these inputs to motor control (Lemon and Griffiths 2005, Nishimura et al. 2007), monkeys and humans show greater functional recovery than rats after a lateral hemisection of the spinal cord—and potentially after other types of incomplete SCIs.

A.6 Conclusion

These findings emphasize the importance of developing therapeutic interventions targeting regeneration and sprouting of the corticospinal tract (Rosenzweig et al. 2010), and neurorehabilitation procedures to enhance the contribution of motor cortex to recovery (Nishimura et al. 2007, van den Brand etl al. 2012). Dramatic differences between rodents and primates also highlight the value of continuing the development of nonhuman primate models for translational SCI research (Courtine et al. 2007, Nout et al. 2012a).

General Discussion

The objective of the present thesis was to elucidate domains of neural control of walking after incomplete spinal cord injury. These domains of neural control were revealed by the respective contributions of a multitude of gait-related parameters to the degree of impairment that may be distinctly modulated after insults to the spinal cord.

Gait analysis has been performed in patients with neuromotor disorders for decades and the relevance of the assessment of locomotor behavior to capture neurological alterations and recovery is undisputed (Ditunno and Scivoletto 2009). However, gait analysis is performed inconsistently and outcome measures may range from simple measures of walking speed to complex activity mapping of motor pools in the spinal cord (Ivanenko et al. 2008). The selection and subsequent analysis of specific outcome measures is crucial as they capture particular aspects of human gait and may therefore reveal different underlying mechanisms. For this reason multiple variables of different modalities were included in the present thesis to evaluate their controllability in iSCI patients and their respective contributions to overall gait pattern and its recovery.

Walking pattern and neural control of walking in iSCI

In the first study we found that the inralimb coordination (i.e. gait quality), represented by the spatio-temporal hip-knee angular coordination (cyclogram), was very distinctly affected in iSCI patients and strongly correlated with the corresponding preferred walking speed. In the second study we showed that the cyclogram highly contributed to the pathology of iSCI walking (first domain, PC1), showing a gradient of impairment along the first PC axis. For these reasons we suggested the intralimb coordination to be a good readout for walking impairment. Remarkably, despite the correlation with preferred walking speed, a patient with a given impairment was not able to modulate the cyclogram by increasing the speed, although the cycle-to-cycle reproducibility improved. This may imply that an iSCI patient has optimized

(i.e. learned) a particular pathological gait pattern as a consequence of the degree of impairment, which is not responsive to increased neural drive (i.e., speed), which in turn supports the idea that spinal neural networks below the lesion reorganize due to the deprivation of supraspinal input and consequently produce altered motor behavior. This concept goes in line with the hypothesis that recovery takes place due to a relearning of new motor patterns rather than a detoured reinnervation of an innate CPG (Molinari 2009). In the second study we demonstrated that both the self-selected and maximal walking speeds were distinctly diminished in iSCI patients, yet within their range of accomplished speeds patients were able to appropriately produce step length, cadence, and gait-cycle phases that were indistinguishable from healthy control subjects. Numerous studies examining locomotor outcome after iSCI use exactly these measures as their primary endpoints (Gil-Agudo et al. 2011, Krawetz and Nance 1996, Pepin et al. 2003), which may however not be sensitive parameters to reflect impairment and its recovery in iSCI.

Nevertheless, the unimpaired modulation may indicate that these parameters are not critically dependent on an entirely intact input from supraspinal control centers. These measures are more likely controlled on a spinal level, where patterned sensory inputs from muscles, tendons and cutaneous mechanoreceptors are integrated in order to produce corresponding motor output very much in accordance with the concept of a central pattern generator (CPG) (Grillner 1985). The spinal control of these gait parameters was shown in cats deprived of brain input (Barbeau and Rossignol 1987, Lovely et al. 1986). Yet, there are reasons to believe that human locomotion relies on neural input from supraspinal centers, presumably to different degrees and mediated by specific brain regions. Unlike the short-lasting and weaker influence of brain damage on gait in rats (Strata et al. 2004) and cats (Armstrong 1986), altered step length/-frequency and gait cycle timing are the clinical hallmarks of various pathologies affecting the brain (e.g., stroke, Parkinson's disease (Morris et al. 1998, Morris et al. 2005, von Schroeder et al. 1995)), reflecting their dependence on intact input from supraspinal centers. At the same time, the isolated human spinal cord, completely deprived of supraspinal signals, has never been shown to be sufficient to drive independent walking. The third domain of neural control (PC3) that could be discerned most notably comprised of

angular ranges of motion (ROMs). They were altered in some patients but were not related to the degree of overall gait impairment, nor were they consistently modulated by speed. Their contribution to recovery was only minor, suggesting that ROMs might be strongly influenced by additional confounding factors, one of which is probably spasticity.

Plasticity after iSCI

Interestingly, during recovery after iSCI the time-distance measures majorly contributed to the overall change in gait pattern over time. In actual fact, these parameters were simply well controlled at any given point in time, changing as a consequence of improved walking speed rather than representing true recovery as a manifestation of neural reorganization. Actual recovery was rather revealed by the complex intralimb coordination and movement dynamics (walking speed, angular velocity) that were shown to be highly affected by the existing impairment and also improved over time. As stated previously, it might be that the deviation of the cyclogram shape reflects the amount of spinal injury, or, more precisely, the degree of reorganization within intraspinal neural networks. This, on the other hand, raises the question as to why time-distance measures are not affected by the restructuring of spinal neural connections. The answer may be found when scrutinizing spinal reflexes. It has been shown that spinal reflex responses change their characteristics with a deterioration of function (Dietz et al. 2009), shifting from a dominant early to a dominant late component in complete SCI patients. With locomotor training and improved walking abilities these alterations can be reversed in iSCI subjects (Hubli et al. 2012). It may therefore be that the more complex coordination of lower-limb segments is mediated by a more elaborate network of intraspinal neurons that are involved in the long-latency spinal reflex circuit while the control of time-distance measures are dependent on less relay neurons assessed by short-latency spinal reflexes and are therefore less prone to reorganization. Yet, not all plastic changes within the spinal cord may be revealed by electrophysiological recordings and even less so by functional readouts. In a series of patients with holocord syringomyelia we showed that morphological alterations affecting the entire cervical spinal cord, in extreme cases ranging from the brainstem down to the lumbar spinal cord, was only detected by

sensitive segmental assessments of sensory pathways, especially the spinothalamic tract, but revealed normal findings in any other measure. This was even more surprising given the probable loss in cross-sectional spinal cord area as revealed by MRI. These findings demonstrate that the spinal cord is capable of large-scale adaptations as a consequence of slowly evolving, space-consuming pathologies in a similar way as has been shown in the brain (e.g. hydrocephalus, brain tumor (Desmurget et al. 2007, Onizuka et al. 2001)).

From bench to bedside

In preclinical animal studies, extensive plastic changes have been shown to take place after a lesion to the spinal cord (Ghosh et al. 2009, van den Brand et al. 2012, Zorner et al. 2014). However, the restorative processes are still mainly limited to the outgrowth of collaterals by uninjured neurons rather than the regeneration of injured axons. Near-future clinical studies may therefore focus on the restoration of function below the level of lesion. As discussed earlier, the intralimb coordination may reflect the severity of injury and thus the reduction of supraspinal drive leading to alterations of spinal networks below the lesion. In order to prevent a deterioration of function and to reactivate these neurons deprived of supraspinal input (Beauparlant et al. 2013), epidural spinal cord stimulation in combination with the administration of specific pharmacological agents and locomotor training were shown to restore functional walking in rats with severe spinal cord injuries (Courtine et al. 2009, van den Brand et al. 2012). Even though it is unquestioned that human locomotion differs from quadrupedal locomotion, given the common principles and behaviors induced by injury, it seems reasonable to assume that human iSCI subjects would profit from this kind of treatment. One might suspect that iSCI patients would profit even more from a surrogate supraspinal drive than rats, which are most likely less dependent on brain input. In fact, the restoration of voluntary motor control was shown in a series of clinically motor complete (AIS A/B) patients, who were implanted with an epidural stimulator (Angeli et al. 2014). Even though they were clinically classified as motor complete patients, it is most likely that these patients had preserved neural connections across the injury site. It is nonetheless important to note that these patients regained

volitional access to their previously dormant spinal networks, and that these pathways may be strengthened (i.e., undergo plastic changes) by activity. It might be due to the high dependence on supraspinal drive that the pathways conveying voluntary drive recover partial function even in chronic SCI. Furthermore, the corticospinal tract shows greater extent of recovery in humans and monkeys compared to rats (Friedli et al., *in preparation*).

From bedside to activity

Underlying mechanisms of manifested changes are especially difficult to unveil in human subjects. A clear and complete attribution of particular aspects of gait control to a specific locus in the CNS is probably neither possible nor correct. Therefore, the search for sensitive recordings that presumably assess specific pathways or the activity of relatively defined neuron populations is critical and highly valuable. The continuous sophistication of anatomical and functional imaging techniques (Edlow and Wu 2012, Freund et al. 2013a, Freund et al. 2013b) allows for more detailed insights into structural and activity changes within otherwise concealed areas of the CNS. Electrophysiological techniques have advanced our knowledge about the integrity and recovery potential of distinct motor and sensory conducting fiber tracts (Curt et al. 2008, Haefeli et al. 2013, Kramer et al. 2010). Despite the ongoing progress of recording tools and diversity of outcome measures the current state-of-the-art assessments still lack in sensitivity and resolution, as could be seen in the patients with an extensive holocord syrinx who remained almost asymptomatic. Analogously, ASIA B patients, clinically defined as motor complete patients, regained voluntary control of their lower limbs, which is commonly agreed to be rather impossible. In spite of regained voluntary leg control, these patients were not able to recover functional ambulation. One should keep in mind that the yield of bedside measurements (i.e., performed in a lying or resting position) may not be transferred to function during specific activities. The activity state of the spinal cord is crucially dependent on body position and task performed (Dietz et al. 2001, Dietz 2011, Michel et al. 2008). It is therefore imperative to evaluate functional capacity and behavior during an adequate activity state, making gait analysis all the more important.

Limitations

One prevailing drawback of studies with iSCI patients is the large phenotypic variance of the inherently heterogeneous population. This precondition would require a large sample size, which is rather difficult to attain given the limited number of patients at our disposal. A subject of perpetual discussion when performing gait analysis is the choice of walking speed and surface (i.e., overground, treadmill). We decided to evaluate locomotion at patients' preferred walking speed, revealing their inherent gait pattern where impairments may be revealed as unbiased as possible, not confounded by the imposition of an unnatural walking speed/gait pattern. Additionally, in the cross-sectional study (No. 2) we analyzed the walking patterns at different speeds on the treadmill in order examine the ability to modulate specific gait characteristics.

The present thesis studied walking pattern and locomotor control via a multitude of kinematic, electrophysiological and clinical parameters, leaving out electromyographic (EMG) data. This was mainly due to the quality and inconsistency of the acquired EMG data, making it difficult to judge whether weak or absent signals were due to diminished muscle activity or problems with data acquisition.

Conclusion

Distinct clusters of gait-related parameters suggested different domains of locomotor control in iSCI subjects. The outcomes of clinical trials critically depend on the choice of the endpoint variables that, if not carefully chosen, may reveal an incomplete and possibly skewed picture of the actual impairment and recovery. We could show that complex intralimb coordination reflected the impairment in iSCI gait control while time-distance parameters were well controlled already at an early time point of recovery. However, pathological alterations within the CNS may not always be revealed by functional assessments if the changes occur on a very slow time scale and are thus masked by spinal plasticity.

Outlook

Neural basis of locomotor control

Even in animals it is not entirely clear to what extent specific regions of the CNS are involved in the control of gait and how this organization may be altered after injury. In order to address this question different approaches may be chosen:

Reflex behavior and modulation

It has been shown that specific reflexes may reveal the state of spinal neural networks that are involved in locomotor activity. Cutaneous spinal reflex responses in patients with a complete SCI were shown to change their configuration over time, accompanied by an exhaustion of EMG activity in lower-limb muscles during assisted walking (Dietz et al. 2009). In motor incomplete non-ambulatory SCI subjects a locomotor improvement after functional training was accompanied by a change in spinal reflex behavior (Hubli et al. 2012). Thompson and colleagues showed that a down-conditioning of the soleus H-reflex resulted in improved locomotion, suggesting that plasticity may be induced in specific spinal pathways that subserve motor behaviors (Thompson et al. 2013). Therefore, combining the assessment of reflex behavior and detailed gait analysis may lead to a more profound understanding of pathways involved in alterations of gait pattern.

Modulation of cortical input

It is relatively undisputed that humans rely on supraspinal (cortical and subcortical) input during locomotion to a greater extent than animals. Transient reduction or alteration of supraspinal drive during walking may reveal its contribution to that behavior. Dual task performance has been studied in able-bodied subjects and populations with neurological diseases (e.g., Parkinson's disease, stroke (Al-Yahya et al. 2011), but little is known about the effects of concurrent tasks on walking performance and gait

pattern in iSCI patients (Lajoie et al. 1999). A frequently observed phenomenon in patients with gait disorders, including iSCI, is the increased reliance on visual feedback (patients often look at their feet while walking), which would suggest a higher dependence on supraspinal control compared to healthy subjects. However, as was shown in the present thesis, patients adopt and optimize new gait patterns based on their specific deficits while spinal networks undergo reorganization induced by partial deprivation of supraspinal input. This may conjecture that the spinal cord of iSCI patients has acquired more autonomy with respect to locomotor function, i.e. depends less on brain input. Whether this hypothesis is justified may also be addressed by comparing the modulation of evoked motor responses mediated via corticospinal pathways during walking in iSCI and healthy subjects (Schubert et al. 1997).

Gait impairment across different neurological disorders

Another approach to try and disentangle the relative input of distinct motor regions is the comparison of specific matching gait parameters across different neurological disorders. Preferentially, patients with relatively defined anatomical lesions would be included in order to investigate the respective alteration in gait pattern caused by the loss of function of these particular areas.

EMG coherence analysis

One major limitation of this thesis was the lack of investigation of EMG signals. It has been shown that the frequency analysis of intramuscular and intermuscular EMG coherence may reveal information on the origin of innervation. Coherence in a specific frequency band (20 – 40 Hz) was shown to be mediated by corticospinal drive in nonhuman primates (Baker et al. 1999) while the coherence at frequencies between 8 and 20 Hz were shown to be reduced in SCI patients (Hansen et al. 2005).

Sensory-motor integration

This thesis specifically investigated motor control of walking and the recovery of locomotor function after iSCI. However, the sensory system undoubtedly plays a crucial role in motor control and recovery but has

been less extensively studied in the context of locomotor function. In a small subset of patients, though, who were included in study 3 of this thesis, clinical and electrophysiological assessments revealed a predominant affectedness of the dorsal column leading to a pronounced sensory loss while motor pathways and muscle strength were less affected. A dramatic deterioration of walking pattern could be observed in these patients, which exceeded the impairment seen in iSCI patients with injuries predominantly affecting motor pathways. Apparently, an interruption of information from the lower body to supraspinal centers was more detrimental for walking function, at least in a subacute phase, even though motor neurons below the level of lesion were not directly affected by the injury. During the course of rehabilitation, these patients improved their locomotor function in the absence of substantial improvements of central sensory conductivity (SSEP). It is also known from partially deafferented patients where peripheral sensory nerves are affected (e.g., neuropathies) that motor function may be considerably impaired (Lajoie et al. 1996, Sainburg et al. 1993). However, walking ability could be relearned but was controlled completely differently (i.e., in a top-down, feedforward fashion). Studying specific groups of patients may provide the opportunity to elucidate how sensory information is integrated at different levels of the neuraxis and how this affects locomotor recovery.

From bench to bedside to activity

The state of the spinal cord was shown to be highly task-dependent (de Leon et al. 1998, Dietz et al. 2001, Dietz 2011, Michel et al. 2008) meaning that motor output may be differently modulated depending on whether a person is lying in bed or walking over ground. It was also shown in study 2 of this thesis that a static measure of muscle force (lower extremity motor score) was only weakly related to locomotor function and recovery. Therefore, bedside tests, even though clinically meaningful and unquestionably required especially in acute patients (i.e., who are not able to sit or stand), may not be accurate at evaluating function and predicting functional outcome. Restoration of voluntary function in clinically complete (but anatomically incomplete) SCI subjects (Angeli et al. 2014, Herkema et al. 2011) serves as a proof of concept of the effect of epidural spinal cord stimulation, but the treatment failed to achieve

functional recovery (i.e., community ambulation). A next step is therefore that this kind of treatment is applied in patients with residual motor function at a non-ambulatory level who preferentially regain community walking.

References

Abel R, Schablowski M, Rupp R, Gerner HJ. Gait analysis on the treadmill - monitoring exercise in the treatment of paraplegia. Spinal Cord. 2002; 40(1):17-22.

Al-Yahya E, Dawes H, Smith L, Dennis A, Howells K, Cockburn J. Cognitive motor interference while walking: a systematic review and meta-analysis. Neuroscience and biobehavioral reviews. 2011; 35(3):715-28.

Angeli CA, Edgerton VR, Gerasimenko YP, Harkema SJ. Altering spinal cord excitability enables voluntary movements after chronic complete paralysis in humans. Brain. 2014; 137(Pt 5):1394-409.

Awai L, Curt A. Intralimb coordination as a sensitive indicator of motor-control impairment after spinal cord injury. Front Hum Neurosci. 2014; 8:148.

Bachmann LC, Matis A, Lindau NT, Felder P, Gullo M, Schwab ME. Deep brain stimulation of the midbrain locomotor region improves paretic hindlimb function after spinal cord injury in rats. Sci Transl Med. 2013; 5(208):208ra146.

Baker SN, Kilner JM, Pinches EM, Lemon RN. The role of synchrony and oscillations in the motor output. Exp Brain Res. 1999; 128(1-2):109-17.

Barbeau H, Rossignol S. Recovery of locomotion after chronic spinalization in the adult cat. Brain Res. 1987; 412(1):84-95.

Beauparlant J, van den Brand R, Barraud Q, Friedli L, Musienko P, Dietz V, et al. Undirected compensatory plasticity contributes to neuronal dysfunction after severe spinal cord injury. Brain. 2013; 136(Pt 11):3347-61.

Behrman AL, Ardolino E, Vanhiel LR, Kern M, Atkinson D, Lorenz DJ, et al. Assessment of functional improvement without compensation reduces variability of outcome measures after human spinal cord injury. Arch Phys Med Rehabil. 2012; 93(9):1518-29.

Borghese NA, Bianchi L, Lacquaniti F. Kinematic determinants of human locomotion. J Physiol. 1996; 494 (Pt 3):863-79.

Brown-Sequard CE. Lectures on the physiology and pathology of the central nervous system and on the treatment of organic nervous affections. Lancet. 1868; 2:93-595,659-62,755-7,821-3.

Buurke JH, Nene AV, Kwakkel G, Erren-Wolters V, Ijzerman MJ, Hermens HJ. Recovery of gait after stroke: what changes? Neurorehabil Neural Repair. 2008; 22(6):676-83.

Calancie B, Lutton S, Broton JG. Central nervous system plasticity after spinal cord injury in man: interlimb reflexes and the influence of cutaneous stimulation. Electroencephalogr Clin Neurophysiol. 1996; 101(4):304-15.

Carmichael ST, Chesselet MF. Synchronous neuronal activity is a signal for axonal sprouting after cortical lesions in the adult. J Neurosci. 2002; 22(14):6062-70.

Cattell RB. Scree test for the number of factors. Multivar Behav Res. 1966; 1(2):245-76.

Chamberlain MC, Tredway TL. Adult primary intradural spinal cord tumors: a review. Curr Neurol Neruosci Rep. 2011; 11(3):320-8.

Chen G, Patten C, Kothari DH, Zajac FE. Gait differences between individuals with post-stroke hemiparesis and non-disabled controls at matched speeds. Gait Posture. 2005; 22(1):51-6.

Cotes JE, Meade F. The Energy expenditure and mechanical energy demand in walking. Ergonomics. 1960; 3(2):97-119.

Courtemanche R, Teasdale N, Boucher P, Fleury M, Lajoie Y, Bard C. Gait problems in diabetic neuropathic patients. Arch Phys Med Rehabil. 1996; 77(9):849-55.

Courtine G, Roy RR, Raven J, Hodgson J, McKay H, Yang H, et al. Performance of locomotion and foot grasping following a unilateral thoracic corticospinal tract lesion in monkeys (Macaca mulatta). Brain. 2005; 128(Pt 10):2338-58.

Courtine G, Bunge MB, Fawcett JW, Grossman RG, Kaas JH, Lemon R, et al. Can experiments in nonhuman primates expedite the translation of treatments for spinal cord injury in humans? Nature medicine. 2007; 13(5):561-6.

Courtine G, Song B, Roy RR, Zhong H, Herrmann JE, Ao Y, et al. Recovery of supraspinal control of stepping via indirect propriospinal relay connections after spinal cord injury. Nat Med. 2008; 14(1):69-74.

Courtine G, Gerasimenko Y, van den Brand R, Yew A, Musienko P, Zhong H, et al. Transformation of nonfunctional spinal circuits into functional states after the loss of brain input. Nature neuroscience. 2009; 12(10):1333-42.

Curt A, Dietz V. Traumatic cervical spinal cord injury: relation between somatosensory evoked potentials, neurological deficit, and hand function. Arch Phys Med Rehabil. 1996a; 77(1):48-53.

Curt A, Dietz V. Nerve conduction study in cervical spinal cord injury: significance for hand function. NeuroRehabilitation. 1996b; 7(3):165-73.

Curt A, Dietz V. Ambulatory capacity in spinal cord injury: significance of somatosensory evoked potentials and ASIA protocol in predicting outcome. Arch Phys Med Rehabil. 1997; 78(1):39-43.

Curt A, Dietz V. Electrophysiological recordings in patients with spinal cord injury: significance for predicting outcome. Spinal Cord. 1999; 37(3):157-65.

Curt A, Ellaway PH. Clinical neurophysiology in the prognosis and monitoring of traumatic spinal cord injury. Handb Clin Neurol. 2012; 109:63-75.

Curt A, Keck ME, Dietz V. Functional outcome following spinal cord injury: significance of motor-evoked potentials and ASIA scores. Arch Phys Med Rehabil. 1998; 79(1):81-6.

Curt A, Van Hedel HJ, Klaus D, Dietz V. Recovery from a spinal cord injury: significance of compensation, neural plasticity, and repair. J Neurotrauma. 2008; 25(6):677-85.

De Leon RD, Hodgson JA, Roy RR, Edgerton VR. Full weight-bearing hindlimb standing following stand training in the adult spinal cat. Journal of neurophysiology. 1998; 80(1):83-91.

Desmurget M, Bonnetblanc F, Duffau H. Contrasting acute and slow-growing lesions: a new door to brain plasticity. Brain. 2007; 130(Pt 4):898-914.

Dietz V. Behavior of spinal neurons deprived of supraspinal input. Nat Rev Neurol. 2010; 6(3):167-74.

Dietz V. Recent advances in spinal cord neurology. Journal of neurology. 2010; 257(10):1770-3.

Dietz V. Quadrupedal coordination of bipedal gait: implications for movement disorders. Journal of neurology. 2011; 258(8):1406-12.

Dietz V, Curt A. Neurological aspects of spinal-cord repair: promises and challenges. Lancet neurology. 2006; 5(8):688-94.

Dietz V, Colombo G, Jensen L. Locomotor activity in spinal man. Lancet. 1994; 344(8932):1260-3.

Dietz V, Fouad K, Bastiaanse CM. Neuronal coordination of arm and leg movements during human locomotion. Eur J Neurosci. 2001; 14(11):1906-14.

Dietz V, Colombo G, Jensen L, Baumgartner L. Locomotor capacity of spinal cord in paraplegic patients. Ann Neurol. 1995; 37(5):574-82.

Dietz V, Grillner S, Trepp A, Hubli M, Bolliger M. Changes in spinal reflex and locomotor activity after a complete spinal cord injury: a common mechanism? Brain. 2009; 132(Pt 8):2196-205.

Dimitrijevic MR, Gerasimenko Y, Pinter MM. Evidence for a spinal central pattern generator in humans. Annals of the New York Academy of Sciences. 1998; 860:360-76.

Ditunno J, Scivoletto G. Clinical relevance of gait research applied to clinical trials in spinal cord injury. Brain research bulletin. 2009; 78(1):35-42.

Ditunno JF, Jr., Barbeau H, Dobkin BH, Elashoff R, Harkema S, Marino RJ, et al. Validity of the walking scale for spinal cord injury and other domains of function in a multicenter clinical trial. Neurorehabil Neural Repair. 2007; 21(6):539-50.

Dlouhy BJ, Dahdaleh NS, Howard MA, 3rd. Radiographic and intraoperative imaging of a hemisection of the spinal cord resulting in a pure Brown-Sequard syndrome: case report and review of the literature. Journal of neurosurgical sciences. 2013; 57(1):81-6.

Dobkin B, Apple D, Barbeau H, Basso M, Behrman A, Deforge D, et al. Weight-supported treadmill vs over-ground training for walking after acute incomplete SCI. Neurology. 2006; 66(4):484-93.

Dominici N, Keller U, Vallery H, Friedli L, van den Brand R, Starkey ML, et al. Versatile robotic interface to evaluate, enable and train locomotion and balance after neuromotor disorders. Nature medicine. 2012; 18(7):1142-7.

Duysens J, Van de Crommert HW. Neural control of locomotion; The central pattern generator from cats to humans. Gait Posture. 1998; 7(2):131-41.

Edlow BL, Wu O. Advanced neuroimaging in traumatic brain injury. Semin Neurol. 2012; 32(4):374-400.

Emery E, Hort-Legrand C, Hurth M, Metral S. Correlations between clinical deficits, motor and sensory evoked potentials and radiologic aspects of MRI in malformative syringomyelia. 27 Cases. Neurophysiol Clin. 1998; 28(1):56-72.

Fawcett JW, Curt A, Steeves JD, Coleman WP, Tuszynski MH, Lammertse D, et al. Guidelines for the conduct of clinical trials for spinal cord injury as developed by the ICCP panel: spontaneous recovery after spinal cord injury and statistical power needed for therapeutic clinical trials. Spinal cord. 2007; 45(3):190-205.

Ferguson AR, Stuck ED, Nielson JL. Syndromics: A Bioinformatics Approach for Neurotrauma Research. Translational stroke research. 2011; 2(4):438-54.

Ferguson AR, Irvine KA, Gensel JC, Nielson JL, Lin A, Ly J, et al. Derivation of Multivariate Syndromic Outcome Metrics for Consistent Testing across Multiple Models of Cervical Spinal Cord Injury in Rats. PloS one. 2013; 8(3):e59712.

Feuillet L, Dufour H, Pelletier J. Brain of a white-collar worker. Lancet. 2007; 370(9583):262.

Field-Fote EC. Combined use of body weight support, functional electric stimulation, and treadmill training to improve walking ability in individuals with chronic incomplete spinal cord injury. Arch Phys Med Rehabil. 2001; 82(6):818-24.

Field-Fote EC, Tepavac D. Improved intralimb coordination in people with incomplete spinal cord injury following training with body weight support and electrical stimulation. Phys Ther. 2002; 82(7):707-15.

Field-Fote EC, Fluet GG, Schafer SD, Schneider EM, Smith R, Downey PA, et al. The Spinal Cord Injury Functional Ambulation Inventory (SCI-FAI). J Rehabil Med. 2001; 33(4):177-81.

Filli L, Zorner B, Weinmann O, Schwab ME. Motor deficits and recovery in rats with unilateral spinal cord hemisection mimic the Brown-Sequard syndrome. Brain. 2011; 134(Pt 8):2261-73.

Fishman PS. Retrograde changes in the corticospinal tract of posttraumatic paraplegics. Arch Neurol. 1987; 44(10):1082-4.

Freund P, Curt A, Friston K, Thompson A. Tracking changes following spinal cord injury: insights from neuroimaging. Neuroscientist. 2013a; 19(2):116-28.

Freund P, Weiskopf N, Ashburner J, Wolf K, Sutter R, Altmann DR, et al. MRI investigation of the sensorimotor cortex and the corticospinal tract after acute spinal cord injury: a prospective longitudinal study. Lancet neurology. 2013b; 12(9):873-81.

Furlan JC, Noonan V, Singh A, Fehlings MG. Assessment of disability in patients with acute traumatic spinal cord injury: a systematic review of the literature. J Neurotrauma. 2011; 28(8):1413-30.

Gezen F, Kahraman S, Canakci Z, Beduk A. Review of 36 cases of spinal cord meningioma. Spine. 2000; 25(6):727-31.

Ghosh A, Sydekum E, Haiss F, Peduzzi S, Zorner B, Schneider R, et al. Functional and anatomical reorganization of the sensory-motor cortex after incomplete spinal cord injury in adult rats. J Neurosci. 2009; 29(39):12210-9.

Gil-Agudo A, Perez-Nombela S, Forner-Cordero A, Perez-Rizo E, Crespo-Ruiz B, del Ama-Espinosa A. Gait kinematic analysis in patients with a mild form of central cord syndrome. J Neuroeng Rehabil. 2011; 8:7.

Gladstone DJ, Danells CJ, Black SE. The fugl-meyer assessment of motor recovery after stroke: a critical review of its measurement properties. Neurorehabil Neural Repair. 2002; 16(3):232-40.

Gordon J, Ghilardi MF, Ghez C. Impairments of reaching movements in patients without proprioception. I. Spatial errors. J Neurophysiol. 1995; 73(1):347-60.

Grant R, Hadley DM, Macpherson P, Condon B, Patterson J, Bone I, et al. Syringomyelia: cyst measurement by magnetic resonance imaging and comparison with symptoms, signs and disability. J Neurol Neurosurg Psychiatry. 1987; 50(8):1008-14.

Grasso R, Bianchi L, Lacquaniti F. Motor patterns for human gait: backward versus forward locomotion. J Neurophysiol. 1998; 80(4):1868-85.

Grillner S. Neurobiological bases of rhythmic motor acts in vertebrates. Science. 1985; 228(4696):143-9.

Gurfinkel VS, Levik YS, Kazennikov OV, Selionov VA. Locomotor-like movements evoked by leg muscle vibration in humans. Eur J Neurosci. 1998; 10(5):1608-12.

Haefeli J, Kramer JL, Blum J, Curt A. Assessment of Spinothalamic Tract Function Beyond Pinprick in Spinal Cord Lesions: A Contact Heat Evoked Potential Study. Neurorehabil Neural Repair. 2013.

Hanlon M, Anderson R. Prediction methods to account for the effect of gait speed on lower limb angular kinematics. Gait Posture. 2006; 24(3):280-7.

Hansen NL, Conway BA, Halliday DM, Hansen S, Pyndt HS, Biering-Sorensen F, et al. Reduction of common synaptic drive to ankle dorsiflexor motoneurons during walking in patients with spinal cord lesion. Journal of neurophysiology. 2005; 94(2):934-42.

Harkema S, Gerasimenko Y, Hodes J, Burdick J, Angeli C, Chen Y, et al. Effect of epidural stimulation of the lumbosacral spinal cord on voluntary movement, standing, and assisted stepping after motor complete paraplegia: a case study. Lancet. 2011; 377(9781):1938-47.

Hawthorne AL, Hu H, Kundu B, Steinmetz MP, Wylie CJ, Deneris ES, et al. The unusual response of serotonergic neurons after CNS Injury: lack of axonal dieback and enhanced sprouting within the inhibitory environment of the glial scar. J Neurosci. 2011; 31(15):5605-16.

Hicheur H, Terekhov AV, Berthoz A. Intersegmental coordination during human locomotion: does planar covariation of elevation angles reflect central constraints? Journal of neurophysiology. 2006; 96(3):1406-19.

Horsfield MA, Sala S, Neema M, Absinta M, Bakshi A, Sormani MP, et al. Rapid semi-automatic segmentation of the spinal cord from magnetic resonance images: application in multiple sclerosis. Neuroimage. 2010; 50(2):446-55.

Hubli M, Bolliger M, Dietz V. Neuronal dysfunction in chronic spinal cord injury. Spinal Cord. 2011; 49(5):582-7.

Hubli M, Dietz V, Bolliger M. Spinal reflex activity: a marker for neuronal functionality after spinal cord injury. Neurorehabil Neural Repair. 2012; 26(2):188-96.

Hug A, Weidner N. From bench to beside to cure spinal cord injury: lost in translation? Int Rev Neurobiol. 2012; 106:173-96.

Husted JA, Cook RJ, Farewell VT, Gladman DD. Methods for assessing responsiveness: a critical review and recommendations. J Clin Epidemiol. 2000; 53(5):459-68.

Ivanenko YP, Poppele RE, Lacquaniti F. Distributed neural networks for controlling human locomotion: lessons from normal and SCI subjects. Brain Res Bull. 2009; 78(1):13-21.

Ivanenko YP, Cappellini G, Poppele RE, Lacquaniti F. Spatiotemporal organization of alpha-motoneuron activity in the human spinal cord during different gaits and gait transitions. Eur J Neurosci. 2008; 27(12):3351-68.

Ivanenko YP, Cappellini G, Dominici N, Poppele RE, Lacquaniti F. Modular control of limb movements during human locomotion. J Neurosci. 2007; 27(41):11149-61.

Jabbari B, Geyer C, Gunderson C, Chu A, Brophy J, McBurney JW, et al. Somatosensory evoked potentials and magnetic resonance imaging in syringomyelia. Electroencephalogr Clin Neurophysiol. 1990; 77(4):277-85.

Kalsi-Ryan S, Curt A, Verrier MC, Fehlings MG. Development of the Graded Redefined Assessment of Strength, Sensibility and Prehension (GRASSP): reviewing measurement specific to the upper limb in tetraplegia. J Neurosurg Spine. 2012; 17(1 Suppl):65-76.

Kamper DG, McKenna-Cole AN, Kahn LE, Reinkensmeyer DJ. Alterations in reaching after stroke and their relation to movement direction and impairment severity. Arch Phys Med Rehabil. 2002; 83(5):702-7.

Kato T, Honmou O, Uede T, Hashi K, Kocsis JD. Transplantation of human olfactory ensheathing cells elicits remyelination of demyelinated rat spinal cord. Glia. 2000; 30(3):209-18.

Kidd D, Stewart G, Baldry J, Johnson J, Rossiter D, Petruckevitch A, et al. The Functional Independence Measure: a comparative validity and reliability study. Disability and rehabilitation. 1995; 17(1):10-4.

Kiehn O. Locomotor circuits in the mammalian spinal cord. Annu Rev Neurosci. 2006; 29:279-306.

Kim CM, Eng JJ, Whittaker MW. Level walking and ambulatory capacity in persons with incomplete spinal cord injury: relationship with muscle strength. Spinal Cord. 2004; 42(3):156-62.

Kinoshita M, Matsui R, Kato S, Hasegawa T, Kasahara H, Isa K, et al. Genetic dissection of the circuit for hand dexterity in primates. Nature. 2012; 487(7406):235-8.

Kramer JK, Taylor P, Steeves JD, Curt A. Dermatomal somatosensory evoked potentials and electrical perception thresholds during recovery from cervical spinal cord injury. Neurorehabil Neural Repair. 2010; 24(4):309-17.

Kramer JL, Taylor P, Haefeli J, Blum J, Zariffa J, Curt A, et al. Test-retest reliability of contact heat-evoked potentials from cervical dermatomes. J Clin Neurophysiol. 2012; 29(1):70-5.

Krawetz P, Nance P. Gait analysis of spinal cord injured subjects: effects of injury level and spasticity. Arch Phys Med Rehabil. 1996; 77(7):635-8.

Kuhn F, Halder P, Spiess MR, Schubert M. One-year evolution of ulnar somatosensory potentials after trauma in 365 tetraplegic patients: early prediction of potential upper limb function. J Neurotrauma. 2012; 29(10):1829-37.

Kuhn RA. Functional capacity of the isolated human spinal cord. Brain. 1950; 73(1):1-51.

Kumru H, Benito J, Murillo N, Valls-Sole J, Valles M, Lopez-Blazquez R, et al. Effects of high-frequency repetitive transcranial magnetic stimulation on motor and gait improvement in incomplete spinal cord injury patients. Neurorehabil Neural Repair. 2013; 27(5):421-9.

Kuypers HG. The Descending Pathways to the Spinal Cord, Their Anatomy and Function. Prog Brain Res. 1964; 11:178-202.

Lacquaniti F, Grasso R, Zago M. Motor Patterns in Walking. News Physiol Sci. 1999; 14:168-74.

Lajoie Y, Barbeau H, Hamelin M. Attentional requirements of walking in spinal cord injured patients compared to normal subjects. Spinal Cord. 1999; 37(4):245-50.

Lajoie Y, Teasdale N, Cole JD, Burnett M, Bard C, Fleury M, et al. Gait of a deafferented subject without large myelinated sensory fibers below the neck. Neurology. 1996; 47(1):109-15.

Latt MD, Menz HB, Fung VS, Lord SR. Walking speed, cadence and step length are selected to optimize the stab ility of head and pelvis accelerations. Exp Brain Res. 2008; 184(2):201-9.

Lemon RN. Descending pathways in motor control. Annual review of neuroscience. 2008; 31:195-218.

Lemon RN, Griffiths J. Comparing the function of the corticospinal system in different species: organizational differences for motor specialization? Muscle Nerve. 2005; 32(3):261-79.

Levi AD, Tator CH, Bunge RP. Clinical syndromes associated with disproportionate weakness of the upper versus the lower extremities after cervical spinal cord injury. Neurosurgery. 1996; 38(1):179-83; discussion 83-5.

Linting M, Meulman JJ, Groenen PJ, van der Koojj AJ. Nonlinear principal components analysis: introduction and application. Psychological methods. 2007; 12(3):336-58.

Little JW, Halar E. Temporal course of motor recovery after Brown-Sequard spinal cord injuries. Paraplegia. 1985; 23(1):39-46.

Lorenz DJ, Datta S, Harkema SJ. Longitudinal patterns of functional recovery in patients with incomplete spinal cord injury receiving activity-based rehabilitation. Arch Phys Med Rehabil. 2012; 93(9):1541-52.

Lovely RG, Gregor RJ, Roy RR, Edgerton VR. Effects of training on the recovery of full-weight-bearing stepping in the adult spinal cat. Experimental neurology. 1986; 92(2):421-35.

Lu P, Blesch A, Graham L, Wang Y, Samara R, Banos K, et al. Motor axonal regeneration after partial and complete spinal cord transection. The Journal of neuroscience : the official journal of the Society for Neuroscience. 2012; 32(24):8208-18.

Lucareli PR, Lima MO, Lima FP, de Almeida JG, Brech GC, D'Andrea Greve JM. Gait analysis following treadmill training with body weight support versus conventional physical therapy: a prospective randomized controlled single blind study. Spinal Cord. 2011; 49(9):1001-7.

Lunenburger L, Bolliger M, Czell D, Muller R, Dietz V. Modulation of locomotor activity in complete spinal cord injury. Exp Brain Res. 2006; 174(4):638-46.

MacLellan MJ, Ivanenko YP, Catavitello G, La Scaleia V, Lacquaniti F. Coupling of upper and lower limb pattern generators during human crawling at different arm/leg speed combinations. Exp Brain Res. 2013; 225(2):217-25.

Manor B, Li L. Characteristics of functional gait among people with and without peripheral neuropathy. Gait Posture. 2009; 30(2):253-6.

Masur H, Oberwittler C, Fahrendorf G, Heyen P, Reuther G, Nedjat S, et al. The relation between functional deficits, motor and sensory conduction times and MRI findings in syringomyelia. Electroencephalogr Clin Neurophysiol. 1992; 85(5):321-30.

McIlroy WJ, Richardson JC. Syringomyelia: a clinical review of 75 cases. Can Med Assoc J. 1965; 93(14):731-4.

Meyer DE, Abrams RA, Kornblum S, Wright CE, Smith JE. Optimality in human motor performance: ideal control of rapid aimed movements. Psychol Rev. 1988; 95(3):340-70.

Michel J, van Hedel HJ, Dietz V. Obstacle stepping involves spinal anticipatory activity associated with quadrupedal limb coordination. Eur J Neurosci. 2008; 27(7):1867-75.

Milhorat TH, Bolognese PA, Black KS, Woldenberg RF. Acute syringomyelia: case report. Neurosurgery. 2003; 53(5):1220-2.

Mirnezami R, Nicholson J, Darzi A. Preparing for precision medicine. N Engl J Med. 2012; 366(6):489-91.

Molinari M. Plasticity properties of CPG circuits in humans: impact on gait recovery. Brain research bulletin. 2009; 78(1):22-5.

Morris M, Iansek R, Matyas T, Summers J. Abnormalities in the stride length-cadence relation in parkinsonian gait. Mov Disord. 1998; 13(1):61-9.

Morris M, Iansek R, McGinley J, Matyas T, Huxham F. Three-dimensional gait biomechanics in Parkinson's disease: evidence for a centrally mediated amplitude regulation disorder. Mov Disord. 2005; 20(1):40-50.

Muhn N, Baker SK, Hollenberg RD, Meaney BF, Tarnopolsky MA. Syringomyelia presenting as rapidly progressive foot drop. J Clin Neuromuscul Dis. 2002; 3(3):133-4.

Mullner A, Gonzenbach RR, Weinmann O, Schnell L, Liebscher T, Schwab ME. Lamina-specific restoration of serotonergic projections after Nogo-A antibody treatment of spinal cord injury in rats. Eur J Neurosci. 2008; 27(2):326-33.

Musienko P, van den Brand R, Marzendorfer O, Roy RR, Gerasimenko Y, Edgerton VR, et al. Controlling specific locomotor behaviors through multidimensional monoaminergic modulation of spinal circuitries. The Journal of neuroscience : the official journal of the Society for Neuroscience. 2011; 31(25):9264-78.

Nakajima K, Maier MA, Kirkwood PA, Lemon RN. Striking differences in transmission of corticospinal excitation to upper limb motoneurons in two primate species. J Neurophysiol. 2000; 84(2):698-709.

Nakamura R, Handa T, Watanabe S, Morohashi I. Walking cycle after stroke. The Tohoku journal of experimental medicine. 1988; 154(3):241-4.

National SCI Statistical Center. Spinal Cord Injury Facts and Figures at a Glance. Birmingham, AL: University of Alabama at Birmingham; 2013 March 2013.

National Research Council (US) Committee on a Framework for Developing a New Taxonomy of Disease. Toward Precision Medicine: Building a Knowledge Network for Biomedical Research and a New Taxonomy of Disease: Washington (DC): National Academies Press (US); 2011.

Nishimura Y, Onoe H, Morichika Y, Perfiliev S, Tsukada H, Isa T. Time-dependent central compensatory mechanisms of finger dexterity after spinal cord injury. Science. 2007; 318(5853):1150-5.

Nooijen CF, Ter Hoeve N, Field-Fote EC. Gait quality is improved by locomotor training in individuals with SCI regardless of training approach. J Neuroeng Rehabil. 2009; 6:36.

Nout YS, Rosenzweig ES, Brock JH, Strand SC, Moseanko R, Hawbecker S, et al. Animal models of neurologic disorders: a nonhuman primate model of spinal cord injury. Neurotherapeutics. 2012a; 9(2):380-92.

Nout YS, Ferguson AR, Strand SC, Moseanko R, Hawbecker S, Zdunowski S, et al. Methods for functional assessment after C7 spinal cord hemisection in the rhesus monkey. Neurorehabil Neural Repair. 2012b; 26(6):556-69.

Onizuka M, Suyama K, Shibayama A, Hiura T, Horie N, Miyazaki H. Asymptomatic brain tumor detected at brain check-up. Neurol Med Chir. 2001; 41(9):431-5.

Oudega M, Perez MA. Corticospinal reorganization after spinal cord injury. J Physiol. 2012; 590(Pt 16):3647-63.

Pearson K. On lines and planes of closest fit to systems of points in space. Philosophical Magazine. 1901; 2(7-12):559-72.

Pepin A, Norman KE, Barbeau H. Treadmill walking in incomplete spinal-cord-injured subjects: 1. Adaptation to changes in speed. Spinal Cord. 2003; 41(5):257-70.

Petersen JA, Spiess M, Curt A, Dietz V, Schubert M. Spinal cord injury: one-year evolution of motor-evoked potentials and recovery of leg motor function in 255 patients. Neurorehabil Neural Repair. 2012; 26(8):939-48.

Raineteau O, Schwab ME. Plasticity of motor systems after incomplete spinal cord injury. Nature reviews. 2001; 2(4):263-73.

Robinson JL, Smidt GL. Quantitative gait evaluation in the clinic. Phys Ther. 1981; 61(3):351-3.

Rosenzweig ES, Brock JH, Culbertson MD, Lu P, Moseanko R, Edgerton VR, et al. Extensive spinal decussation and bilateral termination of cervical corticospinal projections in rhesus monkeys. J Comp Neurol. 2009; 513(2):151-63.

Rosenzweig ES, Courtine G, Jindrich DL, Brock JH, Ferguson AR, Strand SC, et al. Extensive spontaneous plasticity of corticospinal projections after primate spinal cord injury. Nature neuroscience. 2010; 13(12):1505-10.

Roth EJ, Lawler MH, Yarkony GM. Traumatic central cord syndrome: clinical features and functional outcomes. Arch Phys Med Rehabil. 1990; 71(1):18-23.

Sainburg RL, Poizner H, Ghez C. Loss of proprioception produces deficits in interjoint coordination. J Neurophysiol. 1993; 70(5):2136-47.

Schubert M, Curt A, Jensen L, Dietz V. Corticospinal input in human gait: modulation of magnetically evoked motor responses. Exp Brain Res. 1997; 115(2):234-46.

Schurch B, Wichmann W, Rossier AB. Post-traumatic syringomyelia (cystic myelopathy): a prospective study of 449 patients with spinal cord injury. J Neurol Neurosurg Psychiatry. 1996; 60(1):61-7.

Severinsen K, Jakobsen JK, Pedersen AR, Overgaard K, Andersen H. Effects of resistance training and aerobic training on ambulation in chronic stroke. Am J Phys Med Rehabil. 2014; 93(1):29-42.

Steward O, Zheng B, Tessier-Lavigne M, Hofstadter M, Sharp K, Yee KM. Regenerative growth of corticospinal tract axons via the ventral column after spinal cord injury in mice. J Neurosci. 2008; 28(27):6836-47.

Strata F, Coq JO, Byl N, Merzenich MM. Effects of sensorimotor restriction and anoxia on gait and motor cortex organization: implications for a rodent model of cerebral palsy. Neuroscience. 2004; 129(1):141-56.

Tamburella F, Scivoletto G, Molinari M. Balance training improves static stability and gait in chronic incomplete spinal cord injury subjects: a pilot study. Eur J Phys Rehabil Med. 2013; 49(3):353-64.

Thomas SL, Gorassini MA. Increases in corticospinal tract function by treadmill training after incomplete spinal cord injury. Journal of neurophysiology. 2005; 94(4):2844-55.

Thompson AK, Pomerantz FR, Wolpaw JR. Operant conditioning of a spinal reflex can improve locomotion after spinal cord injury in humans. J Neurosci. 2013; 33(6):2365-75.

Ulrich A, Haefeli J, Blum J, Min K, Curt A. Improved diagnosis of spinal cord disorders with contact heat evoked potentials. Neurology. 2013; 80(15):1393-9.

van den Brand R, Heutschi J, Barraud Q, DiGiovanna J, Bartholdi K, Huerlimann M, et al. Restoring voluntary control of locomotion after paralyzing spinal cord injury. Science. 2012; 336(6085):1182-5.

van Hedel HJ. Gait speed in relation to categories of functional ambulation after spinal cord injury. Neurorehabil Neural Repair. 2009; 23(4):343-50.

van Hedel HJ, Wirz M, Curt A. Improving walking assessment in subjects with an incomplete spinal cord injury: responsiveness. Spinal Cord. 2006; 44(6):352-6.

van Hedel HJ, Wirth B, Curt A. Ankle motor skill is intact in spinal cord injury, unlike stroke: implications for rehabilitation. Neurology. 2010; 74(16):1271-8.

Vernon JD, Silver JR, Ohry A. Post-traumatic syringomyelia. Paraplegia. 1982; 20(6):339-64.

von Schroeder HP, Coutts RD, Lyden PD, Billings E, Jr., Nickel VL. Gait parameters following stroke: a practical assessment. J Rehabil Res Dev. 1995; 32(1):25-31.

Weidner N, Ner A, Salimi N, Tuszynski MH. Spontaneous corticospinal axonal plasticity and functional recovery after adult central nervous system injury. Proceedings of the National Academy of Sciences of the United States of America. 2001; 98(6):3513-8.

Winter DA. Biomechanics and Motor Control of Human Movement. New York: Wiley; 1990.

Winter DA. Foot trajectory in human gait: a precise and multifactorial motor control task. Phys Ther. 1992; 72(1):45-53.

Wirth B, van Hedel H, Curt A. Foot control in incomplete SCI: distinction between paresis and dexterity. Neurological research. 2008; 30(1):52-60.

Wuehr M, Schniepp R, Pradhan C, Ilmberger J, Strupp M, Brandt T, et al. Differential effects of absent visual feedback control on gait variability during different locomotion speeds. Exp Brain Res. 2013; 224(2):287-94.

Wyndaele M, Wyndaele JJ. Incidence, prevalence and epidemiology of spinal cord injury: what learns a worldwide literature survey? Spinal Cord. 2006; 44(9):523-9.

Zager EL, Ojemann RG, Poletti CE. Acute presentations of syringomyelia. Report of three cases. J Neurosurg. 1990; 72(1):133-8.

Zimmerli L, Krewer C, Gassert R, Muller F, Riener R, Lunenburger L. Validation of a mechanism to balance exercise difficulty in robot-assisted upper-extremity rehabilitation after stroke. J Neuroeng Rehabil. 2012; 9:6.

Zorner B, Bachmann LC, Filli L, Kapitza S, Gullo M, Bolliger M, et al. Chasing central nervous system plasticity: the brainstem's contribution to locomotor recovery in rats with spinal cord injury. Brain. 2014; 137(Pt 6):1716-32.

Glossary

10mWT	10-meter walk test
6minWT	6-minute walk test
ACC	Angular component of coefficient of correspondence
ADM	Abductor digiti minimi
ANOVA	Analysis of variance
APB	Abductor pollicis brevis
ASIA	American Spinal Injury Association
BDA	biotinylated dextran amine
BS	Brain stem
C	Cervical
CPG	Central pattern generator
CSF	Cerebrospinal fluid
dCHEP	Dermatomal contact heat evoked potential
dSSEP	Dermatomal somatosensory evoked potential
EMG	Electromyography
EMSCI	Europen Multicenter Study about Spinal Cord Injury
EP	Evoked potential
GRASSP	Graded redefined assessment of strength, sensibility and prehension
HPR	Hand-path ratio
IACUC	Institutional Animal Care and Use Committee
iSCI	Incomplete Spinal cord injury
ISNCSCI	International standards for neurological classification of spinal cord injury
L	Lumbar
LEMS	Lower extremity motor score
MEP	Motor evoked potential
MRI	Magnetic resonance imaging
NCS	Nerve conduction study
NLPCA	Non-linear principal component analysis
OG	Overground
PC	Principal component
PCA	Principal component analysis
ROM	Range of motion
SCI	Spinal cord injury
SCIM	Spinal cord independence measure
SD	Standard deviation
SSD	Sum of squared distances
T	Thoracic
TA	Tibialis anterior
TM	Treadmill
TMS	Transcranial magnetic stimulation
UEMS	Upper extremity motor score
WISCI	Walking index for spinal cord injury

Curriculum Vitae

First name: Lea

Name: Awai

Address

Work:
Forchstrasse 340
8008 Zurich
Switzerland
+41 44 386 37 34
lawai@paralab.balgrist.ch

Private:
Forchstrasse 158
8032 Zurich
Switzerland
+41 76 504 31 91

Date of birth: July 2nd 1984

Nationality: Switzerland and Japan

Education

2010 – 2014	**PhD at ETH Zurich**, Switzerland (*ongoing*) Research conducted at the Spinal Cord Injury Center, Balgrist University Hospital, Zurich, Switzerland
2010 – 2014	**International PhD Program in Neuroscience** Neuroscience Center Zurich (ZNZ), University of Zurich and ETH Zurich
2009	**Research student at Department of Human System Science**, Tokyo Institute of Technology, Tokyo, Japan Studies included research activities and Japanese language.
2006 – 2008	**Master of Science in Human Movement Science**, ETH Zurich, Zurich, Switzerland
2003 – 2006	**Bachelor of Science in Human Movement Science**, ETH Zurich, Zurich, Switzerland
2005 – 2008	**Teaching Certificate for Physical Education** in Secondary and Higher Education

Research Experience

2010 – 2014	**Balgrist University Hospital, University of Zurich, Switzerland** (*ongoing*) Advisor: Armin Curt Study the motor control and recovery after incomplete spinal cord injury in humans using 3-D kinematic motion analysis.
2009	**Department of Human System Science, Tokyo Institute of Technology, Japan** Advisor: Takeo Maruyama Explore the redundancy of information during elaborate, expensive and time-consuming 3-D kinematic gait analysis and simplified, low-cost accelerometer based gait analysis.
2008	**Brain Research Institute, University of Zurich and ETH Zurich, Switzerland** Advisor: Michaela Thallmair In vitro proliferation- and differentiation potential of neuronal stem cells derived from the spinal cord and hippocampus. In vivo proliferation, differentiation and migration of spinal-cord and hippocampus derived neuronal stem cells transplanted into brain of wildtype mice, Nogo-A knock-out mice and heterozygous mice.
2008	**Department of Neuropsychology, University of Zurich, Switzerland** Advisor: Eveline Geiser Meter and rhythm processing in music and speech perception assessed by fMRI and EEG.
2007 – 2008	**Vestibulo-oculomotor lab, University Hospital Zurich, Switzerland** Advisor: Jean Laurens Examine the contributions of the visual system during target tracking and perception of different visual backgrounds to posture control during bipedal stance.

Teaching Experience

2012 – 2014	Supervision of Master's Thesis in Human Movement Science, ETH Zurich
2012 – 2013	"Functional Assessment of Human Spinal Cord Injury": Conduct of the block course attended by undergraduate students in biology of the University of Zurich and ETH Zurich

Attended conferences

International Spinal Cord Society (ISCoS), Istanbul, 2013
Talk: Distinction between spinal and supraspinal control of walking in human incomplete spinal cord injury

International Neurorehabilitation Symposium (INRS), Zurich, 2013
Poster: Supraspinal and spinal neural control of walking in human incomplete spinal cord injury

ZNZ Symposium, Zurich, 2013
Poster: Supraspinal and spinal neural control of walking in human incomplete spinal cord injury

European Society of Movement Analysis for Adults and Children (ESMAC), Stockholm, 2012
Poster: Walking pattern and neural control in incomplete spinal cord injury

NCCR Neuro Concluding Symposium & ZNZ Symposium, Zurich, 2012
Poster: Walking pattern and neural control in incomplete spinal cord injured patients

European Neurotrauma School, London, 2012
Poster: Walking pattern and neural control in incomplete spinal cord injured patients

First Joint Meeting – Spinal Cord Injury Centers Heidelberg & Zurich, Heidelberg, 2012
Talk: Walking pattern and neural control in incomplete spinal cord injury

ZNZ Symposium, Zurich, 2011
Poster: Limited gait-modulatory capacity in spinal cord injury patients

Publications

Awai L, Curt A. *Intralimb coordination as a sensitive indicator of motor-control impairment after spinal cord injury*. Frontiers in human neuroscience, 2014; 8:148.

Awai L, Curt A. *Extensive plasticity of the human spinal cord*. 2014. (submitted).

Awai L, Bolliger M, Ferguson AR, Courtine G, Curt A. *Domains of neural control of walking in human spinal cord injury*. 2014. (submitted).

Friedli L, Rozenzweig ES, Barraud Q, Schubert M, Dominici N, **Awai L**, Nielson JL, Musienko P, Nout-Lomas Y, Zhong H, Zdunowski S, Roy RR, EMSCI Study Group, Stran SC, Havton LA, Beattie MS, Bresnahan JC, Ferguson AR, Curt A, Edgerton VR, Tuszynski MH, Courtine G. *Corticospinal tract plasticity after spinal cord injury supports greater recovery in humans and monkeys than rats*. 2014. (Manuscript in preparation).

Laurens J, **Awai L**, Bockisch CJ, Hegemann S, van Hedel HJ, Dietz V, Straumann D. *Visual contribution to postural stability: Interaction between target fixation or tracking and static or dynamic large-field stimulus*. Gait & posture, 2010; 31(1): p. 37-41.

Acknowledgements

Naturally, my thanks go to my committee members:

I would like to thank my PhD supervisor Martin Schwab for being a role model since years before I even thought of doing a PhD. I was fascinated by the achievements he has contributed to the world over the past decades, yet not losing his humbleness and down-to-earthness.

I would like to thank Armin Curt for guiding me through my PhD, for giving me invaluable insights into clinical research, and for being a pain in the rear, occasionally.

I would like to thank Grégoire Courtine for making it possible to conduct my PhD and for being an example of how enthusiastically and persistently one can pursue his goals.

I would also like to thank the European Commission's Seventh Framework Program for the financial support.

My heartfelt thanks go to my family who supported me throughout the conduction of my PhD thesis, who accepted my limited amount of time I could dispose of, who took over duties I did not manage to carry out, and who always reassured that choosing the right way instead of the easy way would pay off at some point.
ご苦労様。

My sincere thanks go to Raphi, who gave me the strength to carry on, who tried to teach me indulgence, who had to do without a lot of things, who had to endure my unpleasantness and who made me run.

I truly thank Adrian for his support, who had to sacrifice so many things, who showed me lightheartedness and impartiality. ありがとう！

I would also like to thank Jenny for being a great companion, different from others.

Last but by far not least I would like to thank all the subjects who volunteered to be part of our studies. I would particularly like to express my gratitude to all patients for participating in the time-consuming and energy-sapping recordings, who, amidst their lives, found themselves confronted with challenging situations. I thank them for their straightforwardness, for their energy, their strength as well as their sadness and depressiveness, for their trust and for opening my eyes. I wish them all the best.